

Electronic Thesis and Dissertation Repository

---

8-4-2020 11:00 AM

## Nicotinamide mononucleotide imparts protection against Doxorubicin-induced cardiotoxicity by maintaining lysosomal acidification

Nima Nalin, *The University of Western Ontario*

Supervisor: Peng, Tianqing, *The University of Western Ontario*

A thesis submitted in partial fulfillment of the requirements for the Master of Science degree in Pathology and Laboratory Medicine

© Nima Nalin 2020

Follow this and additional works at: <https://ir.lib.uwo.ca/etd>

---

### Recommended Citation

Nalin, Nima, "Nicotinamide mononucleotide imparts protection against Doxorubicin-induced cardiotoxicity by maintaining lysosomal acidification" (2020). *Electronic Thesis and Dissertation Repository*. 7195.  
<https://ir.lib.uwo.ca/etd/7195>

This Dissertation/Thesis is brought to you for free and open access by Scholarship@Western. It has been accepted for inclusion in Electronic Thesis and Dissertation Repository by an authorized administrator of Scholarship@Western. For more information, please contact [wlsadmin@uwo.ca](mailto:wlsadmin@uwo.ca).

## Abstract

Doxorubicin (DOX) blocks the autophagic flux in cardiomyocytes by inhibiting lysosome acidification. The acidic pH of lysosomes is maintained by the V-ATPase pump. NAD<sup>+</sup> is an essential cofactor for the maintenance of cellular homeostasis. DOX treatment significantly depletes the NAD<sup>+</sup> levels in cardiomyocytes. This study investigated the potential of the NAD<sup>+</sup> precursor, nicotinamide mononucleotide (NMN), in preventing DOX-induced cardiotoxicity. DOX induced cell injury and altered the lysosomal pH of H9c2 cells, an *in vitro* model of cardiomyocytes. These effects of DOX were attenuated by NMN. The protection conferred by NMN was offset by inhibition of V-ATPase activity with bafilomycin A. Furthermore, NMN prevented the DOX induced hyperacetylation of the V-ATPase subunit ATP6V0d1, a critical protein involved in the maintenance of V-ATPase activity. In summary, NMN protects cardiomyocytes from DOX induced toxicity by maintaining the pH of lysosomes. Thus, NMN holds potential in combating the deleterious impacts of Doxorubicin on the heart.

Keywords: ATP6V0d1; cardiotoxicity; doxorubicin; lysosome; NAD<sup>+</sup>; NMN; V-ATPase

## Summary for Lay Audience

Cancer is one of the leading causes of death worldwide. Nearly 1 in 2 Canadians develop cancer during their lifetime. The harsh reality of cancer does not end with its onset. The devastating dark side of the available treatment options like chemotherapy impacts the patient's quality of life. Doxorubicin, the chemotherapy antibiotic, is routinely used for the treatment of multiple cancers. Its deadliest side effect is heart injury, which leads to heart failure. In fact, over 50% of the childhood cancer survivors develop heart disease in the later stages of their life. Doxorubicin impairs a cellular process known as autophagy in heart cells. Autophagy or cellular recycling is a self-eating process by which the damaged components in the cells can be degraded and recycled. This recycling process occurs in designated recycling centres or specialized compartments called lysosomes in the cell. Efficient functioning of lysosomes is rendered by their acidic nature or low internal pH. This helps the lysosomal proteins to break down the cellular debris. The low pH in lysosomes is achieved with the help of a cellular pump called V-ATPase positioned on the lysosomal membrane. V-ATPase transports protons into the lysosome and maintains optimal pH. Doxorubicin increases the pH of lysosomes and it could most likely be by damaging the V-ATPase pump, but the exact mechanism remains unknown.

NAD<sup>+</sup> is a critical molecule in the body which is required for many essential reactions in the cell. Doxorubicin decreases the natural levels of NAD<sup>+</sup> in the body and compromises the normal functioning of the cell. NAD<sup>+</sup> depletion affects the lysosome function too. This study aims to identify the impact of Doxorubicin treatment on the pH of lysosomes and the V-ATPase pump in the heart cells. Nicotinamide mononucleotide (NMN) is a vitamin B3 derivative and NAD<sup>+</sup> supplement that provides many essential benefits to the body. The role of NMN in preventing the harmful effects of Doxorubicin have been investigated in this study. The results indicate that NMN has promising potential in protecting the heart from the side effects of Doxorubicin.

## Acknowledgements

I would like to extend my warmest gratitude to my supervisor, Dr. Tianqing Peng, for his continuous guidance and support throughout this program. He has been a wonderful mentor and teacher and I highly appreciate the opportunity to work under his supervision. I am also indebted to my advisory committee members, Dr. Douglas Jones and Dr. Martin Duennwald, for their valuable suggestions, comments and encouragement. I would like to thank my lab members, Dr. Rui Ni, Dr. Ting Cao, Rebecca Dang, Xiaoyun Ji, Xiaodi Sun and Liwen Liang for all their technical help and support. I am grateful to all the staff and students of the Centre for Critical Illness Research, LHRI for helping out with the equipment and experiments.

I would like to acknowledge the critiques and comments from Dr. Zia Khan, Dr. Chandan Chakrabarthy and all my classmates at the journal club. Lastly, I would like to thank Ms. Tracey Koning, Ms. Susan Underhill and all others at the Department of Pathology and Laboratory Medicine, Western University for their administrative and moral support throughout the past two years.

## Dedication

Dedicated to my lovely son, Niranjan, my pillar of strength, Vinu Raj, my wonderful parents, Nalanan and Beena, and all my friends and well-wishers.

# Table of Contents

Abstract.....	ii
Summary for Lay Audience .....	iii
Acknowledgements.....	iv
Dedication.....	v
List of Tables.....	ix
List of Figures .....	x
Chapter 1 .....	1
1 Introduction .....	1
1.1 Anthracyclines.....	2
1.2 Doxorubicin .....	5
1.2.1 Anti-cancer mechanism.....	6
1.3 Doxorubicin Cardiotoxicity.....	7
1.3.1 Pathophysiology .....	8
1.3.2 Risk Factors .....	8
1.3.3 Mechanisms of Cardiotoxicity.....	10
1.4 Autophagy and Cardiovascular diseases .....	12
1.5 V-ATPase.....	15
1.5.1 V-ATPase Structure .....	15
1.5.2 V-ATPase Isoforms.....	18
1.5.3 V-ATPase proton transport mechanism.....	19
1.5.5 V-ATPase inhibitors .....	21
1.5.6 Bafilomycin A .....	23
1.5.7 V-ATPase activity in the heart.....	24
1.6 Nicotinamide Adenine Dinucleotide (NAD+) .....	25
1.6.1 NAD+ Biosynthesis .....	26
1.6.2 NAD+ in the heart.....	29
1.6.3 Role of NAD+ in Autophagy.....	29
1.6.4 Nicotinamide mononucleotide (NMN) .....	30
1.7 Rationale.....	32
1.8 Hypothesis .....	34
1.9 Specific Aims.....	35
Chapter 2.....	36
2 Materials and Methods.....	36

2.1 H9c2 cell culture .....	36
2.2 Isolation and culture of neonatal cardiomyocytes .....	37
2.3 Doxorubicin Cardiotoxicity- <i>in vitro</i> experimental model.....	38
2.4 CCK-8 Assay.....	38
2.5 Lactate Dehydrogenase Release Assay.....	39
2.6 Caspase-3 Activity.....	39
2.7 Lysosomal pH measurement .....	40
2.8 Co-immunoprecipitation (co-IP) and Western Blot Analysis .....	41
2.9 Statistical Analysis.....	44
Chapter 3.....	47
3 Results.....	47
3.1 DOX induces dose-dependent toxicity in H9c2 cells .....	47
3.2 DOX increases LDH release in H9c2 cells .....	49
3.3 DOX treatment increases caspase-3 activity in H9c2 cells.....	51
3.3.1 DOX induces morphological alterations in H9c2 cells .....	53
3.4 DOX treatment prevents lysosomal acidification in H9c2 cells .....	54
3.5 NAD <sup>+</sup> and its precursor NMN prevents DOX-induced toxicity in H9c2 cells.....	56
3.5.1 NMN and NAD <sup>+</sup> prevents DOX-induced increases in LDH release.....	56
3.5.2 NMN and NAD <sup>+</sup> prevents DOX-induced increase in caspase-3 activity .....	58
3.5.3 NMN and NAD <sup>+</sup> increases the viability of DOX-treated H9c2 cells .....	60
3.6 NMN and NAD <sup>+</sup> prevents DOX-induced changes in lysosomal pH .....	62
3.7 V-ATPase inhibitor, Bafilomycin A prevents NMN/NAD <sup>+</sup> imparts protection against DOX cardiotoxicity.....	64
3.7.1 Bafilomycin A prevents NMN/NAD <sup>+</sup> induced decreases in LDH release in DOX- treated H9c2 cells.....	64
3.7.2 Bafilomycin A prevents NMN/NAD <sup>+</sup> induced protection against alterations in lysosomal pH in DOX-treated H9c2 cells .....	67
3.8 NMN prevents hyperacetylation of ATP6V0d1 in DOX-treated neonatal cardiomyocytes.....	69
Chapter 4.....	71
4 Discussion, Limitations and Future Directions .....	71
4.1 Discussion.....	71
4.1.1 Doxorubicin induces toxicity and death in cardiomyocytes .....	72
4.1.2 Doxorubicin inhibits acidification and induces lysosomal dysfunction in cardiomyocytes.....	73
4.1.3 NMN confers protection against Doxorubicin-induced toxicity and death in cardiomyocytes.....	75

4.1.4 NMN protects cardiomyocytes from Doxorubicin-induced alterations in lysosomal pH .....	76
4.1.5 Bafilomycin A abrogates the protective effects of NMN in Doxorubicin-induced cardiotoxicity .....	76
4.1.6 NMN prevents hyperacetylation of the d subunit of V-ATPase pump V <sub>0</sub> domain .....	77
4.2 Concluding Remarks.....	78
4.3 Limitations.....	80
4.4 Future Directions .....	80
5 References.....	82
Curriculum Vitae.....	94



## List of Tables

Table 1: Anthracycline drugs.....	3
Table 2: Natural sources of NMN.....	32
Table 3: D-Hank's Solution (1L).....	36
Table 4: Lysis/Assay Buffer (100mL) .....	40
Table 5: 6X Loading Buffer (100 mL) .....	41
Table 6: 4% Stacking gel (6 mL).....	42
Table 7: 12% Resolving Gel (20mL).....	42
Table 8: Running Buffer pH 8.3 (1L) .....	42
Table 9: Transfer Buffer (1L) .....	43
Table 10: TBST pH 7.6 (1L).....	43
Table 11: Enhanced Chemiluminescence (ECL) Reagent (200mL).....	44
Table 12: Reagent Information .....	45
Table 13: Antibody Information .....	46

## List of Figures

Figure 1.1: Chemical Structure of Anthracyclines. ....	4
Figure 1.2: Anti-cancer mechanism of Doxorubicin. ....	7
Figure 1.3: Risk factors associated with DOX-induced cardiomyopathy.....	9
Figure 1.4: Doxorubicin induces Cardiomyocyte cell death. ....	11
Figure 1.5: Schematic representation of Autophagy.....	14
Figure 1.6: Structure of mammalian V-ATPase. ....	17
Figure 1.7: V-ATPase activity is tightly regulated by reversible disassociation of V0 and V1 domains. ....	20
Figure 1.8: Structures of V-ATPase inhibitors. ....	22
Figure 1.9: Bafilomycin A inhibits the proton transport mechanism of V-ATPase. ....	23
Figure 1.10: Structure of NAD+. ....	26
Figure 1.11: Schematic illustration of NAD+ biosynthesis in mammalian cells.....	28
Figure 1.12: Structure of $\beta$ -NMN. ....	31
Figure 1.13: Schematic illustration of Hypothesis.....	34
Figure 2.1: Schematic representation of the in vitro model used for study. ....	38
Figure 3.1: DOX treatment decreases H9c2 cell viability in a concentration-dependent manner.....	48
Figure 3.2: DOX treatment increases the LDH release in H9c2 cells. ....	50
Figure 3.3: DOX treatment increases the caspase-3 activity in H9c2 cells. ....	52
Figure 3.4: DOX treatment alters the lysosomal pH by preventing acidification in H9c2 cells. ....	55
Figure 3.5: LDH release in (a) DOX, NMN and NMN-DOX treated and (b) DOX, NAD and NAD-DOX treated H9c2 cells. ....	57
Figure 3.6: NMN prevents DOX-induced increases in caspase-3 activity in H9c2 cells.....	58
Figure 3.7: NAD+ prevents DOX-induced increases in caspase-3 activity in H9c2 cells. ....	59
Figure 3.8: NMN increases viability of DOX-treated H9c2 cells. ....	60
Figure 3.9: NAD+ increases viability of DOX-treated H9c2 cells.....	61
Figure 3.10: NMN prevents DOX-induced pH changes.....	62
Figure 3.11: NAD+ prevents DOX-induced pH changes. ....	63
Figure 3.12: Bafilomycin A prevents NMN induced decreases in LDH release in DOX-treated H9c2 cells.....	65

Figure 3.13: Bafilomycin A prevents NAD <sup>+</sup> induced decreases in LDH release in DOX-treated H9c2 cells.....	66
Figure 3.14: Bafilomycin A prevents NMN imparted protection against DOX-induced lysosomal pH alterations.....	67
Figure 3.15: Bafilomycin A prevents NAD <sup>+</sup> imparted protection against DOX-induced lysosomal pH alterations.....	68
Figure 3.16: NMN prevents DOX-induced hyperacetylation of ATP6V0d1.....	70
Figure 4.1: Schematic illustration of the study.....	79

# Chapter 1

## 1 Introduction

Cancer is the leading cause of death in Canada and the Canadian Cancer Society estimates more than 80,000 deaths and 225,000 newly diagnosed cases in the country in 2020. Lung, breast, prostate and colorectal cancers together account for about nearly half of the newly diagnosed cases in Canada. Though the incidence is higher in population aged more than 50, it can affect at any age (1). Chemotherapy is most often used as the treatment option alone or in combination with radiation, surgery etc. The word “chemotherapy” was coined by the renowned German chemist Paul Ehrlich in the early 1900’s to address the use of chemicals to treat disease. Nitrogen mustard was one of the earliest chemotherapy agents used for cancer treatment. Even though the initial hype stirred considerable interest in the drug, it soon subsided as remissions occurred in treated patients (2).

Cancer chemotherapy is a double-edged sword attacking both tumour cells and normal cells alike. This could lead to deleterious side effects and so deciphering the mechanistic action of these drugs in malignant and non-malignant cells is of high importance. Doxorubicin is a commonly administered chemotherapy agent worldwide and it is used in adult and paediatric cancer patients alike with commendable recovery rates. Due to its toxicity profile and bright red appearance, Doxorubicin has been notoriously nicknamed as the “Red Devil”. Alongside the common side effects of most chemotherapeutic antibiotics, like nausea, vomiting, mouth sores and alopecia, Doxorubicin could elicit irreversible damage to the heart as well. Though widely studied, the mechanisms of Doxorubicin triggered cardiac injury remains elusive. Numerous drug candidates have entered clinical trials to combat the side effects of Doxorubicin, but none of them have been completely successful so far (3). This study explores the mechanism and potential of Nicotinamide mononucleotide, a vitamin B3 derivative of natural origin, in preventing the cardiotoxic side effects of Doxorubicin in an *in vitro* model of disease.

## 1.1 Anthracyclines

The efforts to investigate potential anti-neoplastic agents from soil microbes by the Italian company, Farmitalia Research Laboratories, led to the discovery of the first anthracycline antibiotic. Prof. Di Marco and his team isolated and purified a red pigment from a spore forming *Streptomyces peucetius* found in the soil near the Castel del Monte on the shores of the Adriatic Sea. This drug showed promising anti-tumor activity and was named Daunomycin. A similar drug with identical physicochemical properties was isolated by a French research group led by Maurice Dubost from *Streptomyces coeruliorubidus* at about the same time and was named Rubidomycin. The name daunorubicin was hence internationally adopted to avoid conflicts and by late 1960's it was clinically introduced for cancer treatment (4). The success of the new drug soon initiated the drive for development of analogues with higher therapeutic index.

Chemical mutagenesis of *Streptomyces peucetius* led to the development of a variant which produced another anthracycline antibiotic, Doxorubicin. Epirubicin and Idarubicin were synthetically developed from Doxorubicin and Daunorubicin, respectively. Epirubicin exerts lower cardiotoxic effects and Idarubicin is more lipophilic compared to their parent drugs. Several new drugs were later added to this group and the list remains inexhaustive (Table 1). Though anthracyclines showed promise in their efficacy for the treatment of cancer, the toxic side effects mainly related to cardiac health were soon reported in patients, raising concerns. Despite this, anthracycline therapy remains an important cancer treatment regimen after nearly 50 decades of its discovery and is included in the World Health Organization's list of essential medicines. Daunorubicin, Doxorubicin, Epirubicin and Idarubicin are the commonly used anthracyclines in the clinics at present (Figure 1.1) (5,6).

**Table 1: Anthracycline drugs**

<b><u>Anthracycline</u></b>	<b><u>Trade Name</u></b>	<b><u>Indications</u></b>
Daunorubicin	Daunoxome, Cerubidine ®	acute lymphocytic leukemia
Doxorubicin	Doxil®, Rubex ®	solid tumors, hematologic malignancies
Epirubicin	Ellence	axillary node metastases after surgical breast cancer resection
Idarubicin	Idamycin	acute myeloid leukemia
Valrubicin	Valstar, Valtaxin	bladder carcinoma
Aldoxorubicin	-	Under investigation
Annamycin	-	Under investigation
Plicamycin	Mithracin	testicular cancer
Sabarubicin	-	Under investigation
Zoptarelin doxorubicin	-	Under investigation

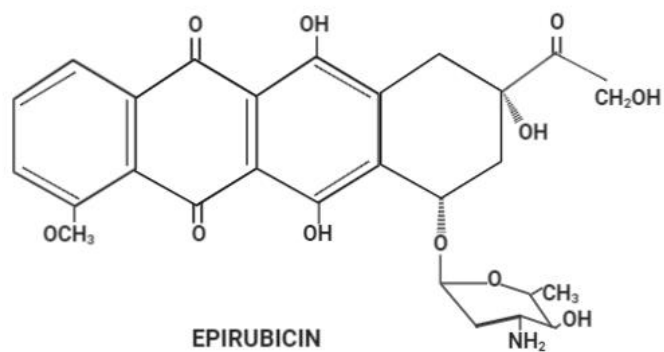
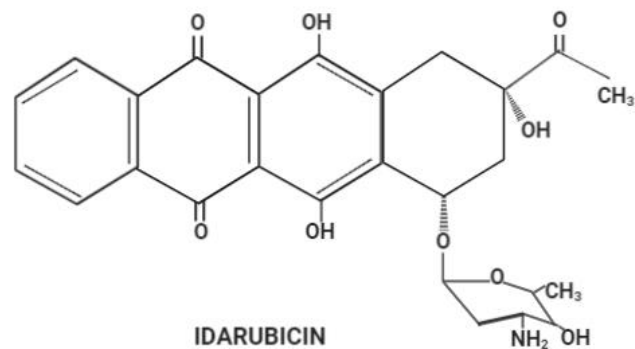
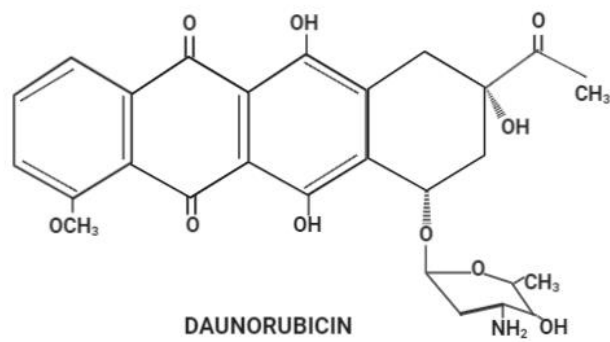
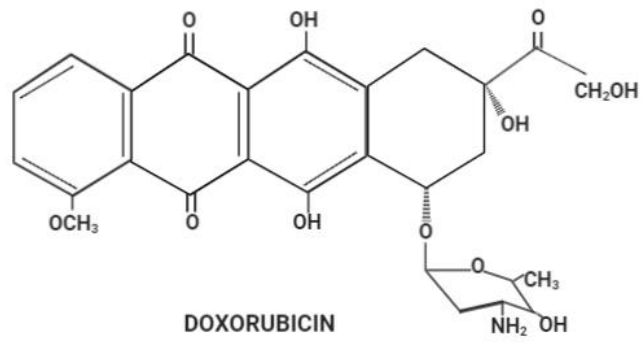


**Figure 1.1: Chemical Structure of Anthracyclines.** The four commonly used anthracycline drugs Doxorubicin, Daunorubicin, Idarubicin and Epirubicin.

## 1.2 Doxorubicin

Doxorubicin (DOX) is produced as a secondary metabolite from the bacterial strain *Streptomyces peucetius* var. *caesius*. It was initially named Adriamycin, in recognition of the Adriatic Sea, from where daunomycin, the first anti-cancer anthracycline was discovered (4). DOX is extensively used in the treatment of solid tumors of the breast, lung, and bladder, cervical cancer, lymphomas and sarcomas, in combination with other drugs such as cyclophosphamide, paclitaxel etc. (7). Attributed to the efficiency of the drug in chemotherapy treatment, the global DOX market is forecasted to be about 1.38 billion USD by the year 2024, with North America contributing the major share followed by Europe and Asia Pacific (8).

The chemical structure of DOX is comprised of a characteristic anthracycline tetracyclic ring with an adjacent quinone-hydroquinone group linked to a sugar moiety, daunosamine, by a glycosidic bond. The presence of a methoxy group attached to the tetracyclic ring and methyl group attached to daunosamine distinguishes DOX from its analogues (9). As the oral bioavailability of DOX is very low (< 1%) due to limited intestinal absorption, it is intravenously administered and undergoes rapid tissue distribution and slow elimination (10). DOX rapidly exits the circulation and accumulates in tissues, mostly in the liver. It does not cross the blood-brain barrier despite being highly penetrative. The metabolism of DOX begins in the liver and transforms to its main active immediate metabolite Doxorubicinol in a NADPH dependent conversion by carbonyl reducing enzymes. The sugar components of DOX and Doxorubicinol undergoes acid catalysed hydrolysis to form the aglycones, doxorubicinone and doxorubicinolone, respectively. These metabolites are then excreted in urine and faeces (11).

More than 2000 analogues of DOX have been synthesized and have been researched for their anti-neoplastic potential. Efforts to develop more efficient and less toxic analogues led to the use of liposomal encapsulation technology. Doxorubicin was the first anti-cancer drug to reach clinical trials as a lipid-based formulation. Liposomes are mostly confined to the vascular system, and limits the exposure of doxorubicin to the myocardial cells having tight junctions. Since the tumour cells are not tightly joined, the liposomal drug can exit the circulation and accumulate in these cells. Phospholipids of the liposomes are derived from natural sources like egg yolk and soya bean and can be eliminated from the circulation within a few hours by plasma protein opsonization. But this short half-life limits its potential to a



certain extent. To overcome this, polymers such as polyethylene glycol (PEG), ganglioside, and cerebroside sulphate that resisted opsonization were incorporated to the liposomal formulation. Pegylated- liposomal DOX is now available under the trade name Doxil<sup>®</sup> and has a circulatory half-life of 3-4 days. Adding a PEG molecule however, because of its large size, could limit the entry of liposome to the tumour cells and decrease the accumulation of DOX. Also, since Doxil<sup>®</sup> has high affinity towards the skin, it causes a dose-limiting hand-foot syndrome (HFS) in nearly 50% of patients treated with the drug. Non-pegylated versions of liposomal encapsulated DOX such as Myocet<sup>®</sup> have been introduced into the North American market but is relatively expensive (12).

### 1.2.1 Anti-cancer mechanism

The chemotherapeutic efficacy of DOX is attributed to its interaction with DNA, topoisomerase inhibition and generation of reactive oxygen species (ROS) (13). It covalently interacts with double stranded DNA by intercalating between the bases. At the maximum saturation level, one molecule of DOX intercalates into every fifth base-pair of DNA. A partial B to A-DNA transition occurs in the structure which accounts for the anti-cancer activity of the drug (14). Topoisomerases are ubiquitous enzymes involved in the replication, transcription, recombination, repair, and chromatin modelling. DOX inhibits topoisomerases and disrupts the repair and replication mechanisms in the nucleus (15,16).

DOX also undergoes reduction to form a semiquinone radical by cellular oxidases, which reacts with oxygen, generating ROS and exerts toxic effects on the cancer cells or gets oxidised back by redox cycling (17). The drug interacts with the plasma proteins too and gets reduced resulting in the formation of the highly potent hydroxyl radicals. Apoptosis is triggered in cells when the repair process in response to DNA damage fails. DOX treatment activates the p53 pathway and downregulates Bcl-2 expression subsequently activating the effector caspases, the mediators of apoptosis (11).

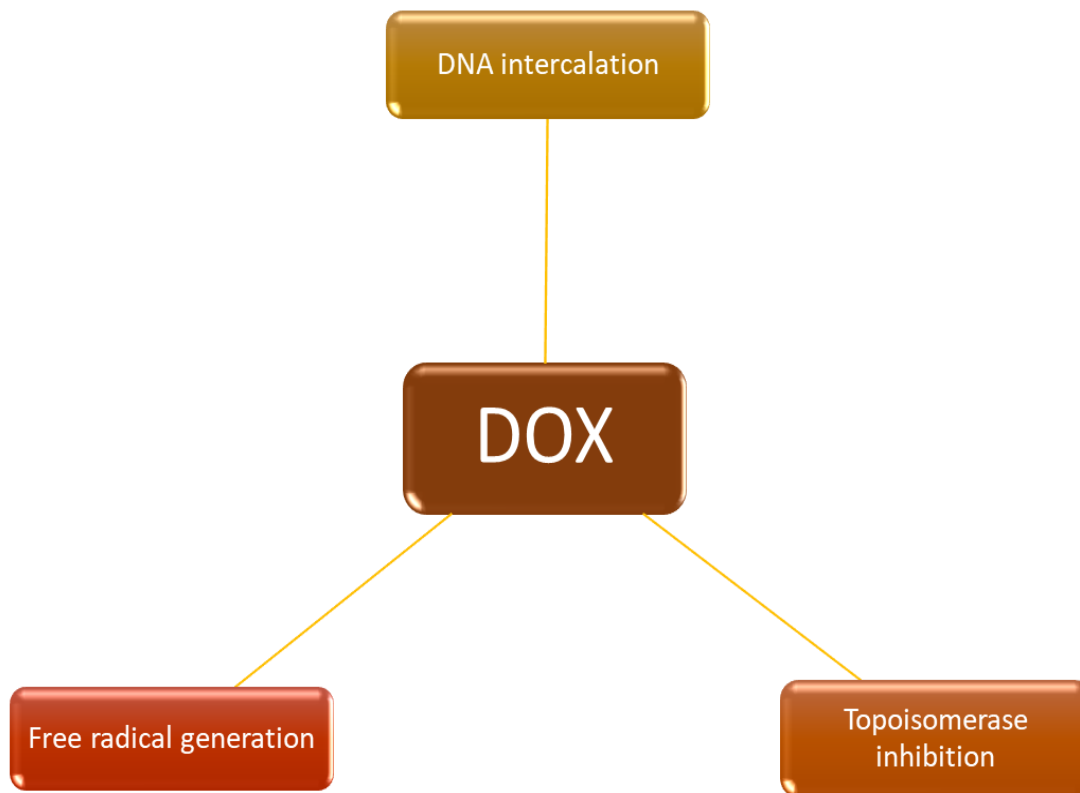


**Figure 1.2: Anti-cancer mechanism of Doxorubicin.** DOX exerts its anti-cancer properties by intercalating into the DNA, inhibiting the topoisomerases and generating free radicals.

### 1.3 Doxorubicin Cardiotoxicity

The adverse effects of DOX and other anthracycline analogues on cardiac health were reported by late 1960's (18). But still, even after nearly 5 decades, it remains a key player in the chemotherapeutic regime amidst the outcomes. Occurrence of cardiac complications is estimated in one among eight DOX-treated patients (19). The cardiotoxic events associated with DOX could be acute which occurs during or immediately after treatment, or chronic, occurring within a year (early-onset) or several years post-treatment (late-onset). Acute DOX cardiotoxicity is reversible, and manifestations could include reduced contractility, pericarditis, myocarditis, sinus tachycardia, ST-T wave changes and decreased QRS complex amplitude. Early-onset chronic complications include dilated cardiomyopathy with reduced ejection fraction, electrical conduction changes, valve damage and reduced contractility.

Late-onset cardiotoxicity is often a silent killer, is irreversible and progresses to heart failure. The progressive nature of chronic DOX cardiotoxicity places the cancer survivors receiving the medication at immense risk and the prognosis remains poor (19–21).

### 1.3.1 Pathophysiology

Dilated cardiac chambers, reduced ventricular ejection fractions, diastolic dysfunction, changes in the ventricular wall thickness are some of the pathological occurrences associated with Doxorubicin treatment. Structural deformities such as myocardial interstitial fibrosis, vacuolated cardiomyocytes, nuclear-chromatin disorganization, distended sarcoplasmic reticulum, damaged mitochondria and increased number of autophagic vacuoles are evident as well (20,22).

### 1.3.2 Risk Factors

Age, gender, cumulative dose, genetic predispositions, and pre-existing medical history are all considered as risk factors leading to DOX induced cardiomyopathy. Nearly 48% of the patients receiving a cumulative dose of more than 700 mg/m<sup>2</sup> of DOX end up having congestive heart failure (20,21,23). More than 57% childhood cancer survivors have been reported to develop chronic cardiac complications (24). Female gender is a further risk factor in paediatric cancer patients while adult males are considered at more risk than their counterparts (25). Individuals having variants of several genes have been associated with increased risk of Anthracycline-induced toxicity as well (26). The epidemiology of DOX induced cardiomyopathy stresses the importance of clinically relevant preventive treatment strategies and hence research into elucidating the pathogenesis of DOX cardiotoxicity is important and would lead to the identification of more molecular targets for drug development (Figure 1.3).

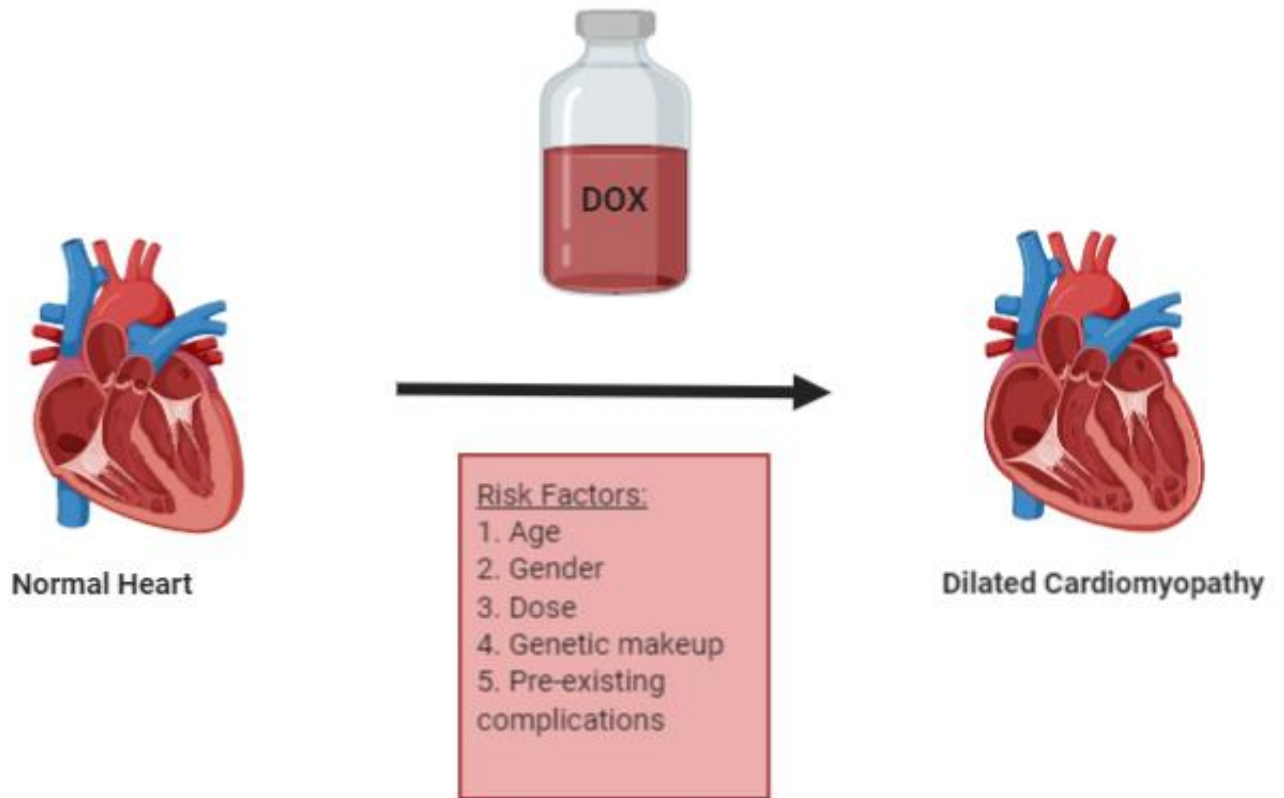


**Figure 1.3: Risk factors associated with DOX-induced cardiomyopathy.**

Incidence of DOX related toxicity and cardiomyopathy increases with age (children and aged), gender, cumulative dose ( $>700 \text{ mg/m}^2$ ), genetic make-up of the individual and pre-existing health conditions.

### 1.3.3 Mechanisms of Cardiotoxicity

Accumulation of DOX in the myocardium, coupled with the low levels of endogenous antioxidants within the heart exponentiate the potent cardiotoxic effects of the drug. DOX rapidly enters the cells by passive diffusion and accumulates in intracellular compartments. The nuclear concentration of DOX is 50-fold more than in the cytoplasm and nearly 2% of the cytosolic load is distributed among other organelles such as Golgi, lysosomes and mitochondria (11). Multiple mechanisms have been identified in the emergence and progression of DOX cardiotoxicity. Increased oxidative stress, disruption of calcium homeostasis, apoptosis activation, DNA damage and autophagic dysregulation have been implicated in the advancement of cardiac dysfunction (27).

DOX gets reduced to a semiquinone radical by cellular oxidases, Nitric oxide synthase (NOS) and nicotinamide adenine dinucleotide phosphate-oxidase (NOX), which then reacts with oxygen and generates free radicals. These radicals damage DNA and attack the membrane lipids. DOX's high affinity toward the cardiac-specific inner mitochondrial membrane lipid, cardiolipin, disrupts the electron transport chain resulting in reduced ATP production and increased mitochondrial ROS generation (28).

Cardiac muscle contractility is mediated by the excitation-contraction coupling in cardiomyocytes regulated by the entry of calcium into the cytoplasm. The intracellular calcium then induces the release of calcium from the sarcoplasmic reticulum (SR) by binding to the ryanodine receptor. This process is termed as calcium-induced calcium release (CICR) and it enables the contraction of cardiomyocytes. The uptake of calcium by the sarcoplasmic reticulum calcium transport ATPase (SERCA) decreases the cytoplasmic calcium levels and induces relaxation of cardiomyocytes. DOX-induces dysregulation of intracellular calcium levels by several mechanisms. DOX binds to the ryanodine receptor and inhibits functioning. It can also interact with luminal calcium binding proteins and the membranous SERCA pump of the SR, and modify their actions resulting in impaired calcium handling and contribute to the ROS pool (29).

The activation of the tumour suppressor p53 pathway by DOX stimulates apoptosis and NF- $\kappa$ B activation induces inflammation and cytokine storm in cardiomyocytes (30). DOX treatment also induced early stages of autophagy and suppressed the later stages resulting in the inhibition of autophagic flux and accumulation of autophagosome generating

oxidative stress in cardiomyocytes (22). The role of ROS in the progressive decline of cardiac health with DOX treatment has been well studied and documented (31). ROS mediated disruptions in nuclear, lysosomal, mitochondrial, and endoplasmic reticulum events have an evident role in the etiology of DOX cardiotoxicity (32). This study focusses on the role of dysfunctional lysosomes in facilitating cardiomyocyte death.

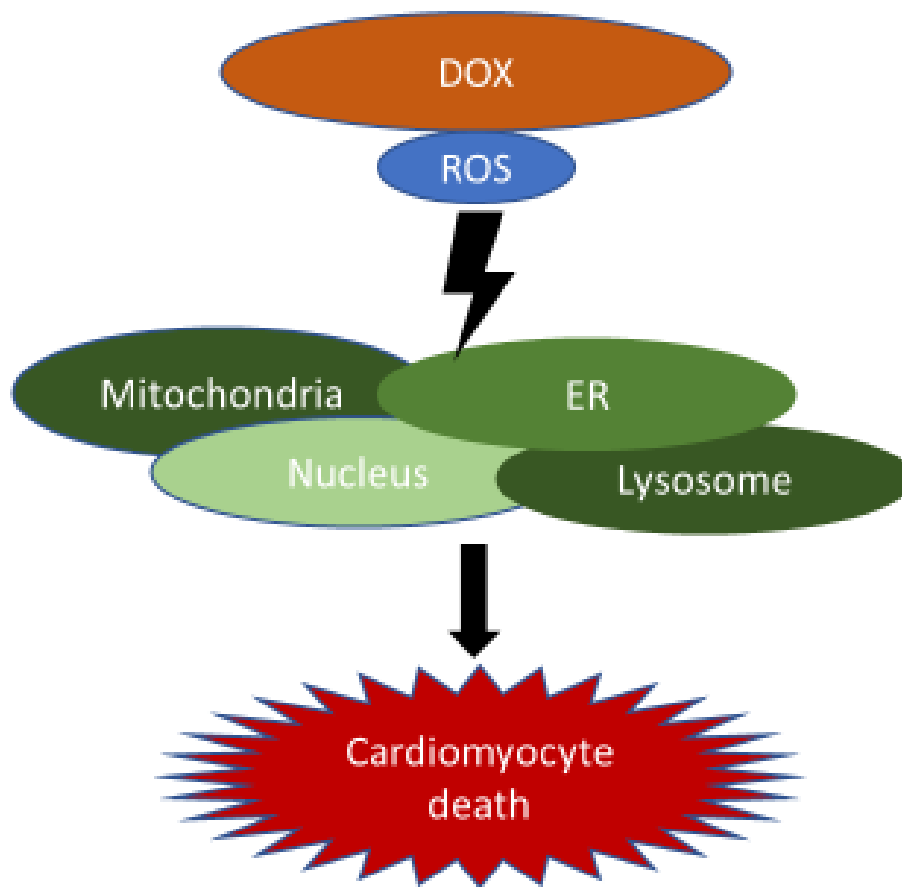


**Figure 1.4: Doxorubicin induces Cardiomyocyte cell death.** DOX-induced ROS generation coupled with low levels of antioxidants in the heart leads to oxidative stress and effects the cardiomyocyte organelles.

## 1.4 Autophagy and Cardiovascular diseases

Under normal physiological conditions, ROS generation from multiple sources contribute to the induction of autophagy and the removal and recycling of damaged organelles and defective proteins within the cell. The cellular debris is sequestered into a double membraned vesicle, the autophagosome, in the endoplasmic reticulum. The loaded autophagosome then fuses with the lysosome which subsequently leads to the degradation of the debris by the lysosomal enzymes and is then released back into the cytosol (33).

The mammalian target of rapamycin complex 1 (mTORC1) and AMP-dependent protein Kinases (AMPK) are the two signalling mechanisms implied in the control of autophagy. mTORC1 signalling cascade is involved in numerous cellular processes regulating growth, based on the nutritional and environmental intimations. Nutrient starvation, cellular stress and certain growth factors negatively regulate mTORC1 and promotes the induction of autophagy (34). Slight increases in the levels of AMP, can be detected by AMPK which in turn phosphorylates many target proteins required for energy homeostasis in the cell. AMPK mediated phosphorylation deactivates the mTORC1 complex, thereby activating the autophagic machinery. AMPK also directly initiates autophagy via mTORC1 independent pathways (35).

Both these signalling pathways are involved in the phosphorylation of the upstream component of autophagy initiation, ULK1 (UNC 51 like kinase 1) kinase complex. mTORC1 binds to ULK1 complex rendering it inactive, while AMPK phosphorylates it and promotes the downstream signalling (35–39). This serine/threonine kinase complex includes the proteins ULK1, FIP200 (focal adhesion kinase family interacting protein of size 200 kDa), ATG13 (autophagy related gene 13) and ATG101. The activated protein complex drives the single membrane phagophore formation by activating the VPS34 (vacuole protein sorting 34) complex comprised of class III phosphatidylinositol 3-kinase (PI3K), VPS34, VPS15 (vacuole protein sorting 15), BECLIN 1 and ATG14 (autophagy related gene 14) (40). Interaction among the VPS34 complex components generates phosphatidylinositol 3-phosphate (PI3P) promoting phagophore elongation and autophagosome formation. The ATG5-ATG12-ATG16L complex dimer then associates with the evolving phagophore and recruits lipidated LC3 (microtubule associated protein 1 light chain 3). Once the autophagosome development is complete, the ATG5-ATG12-ATG16L complex dissociates, leaving the LC3 intact on the luminal and exterior regions of autophagosome. LC3 is

regarded to play a role in the selective uptake of components to be degraded into the autophagosome by interacting with molecules like p62/SQSTM1. This protein is a multifunctional adaptor and binds to ubiquitinated cargos that are directed for clearance (41–44). Rab 7 (GTPase of the Ras-related protein in brain (Rab) family), SNARE complex (soluble N-ethylmaleimide sensitive fusion protein receptor) and lysosome-associated membrane proteins 1 and 2 (LAMP-1 and LAMP-2) along with other factors directs the autophagosome-lysosome fusion forming the autolysosome (45,46). The cargo loaded into the autolysosomes then undergoes degradation in the acidic lysosomal environment by the hydrolytic enzymes and the degraded products are recycled.

Impaired lysosome acidification has been implicated to be fatal in multiple cell types like neurons, hepatocytes, and cardiomyocytes (47–49). The acidic luminal pH (4.5-5) is vital for the maturation and hydrolytic activity of lysosomal enzymes and efficient lysosomal function. Even a slight increase in pH would be detrimental and could result in cell death. Lysosomes contain more than 60 degradative enzymes responsible for breaking down the unfolded proteins, damaged organelles, amino acids, and fatty acids. Myocytes being post-mitotic cells, are considered mostly irreplaceable and are vulnerable to pathological changes. Absence of replication compel these cells to rely on the recycling processes for their survival. Hence lysosomal integrity and functional autophagy are crucial for the smooth functioning of cardiomyocytes. Depressed autophagy in cardiomyocytes leads to the accumulation of the ubiquitinated intracellular cargo meant to be recycled and increases ROS production (50).

Lysosomal dysfunction has been reported in several cardiac complications. Lysosome storage disorders (LSDs) manifest as hypertrophic and dilated cardiomyopathy, coronary artery disorders, and valve defects in the heart. Dysregulations in lysosome biogenesis also contribute towards the development of cardiovascular complications (51). Transcription factor EB (TFEB) regulates the expression of lysosomal proteins and the genes involved in lysosome biogenesis. Decreased expression of TFEB has been linked to cardiac proteinopathy and cardiomyocyte death (51). DOX-induced inhibition of lysosomal acidification blocks the autophagic flux in cardiomyocytes and led to the accumulation of autolysosomes in *in vivo* mice models (52). Stimulating basal autophagy have been reported to protect cardiomyocytes from DOX-induced toxicity probably by eliminating the dysfunctional mitochondria and other organelles and hence reducing ROS production (28).



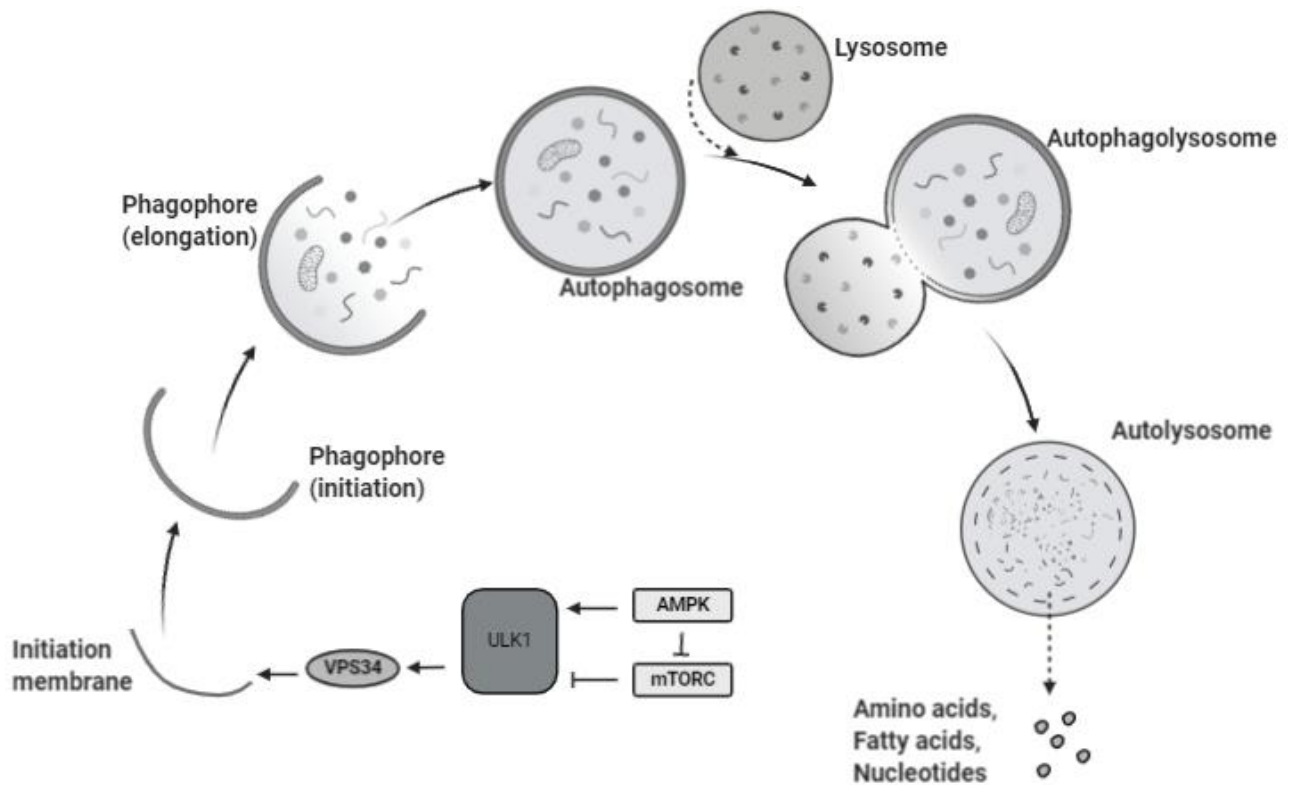


**Figure 1.5: Schematic representation of Autophagy.** Autophagy begins with the formation of an initiation membrane, which develops into a phagophore and elongates to form an autophagosome carrying the cellular debris. Lysosome fuses with the autophagosome forming the autolysosome and the proteolytic enzymes within this structure breaks down the cargo which is then released into the cytosol and recycled.

## 1.5 V-ATPase

Intracellular pH maintenance is accomplished with the help of ion channels, receptors, transporters and pumps (53). The maintenance of the acidic pH gradient in the lysosomes is achieved through the activity of vacuolar ATPase (V-ATPase), an ATP dependent membranous proton pump highly conserved among eukaryotes. It was initially identified and characterised in the yeast, *Saccharomyces cerevisiae* and is structurally similar to the bacterial ATP synthase, F-ATPase (54). Apart from acidification of lysosomes and endosomes, plasma membrane V-ATPases are also involved in other functions such as sperm maturation and bone resorption (55). It has also been associated with cellular processes such as signalling, membrane fusion, membrane trafficking, protein degradation, nutrient homeostasis etc. (56). This multimeric protein has a cytosolic domain  $V_1$  and a membrane domain  $V_0$  that undergoes reversible coupling to transport protons into the lysosomal lumen. ATP hydrolysis occurs at the subunits of  $V_1$  domain which generates the energy required for the translocation of protons through the membrane bound  $V_0$  domain subunits. In yeast, low glucose, low pH and low salt concentrations prevents the assembly of the domains as a measure to conserve ATP and prevent energy expenditure. It has also been shown that increased extracellular pH prevents glucose mediated disassembly of  $V_0$  and  $V_1$  (57). Contrastingly, in mammalian cells, low glucose and amino acid starvation has shown to increase the V-ATPase activity probably to increase the autophagic flux and recycle amino acids within the cell (58).

### 1.5.1 V-ATPase Structure

Mammalian  $V_1$  domain is water-soluble and comprised of 8 subunits A, B, C, D, E, F, G and H. The membrane embedded  $V_0$  domain subunits include a, c, c', d, e, ATP6AP1 and ATP6AP2. Three copies each of A and B subunits of the cytosolic  $V_1$  are arranged as an alternating hexamer. The D and F subunit forms the rotating central stalk (rotor) of the V-ATPase pump. The E and G subunits exist as three heterodimers forming the peripheral stalk (stator) connecting  $V_1$  to subunit a of  $V_0$ . The conformational changes of the linker protein subunit H act as switch in controlling the reversible assembly of  $V_1$ - $V_0$  and prevents ATPase

activity of the pump. The hydrophobic c ring of  $V_0$  comprises of nine copies of c and one copy of c' subunits each containing a single glutamate buried residue which undergoes reversible protonation to translocate protons into the lysosomal lumen. Subunit d links the proteolipid c ring to the rotating central stalk. The transmembrane subunit a binds to subunits H, C and the peripheral stalk in the intact V-ATPase pump. It conducts proton to the glutamate residues of the c ring and enables its exit at the luminal side via two hemi-channels facing the cytoplasmic and luminal side, respectively. Subunit e occupies an adjacent position to subunit a and is highly hydrophobic but its function in mammalian cell remains unknown. ATP6AP1 and ATP6AP2 are two transmembrane accessory proteins located within the c ring. ATP6AP1 acts as a regulatory protein and is involved in vesicular trafficking and bone resorption in osteoclasts. ATP6AP2 is a pro renin receptor and is thought to contribute to V-ATPase mediated control of the renin-angiotensin pathway in regulating blood pressure and electrolyte balance (58–60).

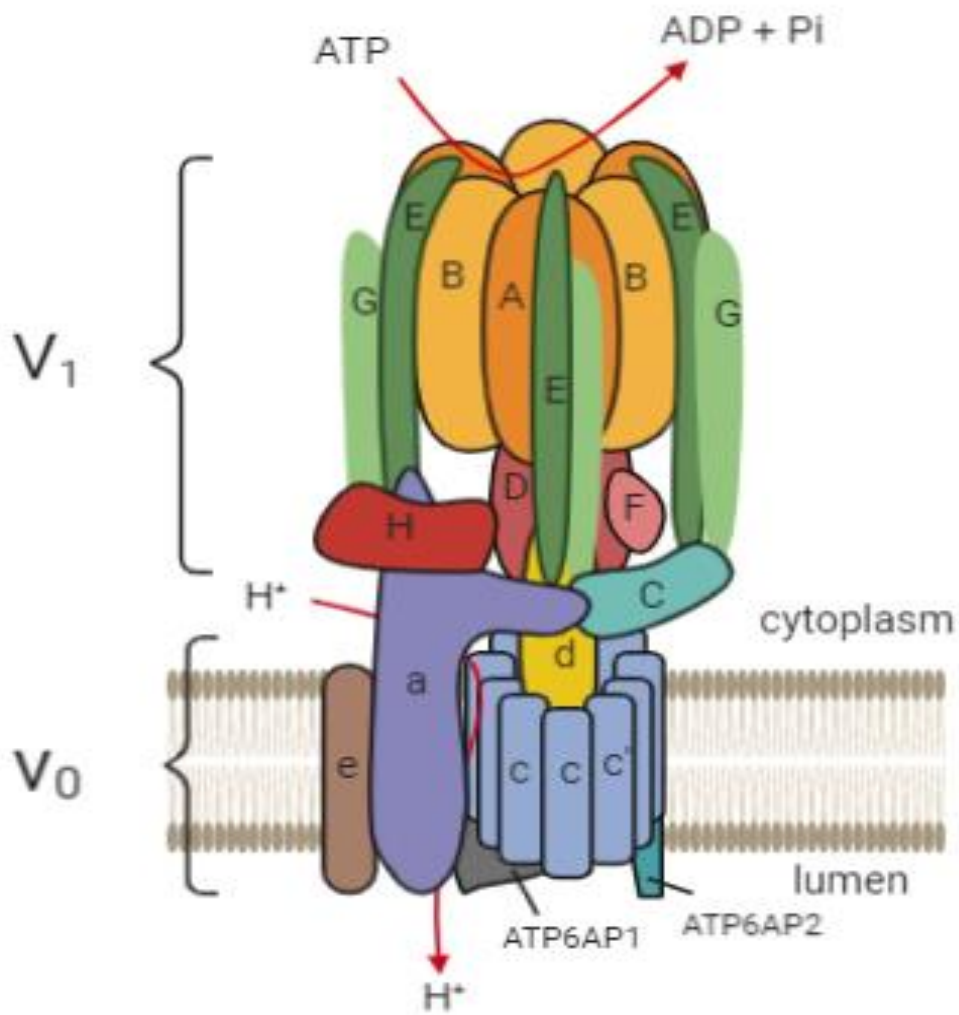


**Figure 1.6: Structure of mammalian V-ATPase.** The mammalian V-ATPase pump has a membrane-embedded V<sub>0</sub> domain and a cytosolic V<sub>1</sub> domain. V<sub>1</sub> has eight subunits (A-H) and V<sub>0</sub> contains five subunits (a, c, c', d, e). ATP6AP1 and ATP6AP2 are the accessory proteins within the c ring of V<sub>0</sub>. ATP hydrolysis at V<sub>1</sub> generates the energy for the transport of protons into the lumen by the V<sub>0</sub>.

## 1.5.2 V-ATPase Isoforms

Multiple subunit isoforms of mammalian V-ATPase have been identified and characterised. Mammalian cells express four isoforms of subunit a and two each of subunits d and e of the  $V_0$  domain. There are three isoforms of C and G of the  $V_1$  domain and two each of subunits B and E.  $V_0a$  is an integral membrane protein of ~110 kDa having a cytosolic N-terminal and 9 transmembrane domains and is the largest subunit of the  $V_0$  domain. The targeting of V-ATPase to the membrane of different cell types is achieved by this subunit. Although ubiquitous, the expression of  $V_0a1$  is high in the brain, localised mainly on the pre-synaptic membrane and synaptic vesicles and is implicated in the acidification of these vesicles. Neuronal cells and endothelium are enriched with  $V_0a2$  and it is found on the intracellular Golgi vesicles. Membranes of lysosomes, osteoclasts and secretory vesicles of pancreatic islet cells express  $V_0a3$  and this isoform is crucial mediator of the bone resorption mechanism.  $V_0a4$  is almost exclusive to the renal cells of the kidney and also found in the inner ear and epididymis (61,62).  $V_0d1$  occurs ubiquitously and  $V_0d2$  is predominantly expressed in the kidney, osteoclasts, and lungs. It is nearly 40 kDa and is considered as one of the linker proteins between the  $V_0$  and  $V_1$  domain at the central stalk of the pump. Heterologous overexpression of this subunit improves the coupling efficiency of the V-ATPase pump (63). Two isoforms of the  $V_0e$  subunits exist, e1 being ubiquitous and e2 found in the brain.  $V_1B1$  and  $V_1B2$  are of nearly 56 kDa, the former being expressed in the kidney, ear and lung and the latter being ubiquitous with enriched expression in the osteoclasts.  $V_1C$  is around 42 kDa and among its isoforms, C1 is ubiquitous. C2a and C2b are specific to lung and kidney, respectively.  $V_1E$  has a molecular weight of 31 kDa and E1 is testis specific while E2 is ubiquitous.  $V_1G$  occurs as a heterodimer with  $V_1E$  and is of 13 kDa. Among its isoforms, the ubiquitous one is  $V_1G1$ .  $V_1G2$  and  $V_1G3$  are expressed in the brain and kidney respectively (54,64).

### 1.5.3 V-ATPase proton transport mechanism

The proton transport mechanism begins with the assembly of the  $V_1$  and  $V_0$  domains. ATP hydrolysis occurs at the catalytic sites of the  $A_3B_3$  hexamer enabling the rotation of the central stalk. The proteolipid c ring attached to the central stalk rotates relative to subunit a held stationary by the peripheral stalk. Protons enter subunit a through the cytoplasmic hemi-channel and protonates the glutamate residues on the c ring which rotates and reaches the luminal hemi-channel. Deprotonation of these residues occur by interaction with a conserved arginine residue of subunit a releasing a proton to the hemi-channel facing the luminal side. For every three ATPs hydrolysed at  $V_1$  domain, ten protons are translocated to the lumen (58,60,65–68). Numerous studies have established the importance of functional V-ATPase in maintaining the autophagic flux, the measure of autophagic degradation activity in the cell. The outcomes observed with the loss of V-ATPase activity and inhibition of lysosome acidification are the formation of enlarged autolysosomes resembling yeast vacuoles mutant for peptidases (69,70).

### 1.5.4 V-ATPase Reversible assembly in mammals

Upon various stimuli such as environmental stress and nutrient depletion, cellular homeostasis must be maintained in mammals by upregulating the recycling capacity of the cells. The rate of autophagy or autophagic flux is enhanced and lysosomal degradation of ubiquitinated cellular debris is increased so that the amino acids, fatty acids, and other molecules are available back in the cytoplasm so that it can be metabolised to generate energy. Based on the requirement, the V-ATPase pump acidifies the lysosomes to achieve optimal recycling capacity. The rotation driven proton pumping mechanism of V-ATPase is tightly regulated by the reversible dissociation of the  $V_1$  and  $V_0$  domains. Though initially described in yeast, a similar mechanism applies to mammalian cells as well.

In response to glucose starvation in mammals, AMPK activity and the phosphatidylinositol 3-kinase/Protein kinase B (PI3K/Akt) signalling pathway activate the assembly of  $V_0$  and  $V_1$  domains, increasing the proton transport and re-establishing the optimal lysosomal pH. During disassembly,  $V_1C$  dissociates from the  $V_1$  domain and separates it from  $V_0$ . The structure of the C resembles a collar and a transient phosphorylation at this subunit is predicted to control its interaction with  $V_1E$ ,  $V_1G$  and  $V_0a$ .  $V_1H$  undergoes a

conformational change to inhibit the ATP hydrolysis at  $V_1$  preventing ATP expenditure and blocks the proton transport at  $V_0$ .  $V_1$ , devoid of the C subunit is found in the cytoplasm as a free water-soluble protein and  $V_0$  remains membrane bound (Figure 1.7) (58,67,71).

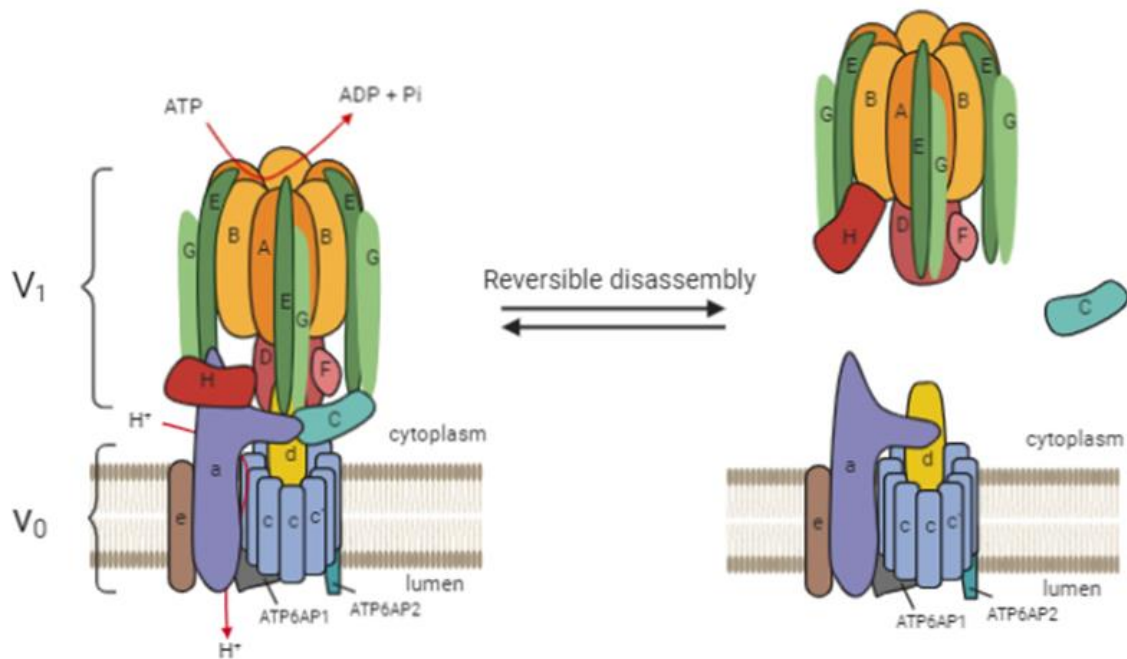


**Figure 1.7: V-ATPase activity is tightly regulated by reversible disassociation of  $V_0$  and  $V_1$  domains.** Upon nutrient depletion, subunit C detaches from cytoplasmic  $V_1$  domain, and separates it from the membrane bound  $V_0$  domain. Subunit H undergoes a conformational change and hinders ATP hydrolysis at  $V_1$  and hence conserves energy. The rotation of the stalk and proton transport at the  $V_0a$  is stalled and the V-ATPase pump becomes inactive.

### 1.5.5 V-ATPase inhibitors

Malfunctional V-ATPase activity have been reported in multiple pathological conditions conferring this ubiquitous pump the status of an attractive therapeutic target. A handful of V-ATPase inhibitors have so far been identified and are available in the market allowing researchers to further study the scope of V-ATPase modulation that could be translated to clinical settings. Bafilomycin A and concanamycin A were the first among a handful to be identified in the 1980's and was isolated from the *Streptomyces sp.* These pleco-macrolide antibiotic V-ATPase inhibitors are characterised by a 6-membered hemiacetal ring connected to the macrolactone ring by a C3 spacer. The macrolactone antibiotic archazolid also inhibits V-ATPase and is highly toxic to cells. Archazolid A has a macrocyclic lactone ring with a thiazole side chain and is produced by the myxobacteria *Archangium gephyra* and *Cystobacter violaceus*. Bafilomycin A, concanamycin A and archazolid inhibits V-ATPase by binding specifically to the subunit c of  $V_0$  (72–74).

A relatively new class of V-ATPase inhibitors were identified in the late 1990's and they shared a common benzolactone enamide structure. Salicylihalamides, lobatamides, oximidines and apicularens belonged to this group and were isolated from natural micro-organism sources. They were peculiar in their inability to inhibit V-ATPases of fungal origin. The benzolactone enamide apicularen binds to the interface of the subunits a and c of the membrane embedded  $V_0$  domain stalling the proton transport. Natural compounds of plant origin, Diphyllin and Celangulin V also inhibited V-ATPase activity *in vitro*. Though the mechanism of inhibition by Diphyllin has not been well characterised, Celangulin V binds to the subunits a, H, and B of V-ATPase (73,75–77).



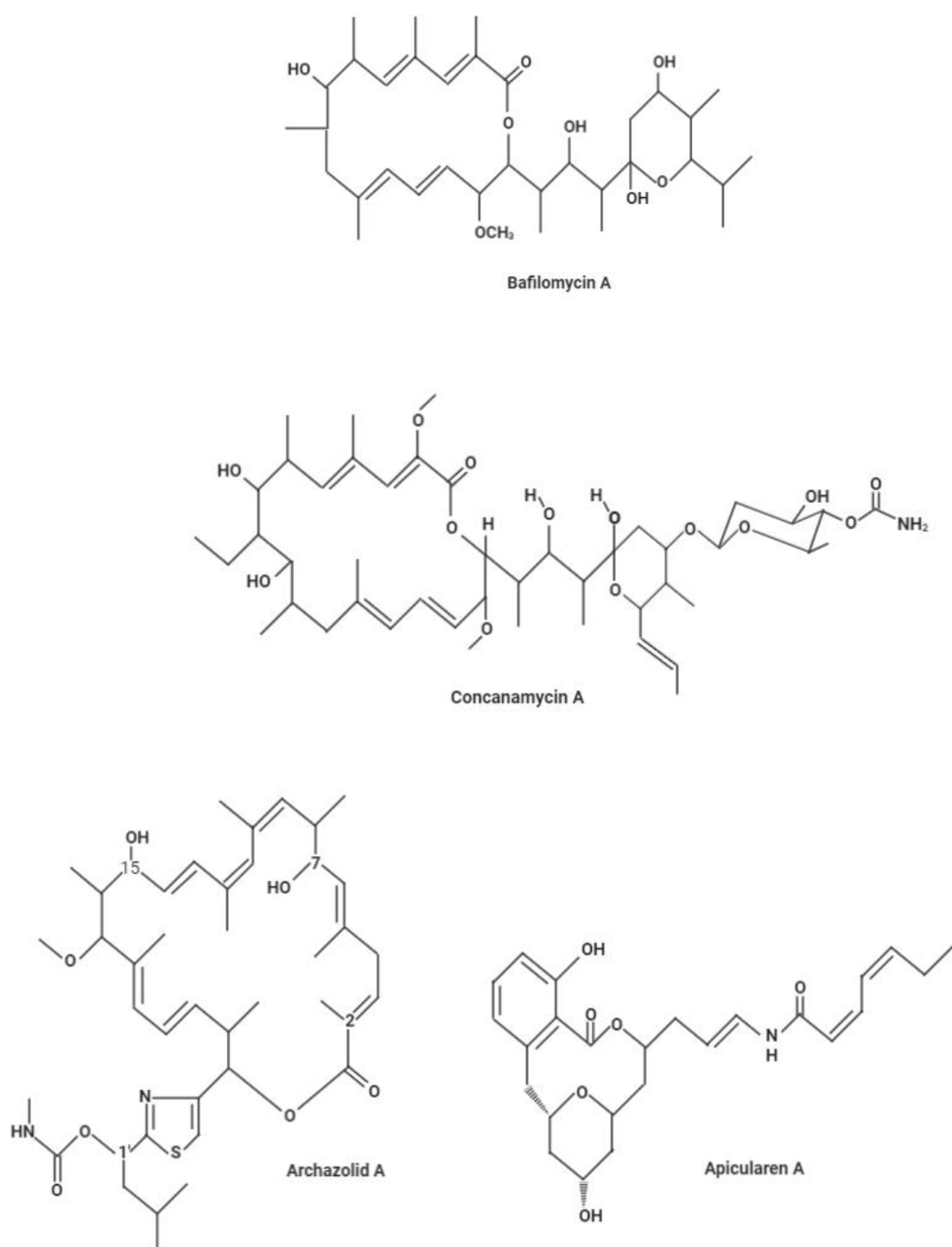


**Figure 1.8: Structures of V-ATPase inhibitors.** The V-ATPase inhibitory capabilities of Bafilomycin, Concanamycin, Archazolid and Apicularen have been characterised and are used as pharmacological tools for studying lysosome function and autophagy

## 1.5.6 Bafilomycin A

Bafilomycin A disrupts autophagy by inhibiting lysosomal acidification and autophagosome-lysosome fusion. It was quite recently reported that the Bafilomycin A inhibits the autophagosome-lysosome fusion via its effects on the  $\text{Ca}^{2+}$  transporter pumps. The proton transport mechanism of V-ATPase is blocked by this macrolide by binding to the subunit c of the  $V_0$  domain. Other ATPases such as ATP2A/SERCA are also moderately inhibited by this antibiotic (78–80). Though its clinical use is limited because of toxicity, Bafilomycin A serves as an important pharmacological tool to study autophagy.

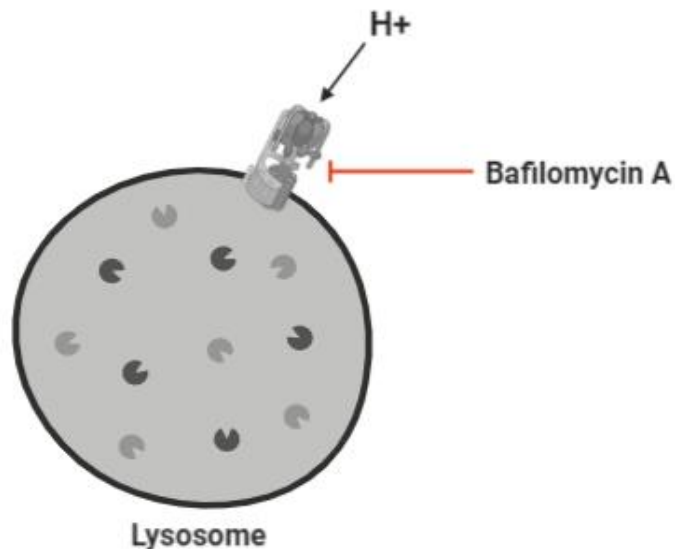


**Figure 1.9: Bafilomycin A inhibits the proton transport mechanism of V-ATPase.**

Bafilomycin A inhibits V-ATPase pump and prevents lysosome acidification and stalls the autophagic machinery in cells.

### 1.5.7 V-ATPase activity in the heart

Decreased V-ATPase activity have been linked to contractile dysfunction in cardiomyocytes. Excessive lipid accumulation impairs the endosomal pump activity and leads to cardiac insulin resistance in rodents and human cardiomyocytes. It is speculated that lipids induce V-ATPase disassembly into  $V_0$  and  $V_1$  and migration of  $V_1$  into the cytoplasm. In response, the long chain fatty acid transporter CD36 in the heart, stimulated by insulin, translocates to sarcolemma from endosomes leading to further increase in up-take and storage of triacylglycerols and elicit insulin resistance (49). Proper regulation of endosomal pH is necessary for directed translocation of glucose transporters (GLUT) in the heart as well. Restoring V-ATPase activity has been hence considered as a promising strategy to combat lipid-induced cardiomyopathy (81).

High-density lipoproteins (HDL) are generally considered as the “good” cholesterol as it aids in reverse cholesterol transport from the tissues to the liver for elimination. The anti-atherogenic property of HDL is mainly attributed to its major component Apolipoprotein A1 (ApoA1). ApoA1 accepts the cell cholesterol with the help of the cell membrane protein ATP-binding cassette A1 (ABCA1) and generates nascent HDL. Activation of ApoA1 occurs when it's lipidated causing the N-terminal to unfold and spontaneously react with the membrane lipids and release nascent HDL from the cell. ABCA1 mediated recruitment of V-ATPase to the cell surface promotes acidification increasing the membrane lipid fluidity and N-terminal unfolding of ApoA1. Thus V-ATPase modulation helps in HDL biogenesis and cholesterol efflux and provides protection from coronary heart disease (82). DOX treatment has been reported to disrupt the basal autophagic flux by inhibiting the lysosomal V-ATPase activity and decreased cardiomyocyte cell survival. Increased lysosomal pH in cardiomyocytes led to the accumulation of autolysosomes and exacerbated oxidative stress (83),(52). Though DOX mediated inhibition of lysosomal acidification has been proved in cardiomyocyte lysosomes, the exact mechanism of V-ATPase modulation remains unclear.

## 1.6 Nicotinamide Adenine Dinucleotide (NAD<sup>+</sup>)

NAD<sup>+</sup> is a major coenzyme present within all living cells and is involved in various essential cellular processes. It was discovered in boiled yeast extracts more than a century ago by Sir Arthur Harden. NAD<sup>+</sup>, its phosphorylated form NADP, and reduced forms NADH and NADPH, are important cofactors in the energy producing and metabolic processes within the cell (84). NAD<sup>+</sup> pools within the mammalian cell occur in the cytosol, nucleus, mitochondria, endoplasmic reticulum and Golgi network (85). NAD<sup>+</sup> consuming enzymes in the cell are sirtuins, poly ADP-ribose polymerases (PARPs) and CD38/157 ectoenzymes. Seven mammalian sirtuins have been identified till date and they are involved in many cellular pathways. These proteins are evolutionarily conserved and belong to class III protein deacetylase family, which are the only histone deacetylases requiring NAD<sup>+</sup> for their activity. Sirtuins cleave NAD<sup>+</sup> forming nicotinamide (NAM) and the acetyl group of the substrate protein is transferred to the ADP-ribose moiety of NAD<sup>+</sup> producing O-acetyl-ADP-ribose and the deacetylated substrate (86). The PARP family of proteins are involved in poly-ADP ribosylation i.e., the transfer of ADP-ribose to target proteins. Members of this family are involved in many vital cellular processes such as DNA synthesis and repair, nucleic acid metabolism and chromatin structure modulation (87). CD38 and CD157 are considered as ectoenzymes, a family of enzymes having an extracellular catalytically active site. These proteins catalyse the conversion of NAD<sup>+</sup> to cyclic ADP-ribose, an important secondary messenger in calcium signalling. They are mainly expressed in immune cells and are also involved in cell adhesion and migration (88).

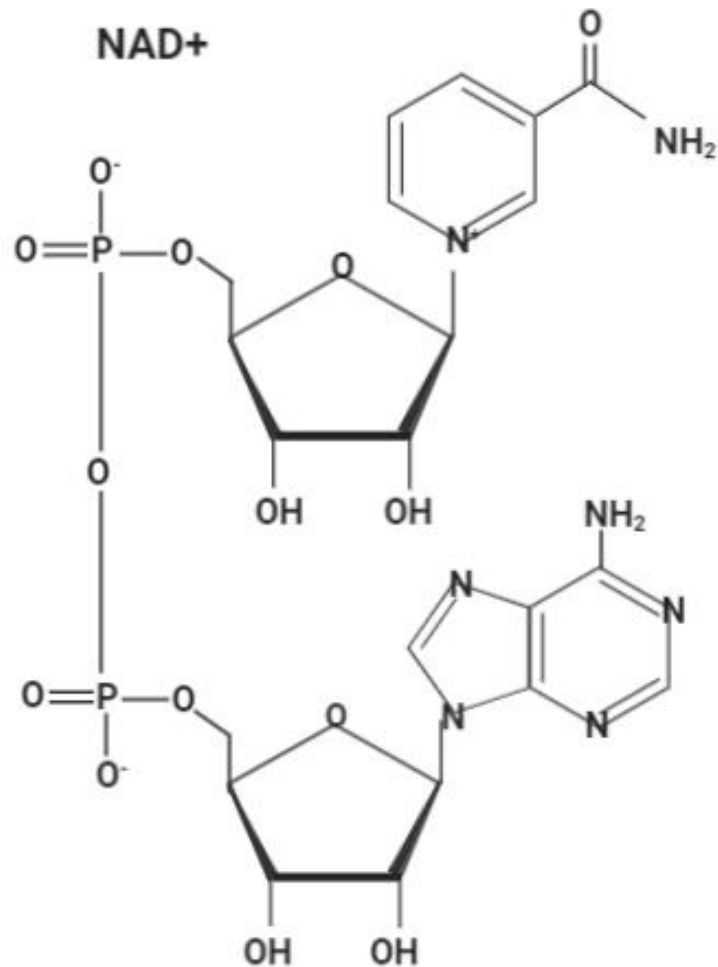


**Figure 1 10: Structure of NAD<sup>+</sup>.**

### 1.6.1 NAD<sup>+</sup> Biosynthesis

The major precursors and intermediates involved in the biosynthesis of NAD<sup>+</sup> are tryptophan, nicotinamide, nicotinic acid, nicotinamide riboside and nicotinamide mononucleotide. These are obtained either from the diet or by the intracellular NAD<sup>+</sup> catabolism. The Preiss-Handler pathway utilizes the enzyme Nicotinic acid phosphoribosyltransferase (NaPRT) to convert dietary Nicotinic acid or Vitamin B3 to NaMN (Nicotinic acid mononucleotide). NaMN/NMN adenylyltransferases (NMNATs) converts NaMN to nicotinic acid dinucleotide (NAAD). NAD<sup>+</sup> is amidated from NAAD by

NAD<sup>+</sup> synthetase enzyme (NADS). The *de novo* pathway involves the essential amino acid tryptophan which is metabolised to Quinolinic acid (QA) via the kynurenine pathway in the liver. It is then converted to NaMN by Quinolinic acid phosphoribosyltransferase (QAPRT) and then to NAD<sup>+</sup> using the Preiss-Handler pathway. The contribution of the *de novo* pathway towards NAD<sup>+</sup> pool in mammals is negligible as tryptophan metabolism contributes to other cellular processes as well. Mammalian NAD<sup>+</sup> synthesis occurs mainly via the salvage pathway involving the conversion of Nicotinamide (NAM), produced from NAD<sup>+</sup> consuming reactions, to Nicotinamide mononucleotide (NMN) by the rate-limiting enzyme Nicotinamide phosphoribosyltransferase (NAMPT). NAM is the by-product of NAD<sup>+</sup> breakdown by sirtuins, PARPs and CD38/157 ectoenzymes. NAMPT is also activated by AMPK, the autophagy stimulating kinase in cells. Nicotinamide Riboside (NR), a Vitamin B3 derivative, also contributes to the NMN pool by Nicotinamide riboside kinase (NRK) mediated enzymatic phosphorylation. Two isoforms of NRK have been discovered, the ubiquitously expressed NRK1 and the skeletal muscle specific NRK2. NMN is then converted to NAD<sup>+</sup> by NMNAT. Three isoforms of NMNAT have been identified so far and they differ in their sub-cellular location and catalytic actions. The ubiquitously expressed NMNAT1 is predominantly found in the nucleus. NMNAT2 is mostly brain-specific and localised in the cytosol and Golgi compartments. NMNAT3 is mitochondrial specific, found in liver, heart, skeletal muscle and also in red blood cells (84,89–92).

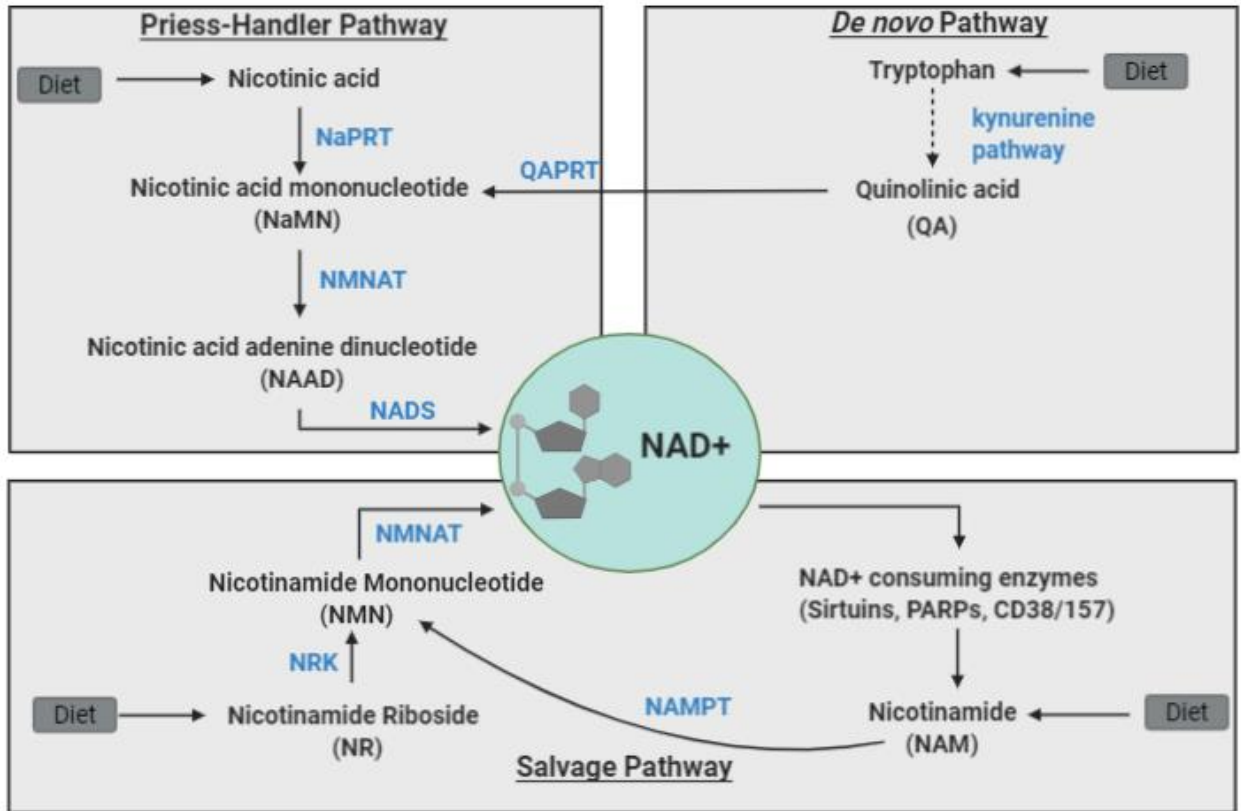


**Figure 1.11: Schematic illustration of NAD<sup>+</sup> biosynthesis in mammalian cells.**

NaPRT- Nicotinic acid phosphoribosyltransferase; NMNAT- NaMN/NMN adenylyltransferases; NADS- NAD<sup>+</sup> synthetase; QAPRT- Quinolinic acid phosphoribosyltransferase; NRK- Nicotinamide riboside kinase; NAMPT- Nicotinamide phosphoribosyltransferase (rate-limiting enzyme) (93).

## 1.6.2 NAD<sup>+</sup> in the heart

The half-life of NAD<sup>+</sup> in mammalian cells is around 10 hours with mitochondrial NAD<sup>+</sup> accounting for nearly 70-75% of the total cellular content in heart cells (84). This is in consistence with the high energy demands of the heart. The levels of the Nicotinic acid converting enzyme NaPRT is low in heart and hence Nicotinamide mediated NAD<sup>+</sup> biosynthesis is thought to be the predominant source of the co-enzyme. NAD<sup>+</sup> depletion has been reported in multiple pathologies associated with the heart. Supplementing NAD<sup>+</sup> has been reported to protect the heart in *in vivo* models of heart failure. Restoring NAD<sup>+</sup> levels in the ischemic and hypertrophic heart prevents disease progression and decreases the risk of heart failure (94). Despite the promising therapeutic effect of NAD<sup>+</sup> upregulation in the heart, the protective mechanism in various cardiovascular pathologies remains largely unanswered. Protein hyperacetylation in failing myocardial cells was attributed to the unavailability of NAD<sup>+</sup> for sirtuin-mediated deacetylation. Altered energy metabolism and decreased NAD<sup>+</sup> biosynthesis was also observed in models of failing heart. NAD<sup>+</sup> precursors reduced the protein acetylation, restored the energy metabolism and increased the synthesis of NAD<sup>+</sup> in the heart thereby preventing further damage to the organ (95).

The delicate balance between NAD<sup>+</sup> synthesis and consumption in the cells are altered during pathological conditions. NAD<sup>+</sup> levels in the cell increase during energy-limiting conditions such as fasting, calorific restriction, low glucose diets or exercise. High fat and high glucose diets as well as oxidative stress deplete NAD<sup>+</sup> levels in the cell and affect downstream cellular processes (94). Boosting NAD<sup>+</sup> levels has been reported to ameliorate multiple pathological conditions such as diabetes, cardiovascular diseases, neuropathies and age-related cellular dysfunction (96). NAD<sup>+</sup> inhibition also blocks autophagic flux (97) and so maintaining the balance between the consumption and synthesis is essential for cellular integrity.

## 1.6.3 Role of NAD<sup>+</sup> in Autophagy

Autophagy plays a central role in maintaining cellular homeostasis particularly in post-mitotic cells like cardiomyocytes. NAD<sup>+</sup> is essential for sustaining the basal autophagic machinery in these cells (98). NAD<sup>+</sup> is reduced to NADH to facilitate cellular ATP



generation through glycolysis in the cytosol, and via the tricarboxylic acid cycle in the mitochondria. Imbalances in the NAD<sup>+</sup>/NADH ratio affect ATP generation and activate the AMPK pathway and autophagy. NAD<sup>+</sup> can be phosphorylated to NADP<sup>+</sup> and then get converted to NADPH which catalyses the formation of the antioxidant glutathione. Reduction in glutathione levels upsets the redox balance in the cell and activates AMPK. NAD<sup>+</sup> depletion and ROS can impair the autophagic machinery by influencing post-translational modifications of autophagy-related proteins. During pathological conditions, PARPs and the CD38/157 ectoenzymes are hyperactivated, and consume the intracellular NAD<sup>+</sup> pools leading to its depletion. PARPs consume nearly 10 - 20% of NAD<sup>+</sup> within minutes of DNA damage. Sirtuin activity is hence reduced and so are the deacetylation processes which are of crucial significance in the regulation of autophagy-related proteins, transcription factors and receptors. Acetylation of transcription factor EB (TFEB), the master regulator of lysosome biogenesis, has been linked to its inability to bind to DNA and negative regulation of lysosomal genes. Though acetylation and deacetylation related functional regulation of multiple other autophagic proteins such as ULK1 and ATG 3,7,5 and 12 have also been identified, the list does not tend to be exhaustive. PARP activation also inhibits mitochondrial ATP synthesis by inactivating sirtuins and induces autophagy by activating the AMPK pathway (85,99).

#### 1.6.4 Nicotinamide mononucleotide (NMN)

Nicotinamide mononucleotide (NMN) or Nicotinamide-1-ium-1-β-D-ribofuranoside 5'-phosphate is an intermediate in the NAD<sup>+</sup> biosynthesis pathway and it is formed by the reaction between nicotinamide (NAM), a phosphate group and a nucleoside containing a ribose moiety. NMN is also formed from NR by enzymatic phosphorylation (Figure 1.11). It has a molecular weight of 334.221 g/mol and exists as two anomers, alpha and beta, the latter being the active form (100). Being a Vitamin B3 derivative, NMN is naturally found abundantly in vegetables like cabbage, broccoli, and cucumbers and in fruits like avocados and tomatoes. The amount of NMN in various food sources has been summarised in Table 2 (101). NMN absorption from food sources begins in the gut within 2-3 minutes where it undergoes dephosphorylation by CD73 to NR and enters the cells with the aid of nucleoside transporters. In the cells, NR is converted back to NMN to synthesize NAD<sup>+</sup>. Recently, a specific NMN transporter has also been identified in cells, encoded by the gene *Slc12a8* that

is highly expressed in the small intestine. Knocking down this gene using lentiviruses in mice significantly reduced the plasma availability of NMN compared to the control. The Slc12a8 NMN transporter has a molecular weight of nearly 90 kDa and is sodium ion dependent (100,102).

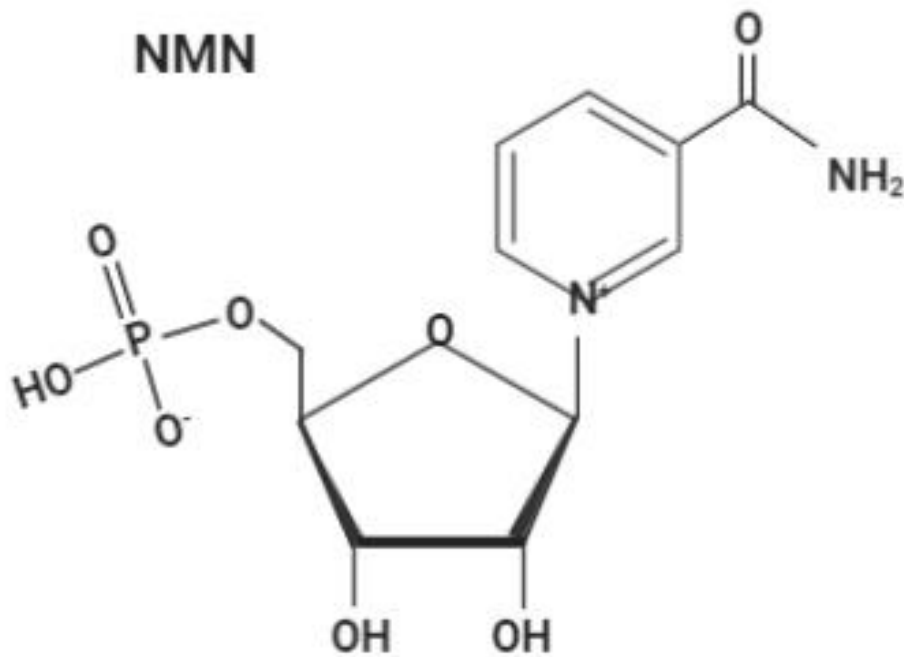


**Figure 1.12: Structure of  $\beta$ -NMN.** Nicotinamide mononucleotide has a phosphate group, Nicotinamide base and ribose sugar

NMN enhanced NAD<sup>+</sup> levels and reversed impaired glucose tolerance and improved insulin sensitivity in rodent models of obesity and diabetes (103,104). NMN administration also prevented ischemic-reperfusion injury in the heart and cerebrum mediated by the sirtuin pathway (105,106). NMN supplementation has been successful in ameliorating alcoholic liver disease, acute kidney injury, retinal degeneration, cerebral haemorrhage and cognitive impairment in animal models (107). Mitochondrial protein hyperacetylation has been implicated as a causative factor in heart failure. Elevation in the NADH/NAD<sup>+</sup> ratio induces mitochondrial protein hyperacetylation and increases the sensitivity of the mitochondrial

permeability transition pore. NMN reverses hyperacetylation and normalizes the NAD<sup>+</sup> redox balance in the heart (108). It also improved cardiac function and bioenergetics in a sirtuin dependent manner in rodent models of cardiomyopathy and so NMN has been evaluated as a potential drug in the treatment of cardiac dysfunctions (109).

**Table 2: Natural sources of NMN**

<u>Source</u>	<u>mg/100 g</u>
Broccoli	0.25 - 1.12
Cabbage	0.0 - 0.90
Avocado	0.36 - 1.60
Cucumber	0.56 - 0.65
Tomato	0.26 - 0.30
Mushroom	0.0 - 1.01
Raw beef	0.06 - 0.42
Shrimp	0.22

## 1.7 Rationale

Autophagic stimulation improves cardiac function by recycling the misfolded and dysfunctional proteins (110). Post-mitotic cells like cardiomyocytes rely highly on the lysosomal recycling mechanisms as they cannot simply be discarded when non-functional, owing to their limited potential to divide (111). Maintaining the autophagic flux in cardiomyocytes is hence beneficial to promote the longevity and functioning of these cells.

Stress triggers autophagic flux in cells to sustain the metabolic demand and organelle biosynthesis (112). Increased NAD<sup>+</sup> synthesis maintains autophagic flux by activating sirtuin deacetylases (97). Sirtuins are implicated in aging, metabolism, and stress. The most extensively studied mammalian sirtuin, SIRT1, has been linked to transcriptional regulation and DNA repair as well (113). The deacetylase activity of sirtuins are attributed to their catalytic pocket having a conserved zinc tetra-thiolate motif (114). SIRT1 inhibition suppresses autophagy in cardiomyocytes and NAD<sup>+</sup> enhances SIRT1 in the nucleus modulating the transcription of proteins regulating autophagy (115). SIRT1 expression is downregulated with DOX treatment and overexpressing this protein attenuates cardiac dysfunction (116). Our lab has previously reported that the NAD<sup>+</sup> precursor, Nicotinamide Riboside (NR) prevented DOX induced accumulation of autolysosomes in mouse hearts and cultured cardiomyocytes by maintaining lysosomal acidification via NAD<sup>+</sup>/Sirt1 signalling (117). It is probable that the maintenance of autophagic flux by sirtuins in cardiomyocytes could be at least to some extent, attributed to the maintenance of lysosomal activity. Up-regulation of the mitochondrial sirtuins has been demonstrated to accelerate the impaired mitophagy by deacetylating the F0-F1 ATPase proton pump in mitochondria (118,119). F0-F1 ATPase and the lysosomal V-ATPase are closely related in terms of structure and function and could have evolved from a common ancestor (120).

Our lab has identified hyperacetylation of the d1 sub-unit of V<sub>0</sub> domain (ATP6V0d1) in response to DOX treatment. It could be speculated that the protective role of NAD<sup>+</sup> up-regulation in DOX-induced cardiotoxicity could be in part via the deacetylation of the V-ATPase pump subunits. NAD<sup>+</sup> precursors like NMN are easily soluble and orally bioavailable and so have been widely researched on rodent models and have entered clinical trials as well (121). This study determines the potential and mechanism of NAD<sup>+</sup> and its precursor, NMN, in preventing DOX-induced changes in lysosomal acidification and hence cardiotoxicity in an *in-vitro* model.

## 1.8 Hypothesis

I hypothesize that

- A) Doxorubicin increases lysosomal pH in H9c2 cells and induces cardiotoxicity.
- B) Boosting NAD<sup>+</sup> using NMN will prevent DOX-induced increases in lysosomal pH and protect H9c2 cells from DOX toxicity.

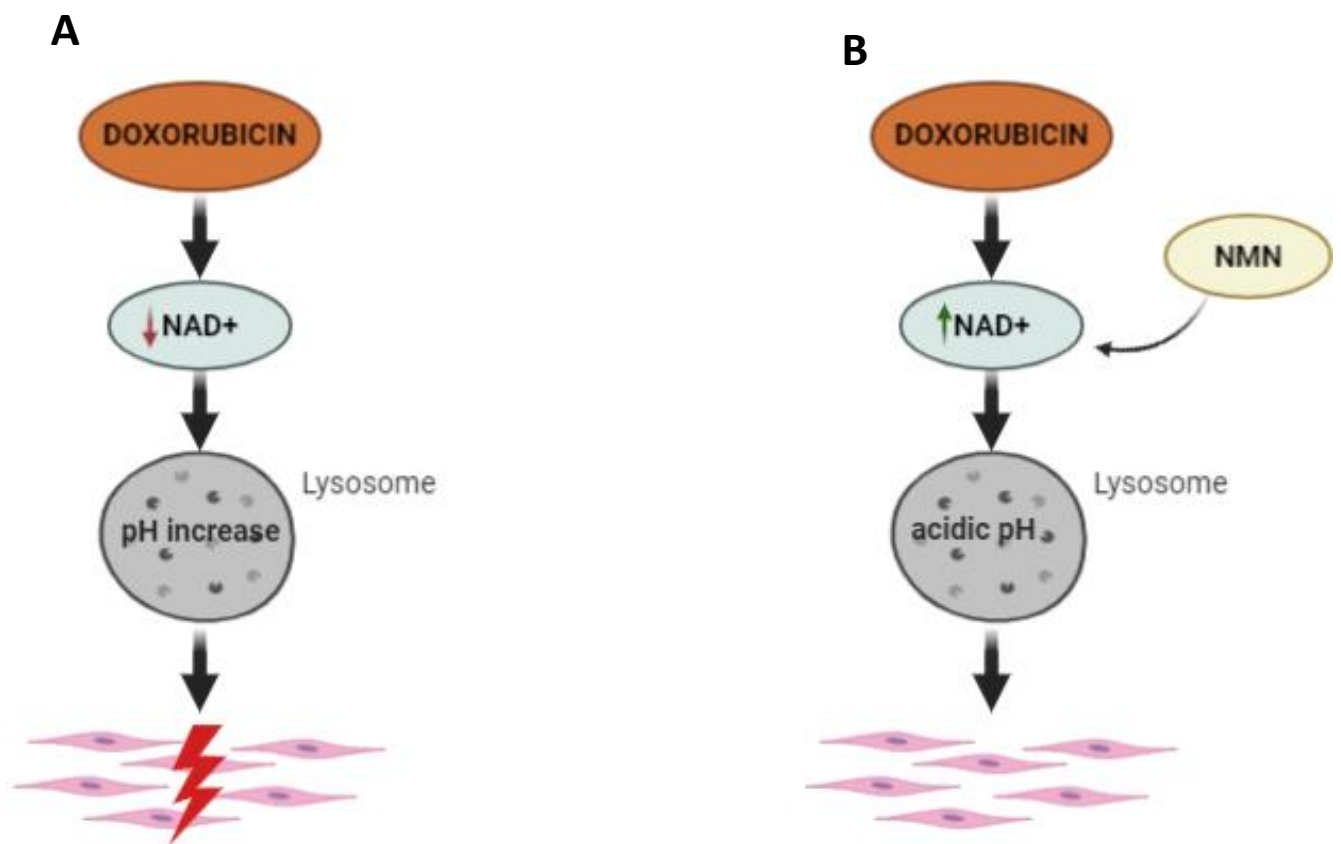


**Figure 1.13:** *Schematic illustration of Hypothesis.* A) DOX treatment inhibits lysosomal acidification in H9c2 cells by depleting NAD<sup>+</sup> levels and induce cardiotoxicity. B) Boosting NAD<sup>+</sup> using NMN maintains the acidic lysosomal pH and protects H9c2 cells from DOX-induced toxicity.

## 1.9 Specific Aims

1. Determine dose-dependent effect of DOX on H9c2 cells.
2. Determine the effect of DOX on the lysosomal pH of H9c2 cells.
3. Analyse the potential of NMN in preventing DOX- induced toxicity in H9c2 cells.
4. Determine the mechanism by which NMN prevents DOX-induced increases in lysosomal pH.

## Chapter 2

### 2 Materials and Methods

#### 2.1 H9c2 cell culture

H9c2 (2-1) (CRL-1446) cells were procured from American Type Culture Collection (ATCC). Cells up to passage 15 were used for this study. The cells were grown in a culture flask incubated at 37°C in a 5% CO<sub>2</sub> humidified air atmosphere. The growth media used was high Dulbecco's Modified Eagle's Medium (DMEM), supplemented with 10% heat-inactivated fetal bovine serum (FBS), penicillin 100 IU/mL, and streptomycin 10 µg/mL. Sub-culturing was done every three days when confluency of 70-80% was attained. Briefly, the media in the flask was discarded and the cells were washed once with D-Hank's solution (Table 3). The cells were then incubated with 0.25% Trypsin at 37°C for 1-2 minutes. Fresh growth media containing 10% FBS was added to the flask to terminate the trypsinization process, and then cells were centrifuged at 125 x g for 5 minutes. The trypsin containing media was discarded and cells were suspended in fresh growth media and re-plated.

**Table 3: D-Hank's Solution (1L)**

KCl	0.4 g
KH <sub>2</sub> PO <sub>4</sub>	0.06 g
NaCl	8 g
D-Glucose	1 g
Phenol red	0.012 g

## 2.2 Isolation and culture of neonatal cardiomyocytes

Primary neonatal cardiomyocytes were isolated from neonatal mice born within 24 hours. Neonatal mice were wiped with 75% alcohol and then killed by decapitation. The chest was cut open at the sternum and the hearts were harvested into D-Hank's solution (Table 1) in a 50 mL tube. The hearts were rinsed in D-Hank's solution twice to remove the blood. Each heart was then divided into 5–6 pieces using a surgical blade and then rinsed again in D-Hank's solution. It was then subjected to the following 3 rounds of digestion;

(1) Heart sections were incubated in Liberase Blendzyme (2.5 mg/mL, Roche Applied Science) for 10 minutes at 37°C in a water bath and the supernatant was discarded.

(2) The sections were again incubated in fresh Liberase Blendzyme solution at 37°C for 15 min with gentle swirling every 5 min. After 15 min, the heart sections were minced to isolate the cardiomyocytes completely. The supernatant containing isolated cardiomyocytes was collected and the digestion was terminated by adding the culture medium, DMEM, supplemented with 10% new-born calf serum (NBCS).

(3) The precipitate was again incubated with fresh Liberase Blendzyme and the digestion procedure was repeated.

The supernatant was then pooled with the earlier one and centrifuged at 200 x g for 5 minutes. The precipitate containing the isolated cardiomyocytes were resuspended in 10% NBCS supplemented DMEM. The cells were then seeded in a culture plate and placed in a CO<sub>2</sub> incubator at 37°C for 120 minutes which allowed fibroblasts to adhere to the plate. After fibroblast adherence, cardiomyocytes were collected and counted. The cardiomyocytes were then seeded into a culture plate, coated with 1% gelatin and incubated in a CO<sub>2</sub> incubator at 37°C. The cardiomyocytes were utilized for experiments after 18 hours. The purity of neonatal cardiomyocytes was characterized by the staining for troponin and was more than 95%.



## 2.3 Doxorubicin Cardiotoxicity- *in vitro* experimental model

H9c2 is an adherent cell line derived from the subclone of the ventricular part of the embryonic BD1X heart tissue of *Rattus norvegicus* and exhibits skeletal and cardiac muscle properties. It is a cell model used as an alternative for cardiomyocytes (122). H9c2 cells and neonatal cardiomyocytes were seeded in multi-welled culture plates at densities required for the assays and incubated at 37°C in a 5% CO<sub>2</sub> humidified air atmosphere. When desired confluency was attained (12-18 hours), cells were treated with NMN or NAD<sup>+</sup> for 24 hours followed by DOX/Bafilomycin A/DOX-Bafilomycin A treatment for further 24 hours. Control cells were supplemented with fresh growth media and were devoid of any treatment throughout the duration of experiment.



**Figure 2.1: Schematic representation of the *in vitro* model used for study.**

## 2.4 CCK-8 Assay

Cell counting kit-8 (CCK-8) (Dojindo Molecular Technologies, Inc), a colorimetric assay, was used to determine the cell viability. The water-soluble tetrazolium salt, WST-8, is reduced by the dehydrogenases in living cells to a yellow colour formazan dye which is measured at an absorbance of 450 nm. H9c2 cells were seeded in a 96-well plate at a density of 10,000 cells per well. After treatment with various drugs, 10 µL of CCK-8 solution, provided by the manufacturer, was added to each well. The plate was incubated at 37°C for

1-4 hours. The absorbance was measured at 450 nm using iMark™ Microplate Absorbance Reader (Bio-Rad Laboratories Inc). The intensity of the yellow dye is directly proportional to the number of living cells. Percentages of viable cells were calculated using the formula:

$$\text{Cell viability \%} = \frac{\text{Abs}_{450} \text{ sample} - \text{Abs}_{450} \text{ blank}}{\text{Abs}_{450} \text{ control} - \text{Abs}_{450} \text{ blank}} \times 100$$

## 2.5 Lactate Dehydrogenase Release Assay

Lactate Dehydrogenase (LDH) is soluble enzyme released from cells due to compromised cell membrane integrity. LDH enzymatically converts iodonitrotetrazolium to a red coloured formazan dye which can be detected using a colorimetric assay at an absorbance of 490 nm. The amount of LDH release is directly proportional to cell damage. LDH-Cytotoxicity Colorimetric Assay Kit (Takara Bio Inc) was used to detect the activity of LDH released from H9c2 cells following treatment. The supernatant was collected in clear optical 96-well microtiter plates and incubated for 30 minutes at room temperature with the reaction mixture containing catalyst and dye solution provided by the manufacturer. The reaction was stopped using 1N HCl and the absorbance was measured at 490 nm using iMark™ Microplate Absorbance Reader (Bio-Rad Laboratories Inc).

## 2.6 Caspase-3 Activity

Caspase-3 belongs to the family of Cysteine-aspartic acid proteases and activation of the enzyme is required for apoptotic cell death. Activated caspase-3 in cell lysates cleaves the peptide substrate acetyl-Asp-Glu-Val-Asp-7-amido-4-methylcoumarin (Ac-DEVD-AMC) and releases fluorescent 7-amino-4-methylcoumarin (AMC) which can be detected at excitation and emission wavelengths of 360 and 460 nm, respectively. Caspase-3 activity in H9c2 cells was determined using the following protocol. Briefly, the cells were lysed using ice-cold lysis buffer (Table 4) and the cell lysates were centrifuged at 10,000 x g for 10 min at 4 °C. The supernatant was collected, and the protein concentration was measured using DC protein assay based on manufacturer's protocol (Bio-Rad Laboratories Inc). 100µg protein was incubated with caspase-3 substrate Ac-DEVD-AMC and Ac-DEVD-AMC in the

presence of inhibitor AC-DEVD-CHO diluted in assay buffer (Table 4) at 37°C for 2 hours. Caspase-3 cleaves the substrate Ac-DEVD-AMC and releases chromophore AMC which can be detected by a fluorescence spectrophotometer with excitation of 355 nm and emission of 460 nm.

**Table 4: Lysis/Assay Buffer (100mL)**

Reagent	Lysis Buffer	Assay buffer
HEPES (1 M, pH=7.4)	5 mL	5 mL
CHAPS	0.1 g	0.1 g
NaCl	-	585 mg
DTT (1 M)	500 $\mu$ L	1 mL
EDTA (0.5 M)	20 $\mu$ L	200 $\mu$ L
NP-40	100 $\mu$ L	-
Glycerol	-	10 mL
H <sub>2</sub> O	94.4 mL	83.8 mL

## 2.7 Lysosomal pH measurement

Changes in lysosomal pH were measured using LysoSensor yellow/blue DND-160 (Invitrogen). This dye imparts yellow fluorescence in acidic environments and blue fluorescence in neutral pH in living cells. The ratio of emission at 460 and 535 nm was used to interpret the pH. H9c2 cells were seeded in 96-well black clear bottom sterile plates at a density of 5000 cells per well. After treatment, the cells were incubated with the dye (1  $\mu$ M) for 5 minutes at 37°C. The fluorescent signals were determined using a Spectra Max M5 Multi Mode Microplate Reader with excitation of 340 nm. The ratio of emission, 460/535 nm, was then calculated for each sample.

## 2.8 Co-immunoprecipitation (co-IP) and Western Blot Analysis

Co-immunoprecipitation was done to pull down the acetylated proteins from neonatal cardiomyocytes following DOX and NMN treatments. Cells were lysed using the lysis buffer (Table 4) and disrupted by ultrasonication and centrifuged at 10,000 x g for 10 minutes at 4°C. Protein was quantified using DC protein assay (Bio-Rad Laboratories Inc) and 400 µg of protein was subjected to immunoprecipitation. Briefly, Anti-acetyl Lysine antibody (abcam) was used to pull down the proteins using Dynabeads™ Protein G Immunoprecipitation Kit (Invitrogen) following the manufacturer's instructions. The protein was then eluted from the beads using the elution buffer supplied in the kit and subjected to SDS- polyacrylamide gel electrophoresis followed by western blot analysis.

The immunoprecipitated protein was mixed with 6X loading buffer (Table 5) in a microtube and incubated at 70°C for 10 minutes on a dry bath for denaturing. The protein was then subjected to sodium dodecyl sulphate-polyacrylamide gel electrophoresis (SDS-PAGE) using a 4% stacking gel (Table 6) and 12% resolving gel (Table 7) using a BIO-RAD Mini-PROTEAN system. 30 µL of proteins were added to the wells of the gel and resolved at 100V with in-house running buffer (Table 8) till the running front reached the end of the gel.

**Table 5: 6X Loading Buffer (100 mL)**

Tris-HCl (1M, pH 6.8)	37.5 mL
SDS	6 g
Bromophenol blue	30 mg
Glycerol	48 mL
β-Mercaptoethanol	9 mL
H <sub>2</sub> O	5.5 mL

**Table 6: 4% Stacking gel (6 mL)**

H <sub>2</sub> O	4.10 mL
30% Acrylamide	1 mL
Tris (1.5M, pH 6.8)	0.75 mL
10% SDS	60 µL
10% Ammonium Persulphate	60 µL
TEMED	6 µL

**Table 7: 12% Resolving Gel (20mL)**

H <sub>2</sub> O	4.10 mL
30% Acrylamide	8 mL
Tris (1.5M, pH 8.8)	7.5 mL
10% SDS	200 µL
10% Ammonium Persulphate	200 µL
TEMED	8 µL

**Table 8: Running Buffer pH 8.3 (1L)**

Tris Base	3.03 g
Glycine	14.41 g
SDS	1 g
H <sub>2</sub> O	1 L
β-Mercaptoethanol	9 mL

The proteins were then transferred from the gel on to a poly vinyl difluoride (PVDF) membrane (Froggabio) by tank blotting in ice-cold transfer buffer (Table 9) at 25 V for 15 hours using the Bio-Rad Mini Trans-Blot electrophoretic transfer cell. The membrane was then blocked using 5% non-fat milk (Bio-Basic) in TBST (Table 10) at room temperature for 1 hour. After blocking, the membrane was incubated overnight at 4°C with primary antibody at manufacturer recommended dilution dissolved in 5% BSA. The membrane was then washed 3 times with TBST for 10 minutes each followed by incubation with secondary antibody dissolved in 5% non-fat milk in TBST for 1 hour at room temperature. After washing the membrane again 3 times for 10 minutes each in TBST, the proteins on the membrane were visualised using a chemiluminescence detection system using enhanced chemiluminescence reagent (Table 11).

**Table 9: Transfer Buffer (1L)**

Tris base	3.03 g
Glycine	14.41 g
Methanol	200 mL
H <sub>2</sub> O	800 mL

**Table 10: TBST pH 7.6 (1L)**

Tris base	2.42 g
NaCl	8 g
H <sub>2</sub> O	1000 mL
Tween 20	1 mL

**Table 11: Enhanced Chemiluminescence (ECL) Reagent (200mL)**

Component	Reagent A	Reagent B
Tris-HCl (1M, pH 8.5)	100 mL	100 mL
Coumaric acid (90 mM)	440 $\mu$ L	-
Luminol (250mM)	1 mL	-
H <sub>2</sub> O <sub>2</sub>	-	60 $\mu$ L

## 2.9 Statistical Analysis

Statistical Analysis was done using Graphpad Prism software version 6.0. All data were presented as mean  $\pm$  standard deviation (SD). One-way analysis of variance (ANOVA) was used for analysing the results. Post-hoc comparisons were done using Tukey HSD or Dunnett's Test as appropriate. A value of  $P < 0.05$  was considered statistically significant. The test used for each experiment has been mentioned in the figure legend.

**Table 12: Reagent Information**

<u>Reagent</u>	<u>Manufacturer</u>	<u>Cat #</u>
DMEM	Gibco, USA	11995-065
DMEM	Wisent Inc, Canada	319010CL
HI FBS	Gibco, USA	12484-028
Penicillin-Streptomycin	Gibco, USA	15140-122
Trypsin-EDTA	Gibco, USA	25200-056
Liberase Blendzyme	Roche Applied Science, Switzerland	05401151001
NBCS	Gibco, USA	26010-074
Gelatin	Sigma, USA	G9382
Triton X-100	Sigma, USA	T9284
NaOH	VWR, USA	BDH7222-1
Tris	Bio Basic, Canada	TB0196
HCl	Sigma, USA	HX0603-4
KCl	Sigma, USA	PX1405-1
KH <sub>2</sub> PO <sub>4</sub>	Bio Basic, Canada	PB0445
NaCl	Bio Basic, Canada	DB0483
D-Glucose	Bio Basic, Canada	GB0219
Phenol red	Sigma, USA	P5530
SDS	Sigma, USA	L3771
Bromophenol Blue	Sigma, USA	20017
Glycerol	Sigma, USA	G5516
β-Mercaptoethanol	Sigma, USA	444203



Acrylamide	Bio Basic, Canada	AB1032
APS	Bio Basic, Canada	AB0072
TEMED	Bio Basic, Canada	TB 0508
Glycine	Bio Basic, Canada	GB0235
Methanol	VWR, USA	BDH1135-4LP
Coumaric acid	Sigma, USA	C9008
Luminol	Sigma, USA	A8511
HEPES	Bio Basic, Canada)	HB0264
CHAPS	Bio Basic, Canada)	CD0110
DTT	Bio Basic, Canada	DB0058
NP-40 Sigma	Sigma, USA	13021
Na <sub>2</sub> HPO <sub>4</sub>	Sigma, USA	S0876
β-NMN	Apex Bio, USA	B7878
NAD <sup>+</sup> , free acid	Calbiochem, Japan	481911
Bafilomycin A	Apex Bio, USA	A8627
Doxorubicin Hydrochloride	Mylan, USA	67457-436-50
EDTA	Sigma, USA	E5134

**Table 13: Antibody Information**

<u>Antibody</u>	<u>Manufacturer</u>	<u>Cat#</u>	<u>Dilution</u>
Anti-ATP6V0D1	Abcam, USA	ab202897	1:1000
Anti-Acetyl Lysine	Abcam, USA	ab22550	1:1000
Anti-GAPDH	Santa Cruz Biotechnology, USA	sc-25778	1:1000

## Chapter 3

### 3 Results

#### 3.1 DOX induces dose-dependent toxicity in H9c2 cells

The toxic effects of DOX on H9c2 cells have been reported from our lab and authors elsewhere (117,123,124). Dose-dependent toxicity along with increased oxidative stress and autophagic flux impairment have been confirmed by these authors. To confirm the toxic effect of DOX on H9c2 cell viability and to determine the dose for further experiments, cells were seeded in 96-well sterile plates at a density of 1000 cells per well. After 24 hours, the cells were treated with DOX at concentrations of 0.5, 1, 2 and 5  $\mu\text{M}$ . Control cells were left untreated. About ~75% of cells were found to be viable with 0.5  $\mu\text{M}$  DOX. 1  $\mu\text{M}$  DOX reduced the number of viable cells by nearly 50%. Less than 30% cells survived with 2 and 5  $\mu\text{M}$  DOX treatment for 24 hours. As shown in Figure 3.1, DOX reduces cell viability in a dose-dependent manner. As mentioned earlier, DOX has high affinity towards mitochondria in cardiomyocytes and 0.5- 1  $\mu\text{M}$  has been considered as clinically relevant plasma concentrations where the mitochondrial accumulation is around 50 -100  $\mu\text{M}$  (125).

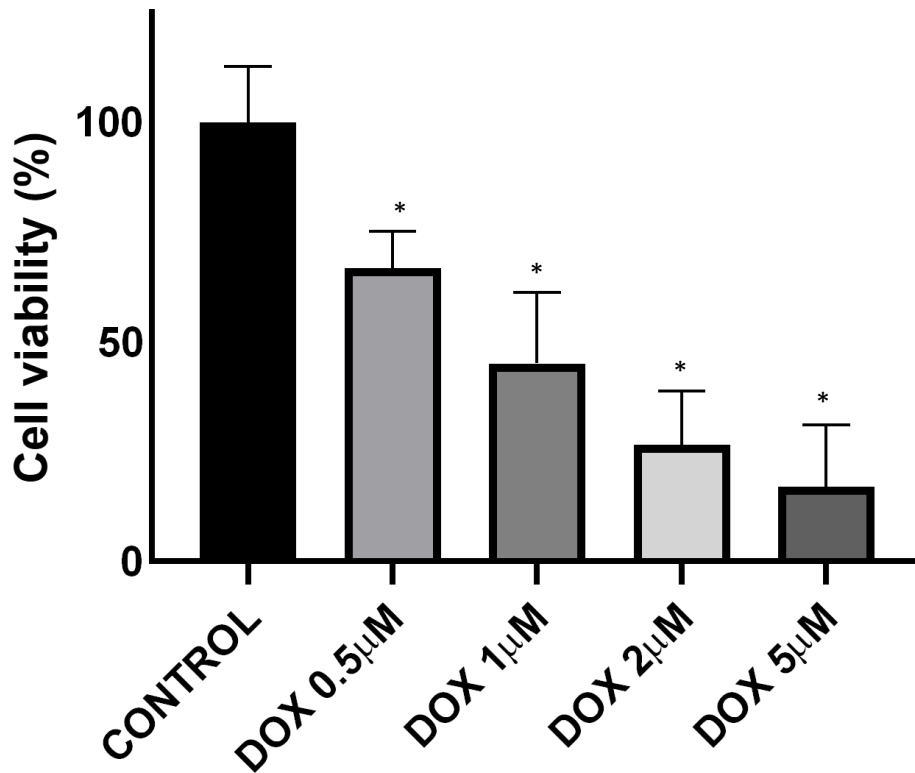


**Figure 3.1: DOX treatment decreased H9c2 cell viability in a concentration-dependent manner.** H9c2 cells were cultured in 96-well plates for 24 hours. The cells were then incubated with DOX at concentrations of 0.5, 1, 2 and 5  $\mu$ M or left untreated for another 24 hours. Cell viability was assessed using CCK-8 method. One-way ANOVA analysis followed by Dunnett's test was used to compare groups (n= 3 independent experiments) (\*P<0.05 versus control)

## 3.2 DOX increases LDH release in H9c2 cells

LDH is a stable cytoplasmic enzyme released into the cell culture medium upon plasma membrane damage. H9c2 cells were seeded in 24-well plates and incubated for 24 hours. The growth media was replaced with DOX containing culture media at concentrations of 1, 2 and 5  $\mu\text{M}$  and incubated for another 24 hours. Control cells were left untreated. The media containing LDH was collected and incubated with an equal volume of reaction mix containing the catalyst and dye solution from the LDH-Cytotoxicity Colorimetric Assay Kit (BioVision Incorporated). The LDH enzyme in the media oxidizes the lactate component of the catalyst to pyruvate which in turn reacts with the tetrazolium salt of the dye solution forming a red coloured formazan dye. This water-soluble formazan dye was detected by a spectrophotometer at 490nm which correlates with the LDH activity in the cells. DOX at all the three concentrations increased the LDH activity by around 0.3-fold to 0.5-fold as seen in Figure 3.2. The LDH release in cells treated with 1 and 2  $\mu\text{M}$  DOX were almost the same and 5  $\mu\text{M}$  DOX showed a slightly higher increase in the enzyme activity compared to the lower concentrations.

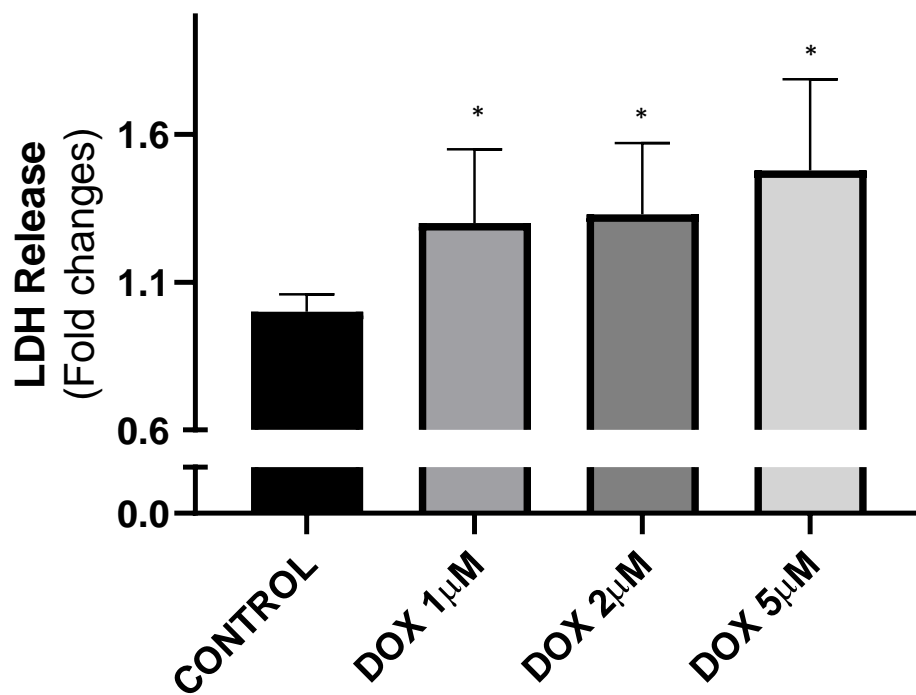


**Figure 3.2: DOX treatment increased the LDH release in H9c2 cells.** H9c2 cells were treated with DOX at concentrations of 1, 2 and 5  $\mu$ M for 24 hours or left untreated. LDH release was measured. One-way ANOVA analysis followed by Dunnett's test was used to compare groups (n= 3 independent experiments) (\*P<0.05 versus control)

### 3.3 DOX treatment increases caspase-3 activity in H9c2 cells

Caspase-3 activation could lead to breakdown of myofibrillar proteins and contractile dysfunction even before cell death in cardiomyocytes (126). H9c2 cells were seeded in 24-well plates at a density of  $1 \times 10^5$  cells per well and incubated for 24 hours. The culture media was replaced with DOX containing culture media at concentrations of 1 and 2  $\mu\text{M}$  and incubated further for 24 hours. Control cells were left untreated. Caspase -3 activity was assessed in the cells. DOX treatment at 1 and 2  $\mu\text{M}$  increased the caspase-3 activity in H9c2 cells by more than 6-fold and 7.5-fold, respectively (Figure 3.3).

Since the moderate injury for H9c2 cells was with 1 $\mu\text{M}$  DOX, when cell viability declined about 50% and caspase 3 activity and LDH release significantly increased, this dose was used to treat H9c2 cells in the subsequent experiments to generate the *in vitro* doxorubicin-induced toxicity model. Further, DOX treatment at 1  $\mu\text{M}$  for 24 hours has been shown to induce autophagic impairment in cardiomyocytes resulting in the accumulation of ubiquitinated proteins as well (127).

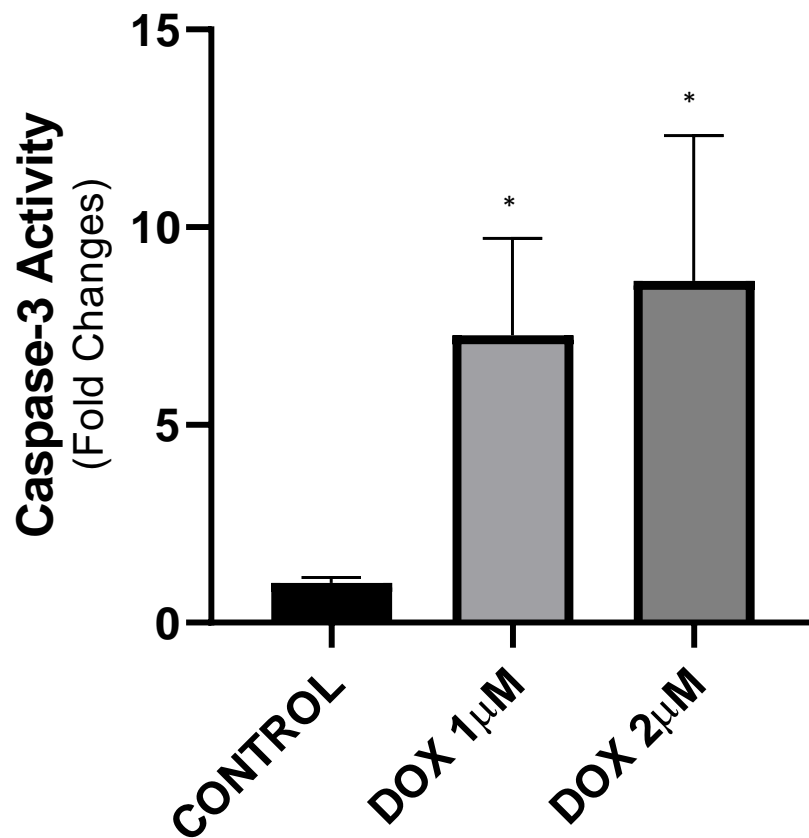
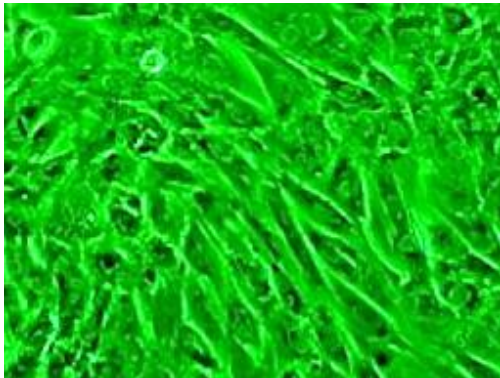


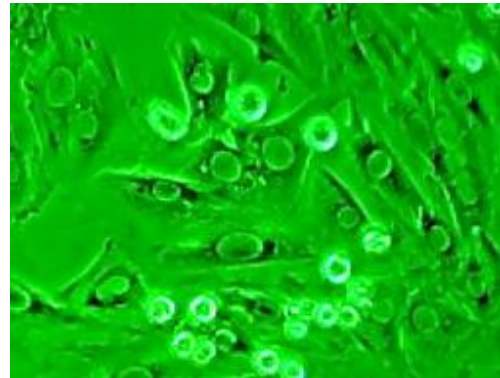
**Figure 3.3: DOX treatment increased the caspase-3 activity in H9c2 cells.** H9c2 cells were incubated with DOX at concentrations of 1 and 2 µM for 24 hours. Control cells were left untreated. One-way ANOVA analysis followed by Dunnett's post hoc test was used to compare groups (n=3 independent experiments) (\*P<0.05 versus control)

### 3.31 DOX induces morphological alterations in H9c2 cells

Normal H9c2 cells are spindle-to stellate-shaped and can be mono- or multi-nucleated (128). H9c2 cells were incubated with 1  $\mu$ M DOX for 24 hours and the morphological changes were examined. Changes in the structure of H9c2 cells were observed along with cytoplasm vacuolation (Figure 3.4).



**Control**



**DOX (1  $\mu$ M)**

**Figure 3.31: DOX induces morphological alteration in H9c2 cells.** H9C2 cells were treated with 1  $\mu$ M DOX for 24 hours. The morphological changes were examined.



### 3.4 DOX treatment prevents lysosomal acidification in H9c2 cells

Efficient lysosomal functioning is enabled with the support of over 60 hydrolytic enzymes within the organelle. These enzymes require an acidic pH of 4.5-5 for the enzymatic breakdown of the cellular debris within the lysosomes. The proton pump V-ATPase pumps  $H^+$  ions into the lysosomal lumen and maintains the pH within the organelle. Lysosomal abnormalities involving dysfunctional hydrolytic enzymes have been implicated in multiple cardiovascular disorders (51). H9c2 cells were incubated with 1  $\mu$ M DOX and 100 nM Bafilomycin A (BafA) for 24 hours. The control cells were untreated. The changes in lysosomal pH were measured using LysoSensor yellow/blue DND-160 (Invitrogen). This ratiometric dye has dual excitation and emission characteristics and this property was exploited for investigating the lysosomal pH as described in the methods section. Bafilomycin A was employed as a positive control for the experiment. It is a potent V-ATPase inhibitor and impairs autophagy by preventing lysosomal acidification. DOX altered the lysosomal pH of H9c2 cells compared to the control (Figure 3.4). The changes in lysosomal pH in response to DOX treatment were similar to the changes in Bafilomycin A treated cells.

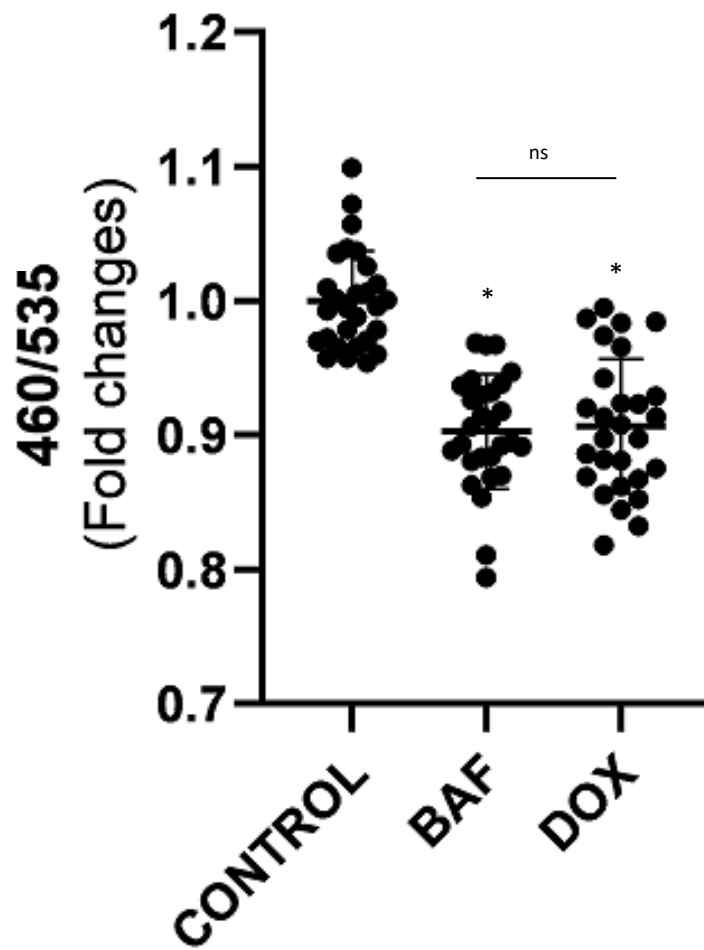


**Figure 3.4: DOX treatment altered the lysosomal pH by preventing acidification in H9c2 cells.** H9c2 cells were treated with DOX (1  $\mu$ M) and Bafilomycin A (BAF) (100 nM) for 24 hours. Control cells were left untreated. The lysosomal pH was determined based on 460/535 ratio. One-way ANOVA analysis followed by Tukey post hoc test was used to compare groups (n= 10) (\*P<0.05 versus control; ns-not significant)

### 3.5 NAD<sup>+</sup> and its precursor NMN prevents DOX-induced toxicity in H9c2 cells

Declined NAD<sup>+</sup> levels are observed in the heart of rodent models of dilated cardiomyopathy in which NAD<sup>+</sup> precursor supplementation improves cardiac function by stabilizing the myocardial NAD<sup>+</sup> levels (129). Systemic NMN administration has been reported to up-regulate the NAD<sup>+</sup> levels in the pancreas, heart, skeletal muscle and liver of rodents under pathological conditions (92). DOX treatment reduces the NAD<sup>+</sup> content in cardiomyocytes. Previous work from our lab has also shown that pre-incubation with NAD<sup>+</sup> precursors enhances the NAD<sup>+</sup> levels in DOX-treated cardiomyocytes (117). Based on our experiments in the lab and literature review, 1mM concentration of NMN and NAD<sup>+</sup> was used for assessing the protection imparted by these drugs in the *in vitro* model of DOX-induced cardiotoxicity (130).

#### 3.5.1 NMN and NAD<sup>+</sup> prevents DOX-induced increases in LDH release

H9c2 cells were pre-incubated with NMN/NAD<sup>+</sup> (1 mM) for 24 hours prior to DOX (1 μM) treatment. Cells were also treated with NMN/NAD<sup>+</sup> alone and control cells were untreated. LDH release was examined in the cells as it is a major index of cell injury. NMN and NAD<sup>+</sup> pre-incubation prevented DOX-induced increases in LDH release by nearly 0.4-fold and 0.5-fold, respectively. NMN and NAD<sup>+</sup> alone did not show much effect on H9c2 cells compared to the control (Figure 3.5a and 3.5b).

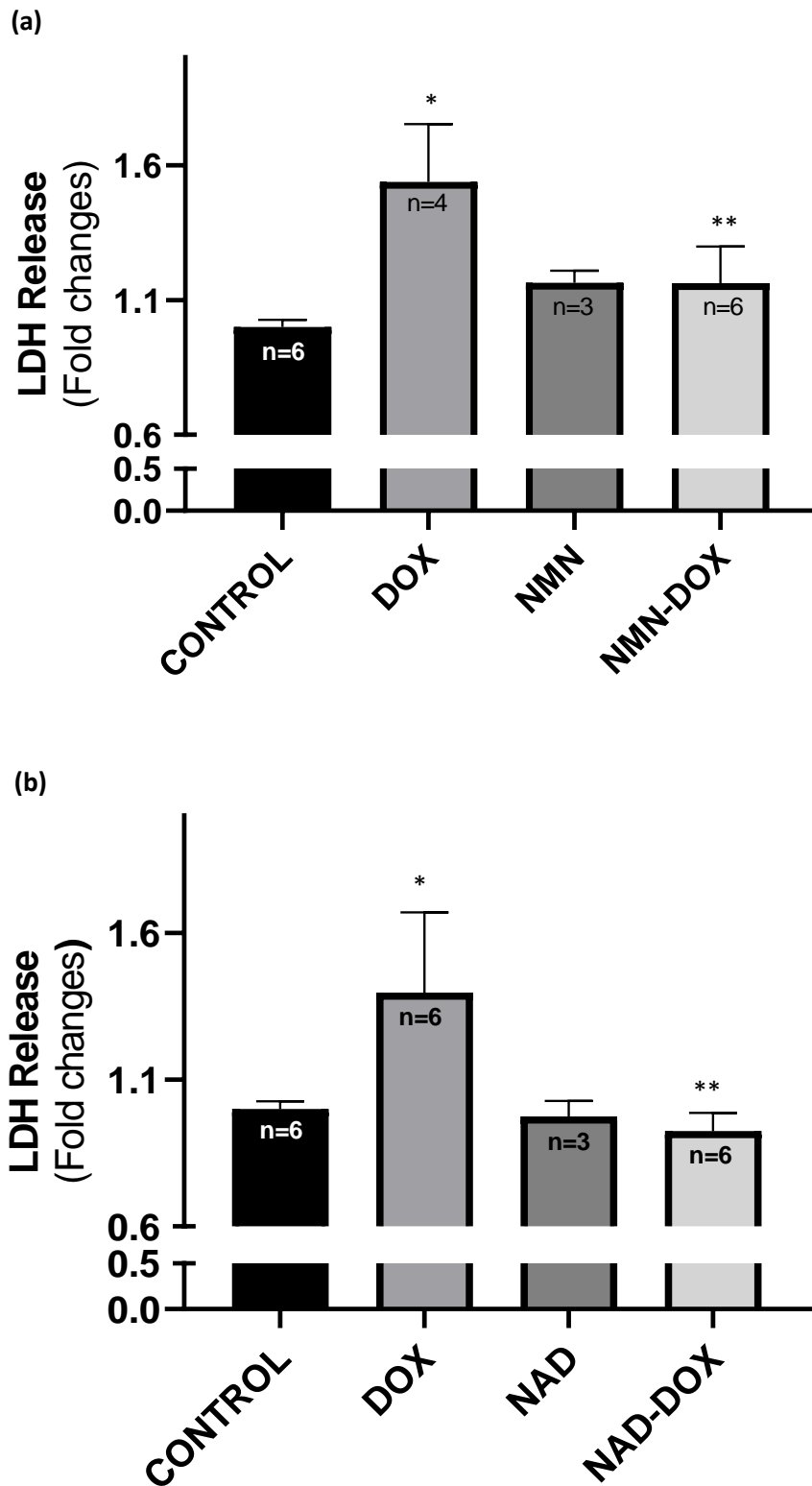


**Figure 3.5: LDH release in (a) DOX, NMN and NMN-DOX treated and (b) DOX, NAD and NAD-DOX treated H9c2 cells. One-way ANOVA analysis followed by Tukey post hoc test was used to compare groups (\* $P < 0.05$  versus control; \*\* $P < 0.05$  versus DOX)**

### 3.5.2 NMN and NAD<sup>+</sup> prevents DOX-induced increase in caspase-3 activity

It has been observed that DOX treatment increases the caspase-3 activity in H9c2 cells. Here, caspase-3 activity was measured in H9c2 cells treated with NMN or NAD<sup>+</sup> prior to DOX treatment. Compared to the DOX-treated group, NMN/NAD<sup>+</sup> pre-incubation prior to DOX, significantly reduced the caspase-3 activity (Figure 3.6 and 3.7).

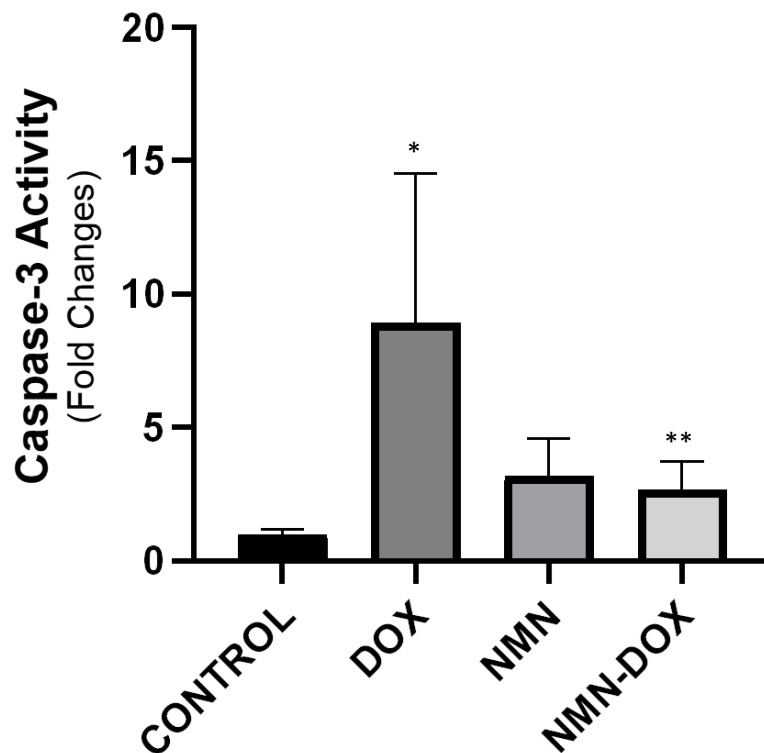


**Figure 3.6: NMN prevents DOX-induced increases in caspase-3 activity in H9c2 cells.**

Caspase -3 activity in DOX, NMN and NMN-DOX treated H9c2 cells. One-way ANOVA analysis followed by Tukey post hoc test was used to compare groups (n=5) (\*P<0.05 versus control; \*\*P<0.05 versus DOX)

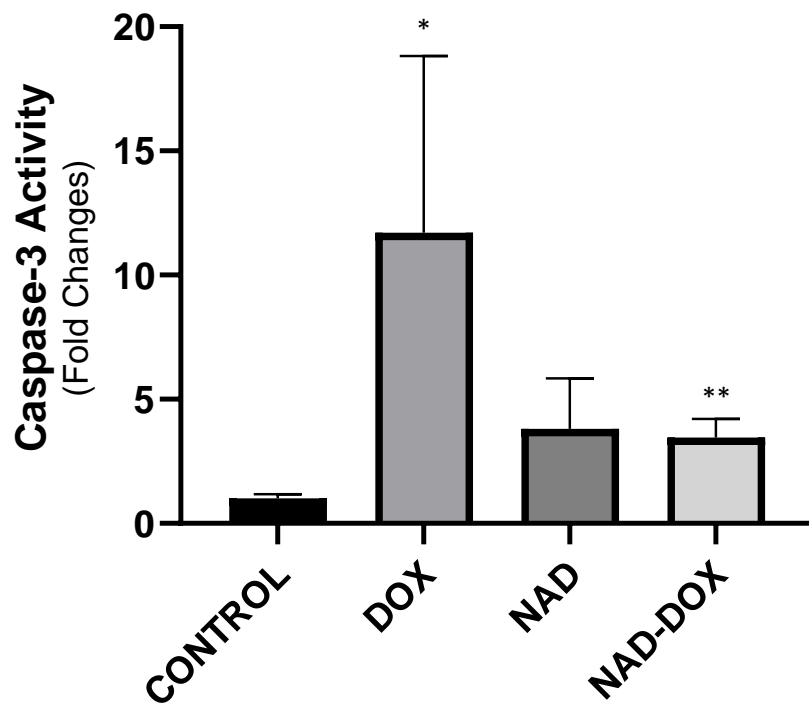


**Figure 3.7: NAD<sup>+</sup> prevents DOX-induced increases in caspase-3 activity in H9c2 cells.**

Caspase-3 activity in DOX, NAD and NAD-DOX treated H9c2 cells. One-way ANOVA analysis followed by Tukey post hoc test was used to compare groups (n=5) (\*P<0.05 versus control; \*\*P<0.05 versus DOX).

### 3.5.3 NMN and NAD<sup>+</sup> increases the viability of DOX-treated H9c2 cells

NAD<sup>+</sup> enhancement attenuated DOX-induced decrease in cell viability. There was nearly 50-80% increase in the number of viable cells after NMN/NAD<sup>+</sup> pre-incubation prior to DOX treatment compared to the cells treated with DOX alone (Figure 3.8 and 3.9). Upregulating NAD<sup>+</sup> levels in H9c2 cells improved the cell viability and decreased LDH release and caspase-3 activity, thereby protecting the cells from the deleterious effects of DOX. Supplementing NAD<sup>+</sup> in H9c2 cells is therefore a good strategy to replenish the DOX depleted cellular pools and protect cells from toxicity.

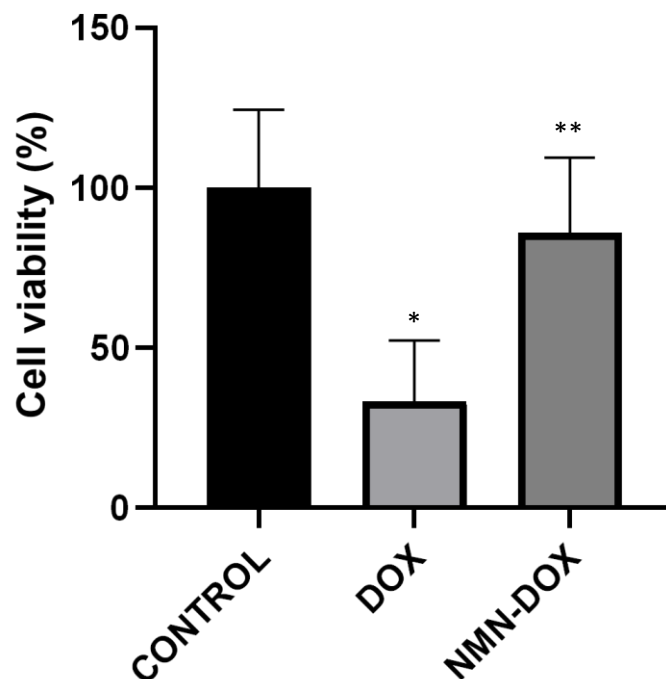


**Figure 3.8: NMN increased viability of DOX-treated H9c2 cells.** Cell viability was assessed in H9c2 cells treated with DOX and NMN-DOX. Control cells were untreated. One-way ANOVA analysis followed by Tukey post hoc test was used to compare groups (n= 3) (\*P<0.05 versus control; \*\*P<0.05 versus DOX)

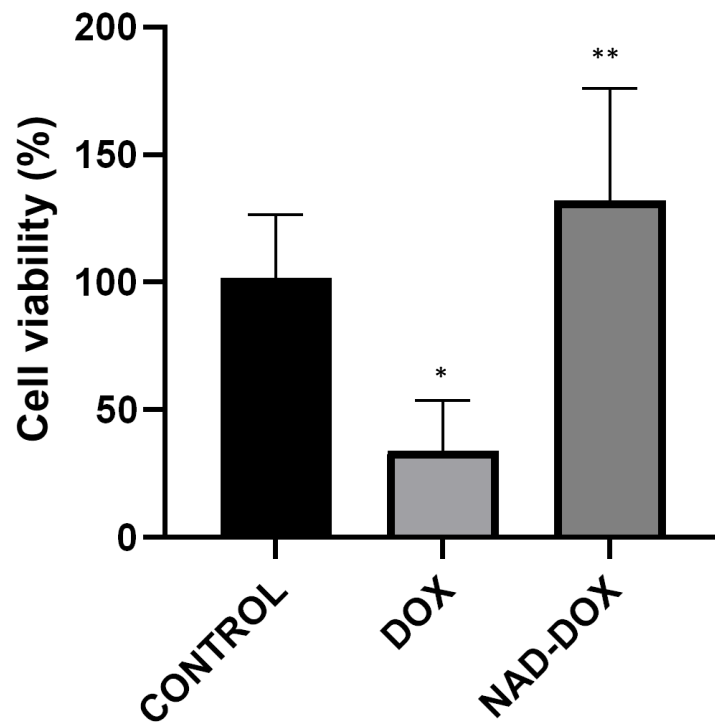


**Figure 3.9: NAD<sup>+</sup> increased viability of DOX-treated H9c2 cells.** Cell viability was assessed in H9c2 cells treated with DOX and NAD-DOX. Control cells were untreated. One-way ANOVA analysis followed by Tukey post hoc test was used to compare groups (n= 3 independent experiments) (\*P<0.05 versus control; \*\*P<0.05 versus DOX)



### 3.6 NMN and NAD<sup>+</sup> prevents DOX-induced changes in lysosomal pH

Since DOX also altered to the lysosomal pH of H9c2 cells apart from being toxic, NAD<sup>+</sup> upregulation in preventing the pH increase was examined. The pH changes were measured using the LysoSensor probe described earlier. Both NMN and NAD<sup>+</sup> treatment prior to DOX incubation prevented the pH alterations (Figure 3.10 and 3.11). Statistically, pH of the NMN/NAD<sup>+</sup> pre-incubated cells did not differ significantly from the control cells.

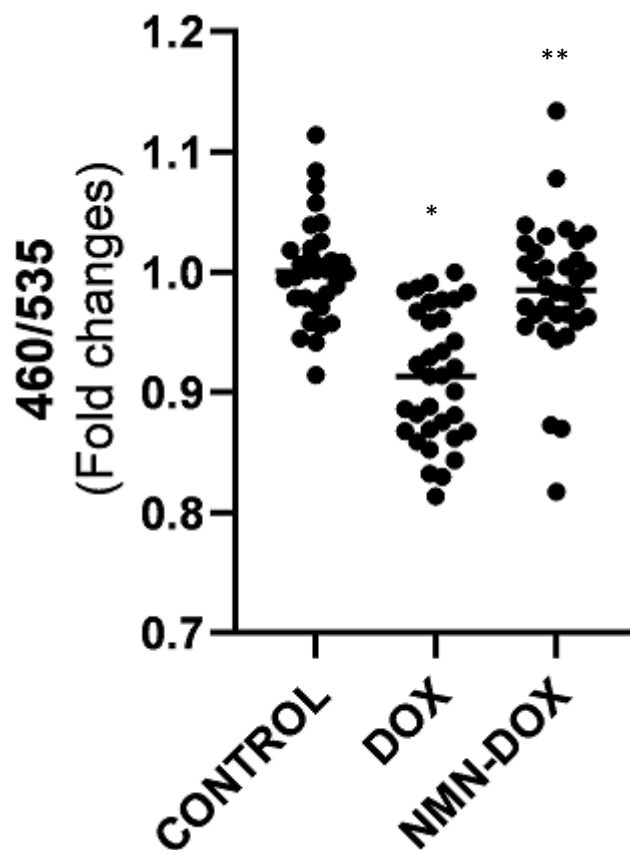


**Figure 3.10: NMN prevented DOX-induced pH changes.** H9c2 cells pre-treated with NMN (1 mM) for 24 hours prior to DOX treatment (1  $\mu$ M) (24 hours). Control cells were left untreated. The lysosomal pH was determined based on 460/535 ratio. One-way ANOVA analysis followed by Tukey post hoc test was used to compare multiple groups (n= 10) (\*P<0.05 versus control; \*\*P<0.05 versus DOX)

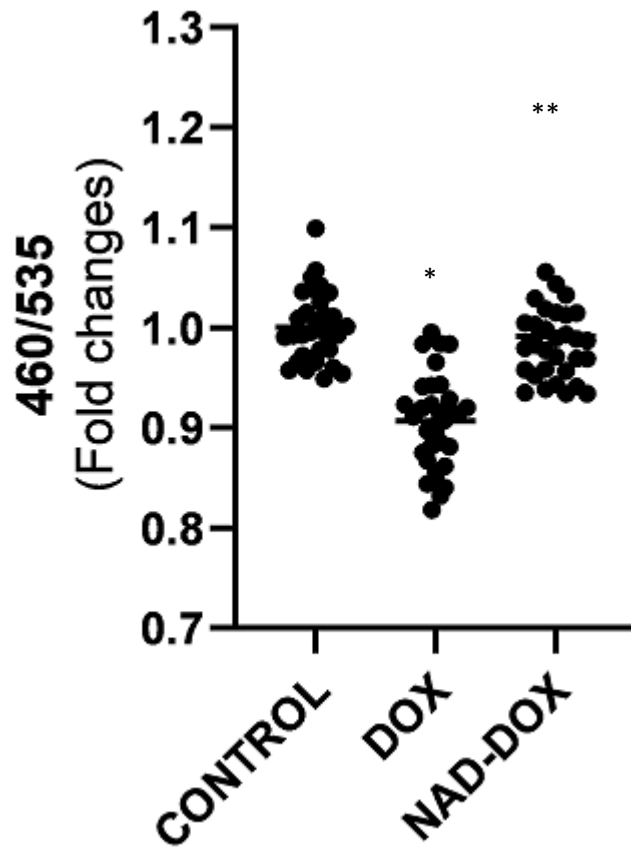


**Figure 3.11: NAD<sup>+</sup> prevented DOX-induced pH changes.** H9c2 cells pre-treated with NAD<sup>+</sup> (1 mM) for 24 hours prior to DOX treatment (1  $\mu$ M) (24 hours). Control cells were left untreated. One-way ANOVA analysis followed by Tukey post hoc test was used to compare multiple groups (n= 10) (\*P<0.05 versus control; \*\*P<0.05 versus DOX).

### 3.7 V-ATPase inhibitor, Bafilomycin A prevents NMN/NAD<sup>+</sup> imparted protection against DOX cardiotoxicity

The V-ATPase inhibitor, Bafilomycin A, was used as a pharmacological tool to confirm the role of V-ATPase pump in DOX cardiotoxicity. Both BAF and DOX had been toxic to H9c2 cells and had induced pH alterations. DOX has already been reported to prevent the autophagic flux in cardiomyocytes by preventing acidification of lysosomes (52) and it had to be confirmed in the *in vitro* model used for this study as well.

#### 3.7.1 Bafilomycin A prevents NMN/NAD<sup>+</sup> induced decreases in LDH release in DOX-treated H9c2 cells

H9c2 cells were pre-incubated with NMN/NAD<sup>+</sup> (1 mM) for 24 hours and then treated with DOX (1 μM) and BAF (1 nM) for another 24 hours. LDH release was measured in the cells as described earlier. BAF treatment further increased the LDH release in H9c2 cells when compared to cells treated with DOX alone. The protective effect of NMN and NAD<sup>+</sup> were abolished by the V-ATPase inhibitor (Figure 3.12 and 3.13).

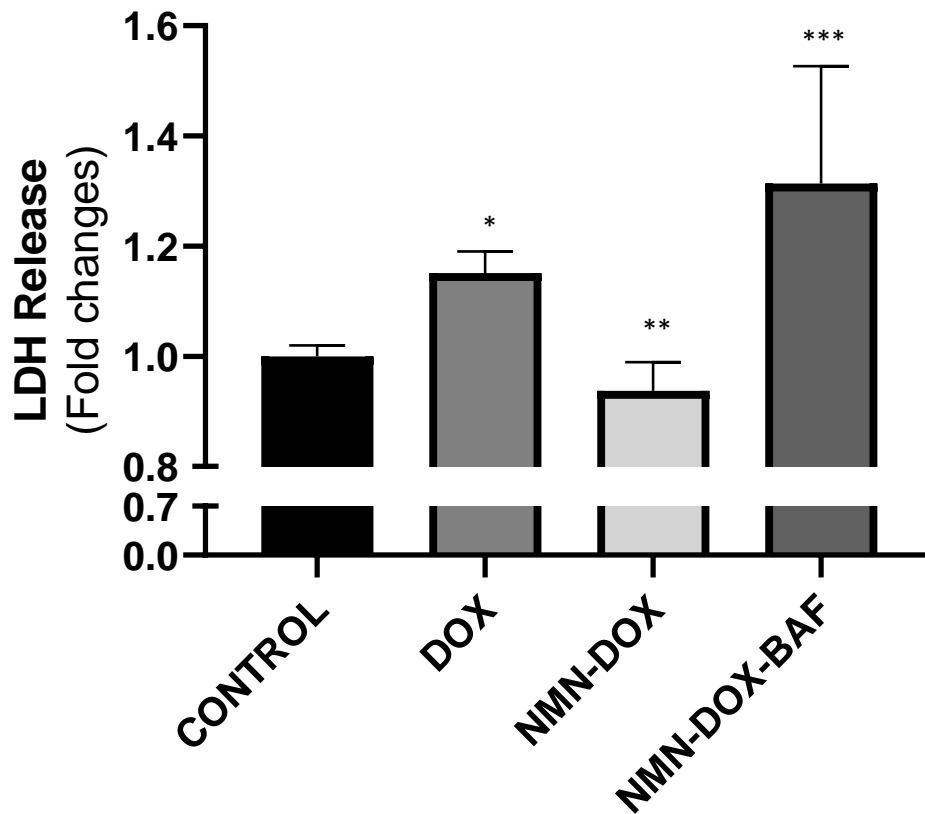


**Figure 3.12: Bafilomycin A prevented NMN induced decreases in LDH release in DOX-treated H9c2 cells.** LDH release in DOX, NMN, NMN-DOX, NMN-DOX-BAF treated H9c2 cells. One-way ANOVA analysis followed by Tukey post hoc test was used to compare groups (n=6) (\*P<0.05 versus control; \*\*P<0.05 versus DOX; \*\*\*P<0.05 versus NMN-DOX)

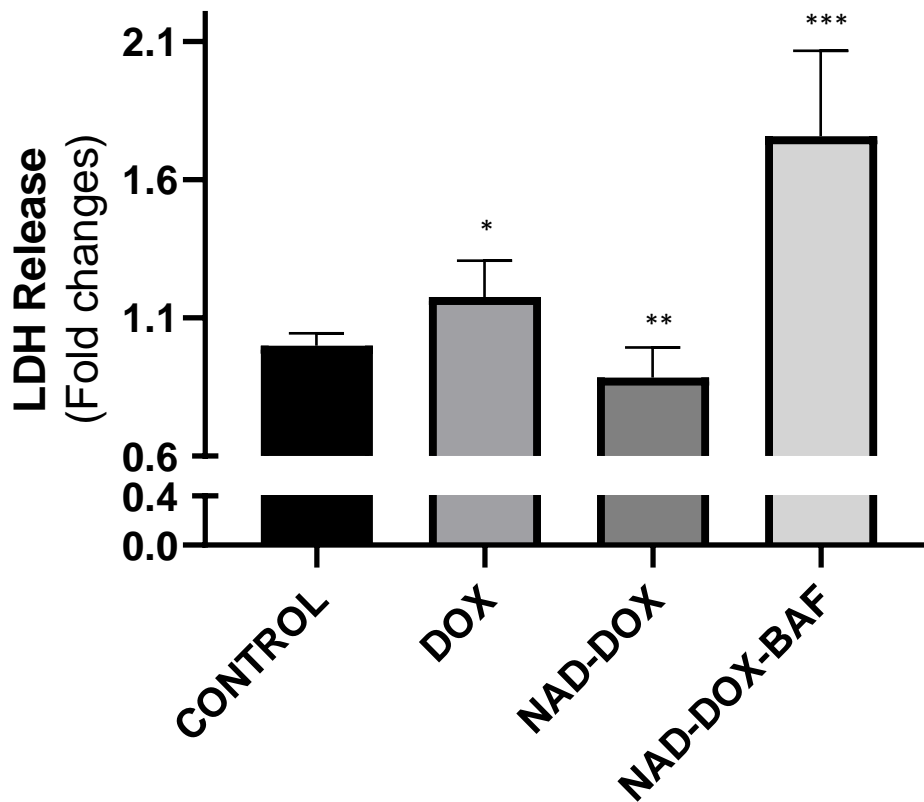


**Figure 3.13: Bafilomycin A prevented NAD<sup>+</sup> induced decreases in LDH release in DOX-treated H9c2 cells.** LDH release in DOX, NAD, NAD-DOX and NAD-DOX-BAF treated H9c2 cells. One-way ANOVA analysis followed by Tukey post hoc test was used to compare groups (n=6) (\*P<0.05 versus control; \*\*P<0.05 versus DOX; \*\*\*P<0.05 versus NMN-DOX)

### 3.7.2 Bafilomycin A prevents NMN/NAD<sup>+</sup> induced protection against alterations in lysosomal pH in DOX-treated H9c2 cells

Whether NAD<sup>+</sup> imparted protection against lysosomal pH changes was via the V-ATPase pump related acidification was to be determined. H9c2 cells were pre-treated with NMN/NAD<sup>+</sup> and then subjected to incubation with DOX (1  $\mu$ M) and BAF (1 nM) for 24 hours. BAF indeed prevented the protective effect of NMN and NAD<sup>+</sup> in maintaining lysosomal pH (Figure 3.14 and 3.15). These results advocate that the protective mechanism of NAD<sup>+</sup> could be by preventing the DOX-induced modifications of the lysosomal V-ATPase pump.

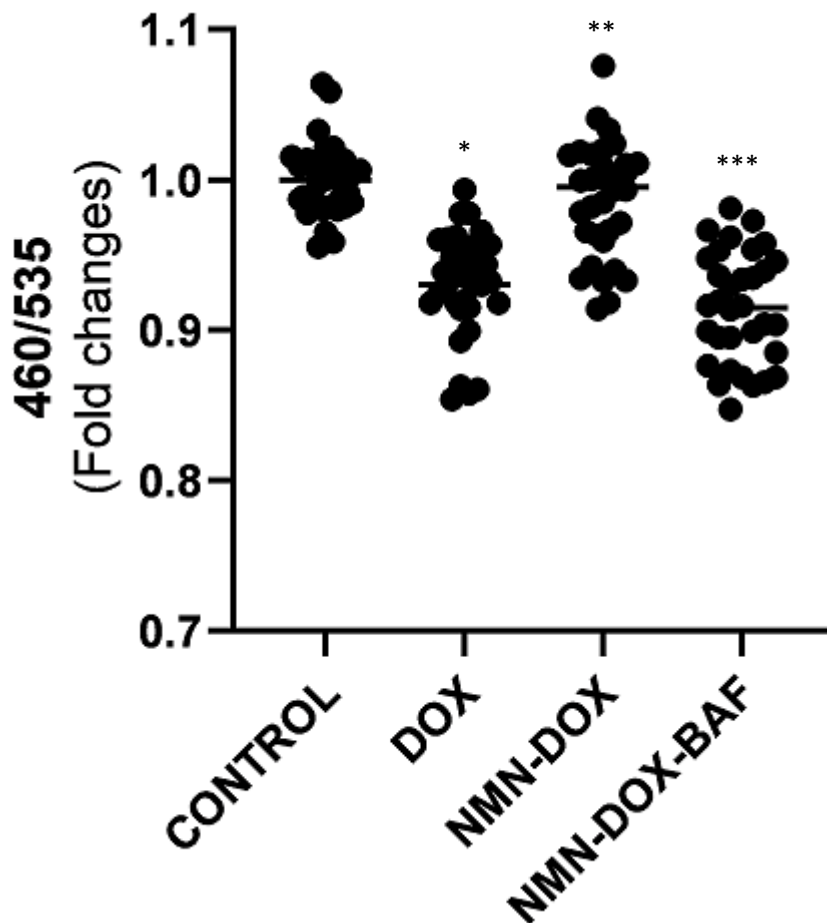


**Figure 3.14: Bafilomycin A prevented NMN imparted protection against DOX-induced lysosomal pH alterations.** H9c2 cells pre-treated with NMN (1 mM) for 24 hours prior to DOX, DOX/BAF treatment (24 hours). Control cells were left untreated. Control cells were left untreated. The lysosomal pH was determined based on 460/535 ratio. One-way ANOVA

analysis followed by Tukey post hoc test was used to compare groups (n= 10) (\*P<0.05 versus control; \*\*P<0.05 versus DOX; \*\*\*P<0.05 versus NMN-DOX)

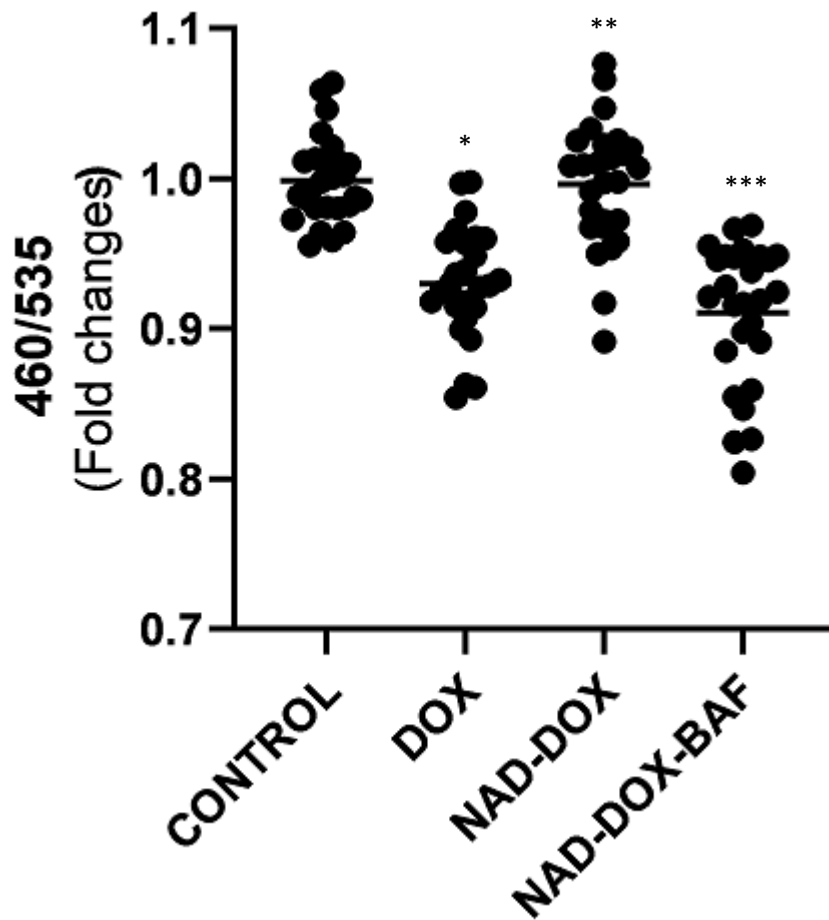


**Figure 3.15: Bafilomycin A prevented NAD<sup>+</sup> imparted protection against DOX-induced lysosomal pH alterations.** H9c2 cells pre-treated with NAD<sup>+</sup> (1 mM) for 24 hours prior to DOX, DOX/BAF treatment (24 hours). Control cells were left untreated. The lysosomal pH was determined based on 460/535 ratio. One-way ANOVA analysis followed by Tukey post hoc test was used to compare groups (n= 10) (\*P<0.05 versus control; \*\*P<0.05 versus DOX; \*\*\*P<0.05 versus NAD-DOX)

### 3.8 NMN prevents hyperacetylation of ATP6V0d1 in DOX-treated neonatal cardiomyocytes

Previous research from our lab had documented hyperacetylation of the d subunit of  $V_0$  domain (ATP6V0d1) of the V-ATPase pump in response to DOX treatment in mouse models of DOX cardiotoxicity and neonatal cardiomyocytes. The protective effect of the  $NAD^+$  precursor, NMN in preventing hyperacetylation was hence worth investigating. This could be one of the mechanisms by which  $NAD^+$  upregulation protects cardiomyocytes against autophagic dysregulation by DOX. Neonatal cardiomyocytes were treated with NMN (1 mM) for 24 hours and then incubated with DOX (1  $\mu$ M) for another 24 hours. Acetylated proteins were co-immunoprecipitated with anti-acetyl lysine antibody and separated on SDS-Page gel. After transferring on to PVDF membrane, the proteins were probed with anti-ATP6V0D1 antibody to identify the acetylation levels on the cells. Coinciding with our earlier findings, DOX treatment induced hyperacetylation of ATP6V0d1. NMN treatment at 1 mM concentration for 24 hours prior to DOX incubation treatment prevented the hyperacetylation of ATP6V0d1 (Figure 3.16).



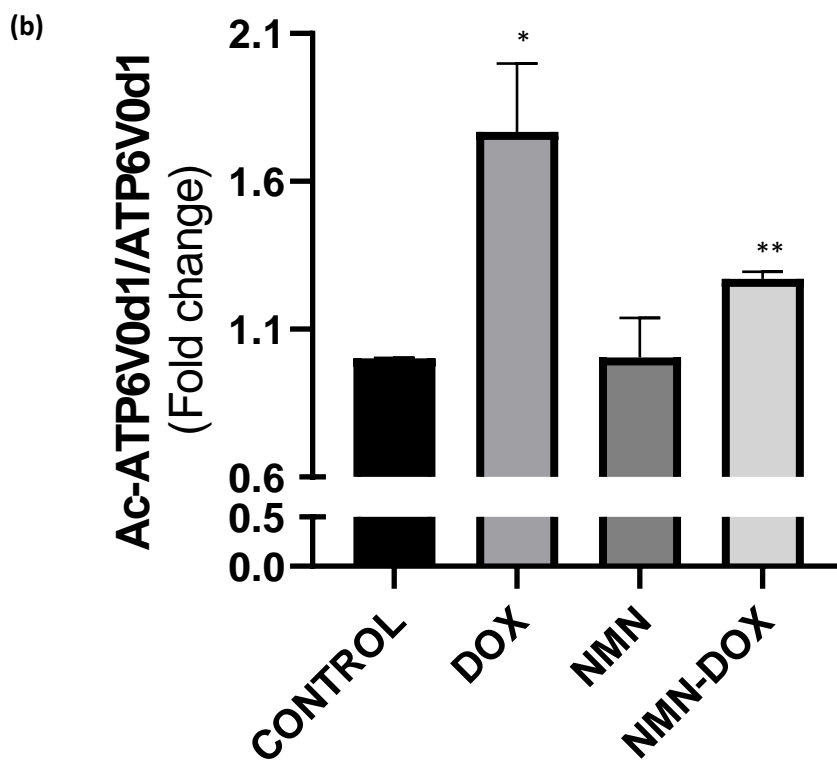
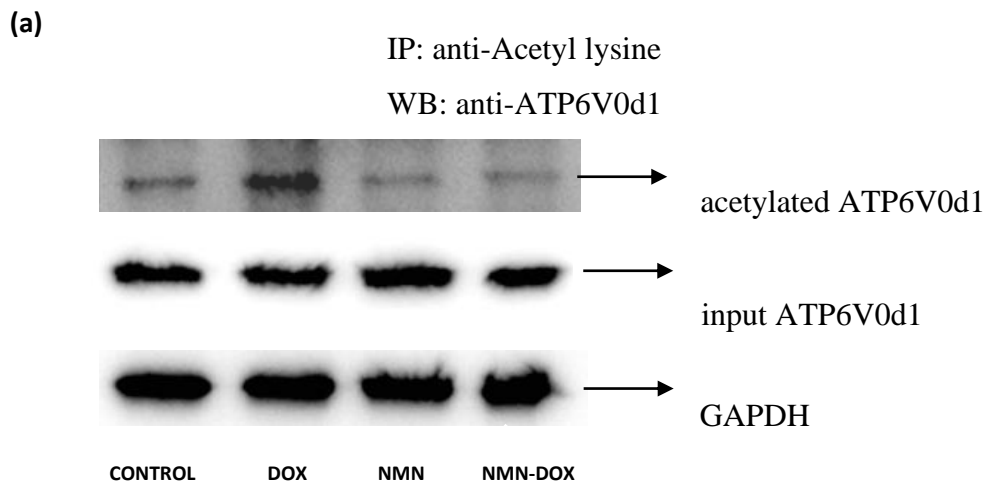


**Figure 3.16: NMN prevented DOX-induced hyperacetylation of ATP6V0d1.**

(a) (Representative image) Neonatal cardiomyocytes were incubated with NMN prior to incubation with or without DOX. Control cells were left untreated. Co-immunoprecipitation of acetylated proteins followed by western blot analysis of ATP6V0d1 was done. (b) Quantification of proteins levels of acetylated ATP6V0d1 relative to ATP6V0d1. One-way ANOVA analysis followed by Tukey post hoc test was used to compare groups (n=3) (\*P<0.05 versus CONTROL; \*\*P<0.05 versus DOX)

## Chapter 4

### 4 Discussion, Limitations and Future Directions

#### 4.1 Discussion

Cancer is a growing burden on the Canadian health sector and the leading cause of death in the country. Several measures have been undertaken by the Government of Canada in addressing this issue and around \$159 million have been invested in cancer research in the country in 2009-10 alone through the Canadian Institute of Cancer Research (131). The government has also invested \$250 million to improve the quality of lives of Canadian Cancer patients and survivors through its initiative, Canadian Partnership Against Cancer, an independent not-for-profit organization. Despite of all these measures, nearly half of all Canadians are expected to develop cancer in their lifetime.

Doxorubicin has been a frontline drug in the treatment of cancer since decades and hence is a major player in the pharmaceutical industry in terms of revenue too. The major concern of this drug is its toxic effect on the heart posing acute and chronic threats. Though Doxorubicin cardiotoxicity has been widely studied, an effective treatment option is yet to be achieved. Cardiac toxicity associated with DOX administration is dependent on risk factors such as cumulative and age. Antioxidant supplementation along with DOX have so far been limited in preventing cardiotoxicity in the clinical scenario (132). Clinical studies on the effectiveness of beta-blockers like carvedilol, Angiotensin II receptor blockers (ARB) and Angiotensin converting enzyme (ACE) inhibitors, in preventing doxorubicin cardiotoxicity have resulted in mixed or no desired outcomes (133). Dexrazoxane, a bis-dioxopiperazine compound is co-administered with Doxorubicin to prevent cardiotoxic occurrences, but reduced chemotherapeutic efficacy and side effects like myelosuppression have been reported in patients (134). Effective treatment strategies in managing the toxic effects of DOX would open more room to exploit the therapeutic potential of the drug.

The role of autophagy in DOX cardiotoxicity has gained considerable interest in recent years. Stimulating basal autophagy by calorific restriction and mTORC inhibition has been demonstrated to reduce DOX toxicity in rodents. Also, interfering with the proteins involved in late autophagic machinery has been reviewed as a promising strategy and could

contribute in alleviating the complication (135). This study focuses on revealing the mechanisms of impaired lysosome acidification in cardiomyocytes causing autophagic disruption in response to doxorubicin treatment. A novel role of NAD<sup>+</sup> precursor, NMN, in establishing the basal autophagic machinery in DOX treated cardiomyocytes by augmenting impaired lysosome acidification been proposed. This study establishes the defects induced by Doxorubicin on the lysosomal V-ATPase, the proton pump essential for regulating pH. Further, the therapeutic scope and mechanism of NMN, the NAD<sup>+</sup> precursor in preventing Doxorubicin-induced autophagic dysregulation by establishing the lysosomal function has been evaluated.

#### 4.1.1 Doxorubicin induces toxicity and death in cardiomyocytes

In the clinical scenario, DOX induces cardiomyocyte death within hours of intravenous administration (136). Dose-dependent toxicity cardiotoxic effects of DOX have been established in this study on the rat myoblast cell line H9c2 and on human induced pluripotent stem cells-derived cardiomyocytes and adult cardiomyocytes by researchers elsewhere. Increases in the LDH release, DNA fragmentation and activation of caspases are observed in these cells (137,138).

Increased LDH activity is evident in human hearts with defects and end-stage failure and early interventions have been reported to improve the clinical outcomes of these patients. LDH is a sensitive method and an early biochemical indicator of myocardial complications. Plasma levels of LDH increase within 8-12 hours of cardiac injury, peaks in 2-3 days and remains elevated for 7-10 days. High serum LDH levels predicts short survival time in patients with multiple myeloma treated with a combinatorial Doxorubicin drug regimen (139–142). DNA fragmentation is a marker of apoptosis and increased levels of fragmented DNA are observed in cardiomyopathy which often transitions to heart failure. Oxidative stress induces high levels of DNA damage in patients with cardiovascular diseases (143,144). Caspases are cysteinyl aspartate specific proteases involved in the cleavage of several proteins propagating cellular homeostasis by inducing apoptosis, proliferation, and inflammation. These proteases are widely expressed, and 12 human caspases have been identified till date. Tightly regulated activation of caspases prevents premature cell death. Activation of caspases in the heart degrades the myofibrillar proteins such as actin and actinin

resulting in the impairment of the myofibrillar ATPase active and contractile dysfunction. In normal conditions, due to their limited proliferative capacity, only around 0.001-0.01% of cardiomyocytes undergo apoptosis. Caspase-3 is an executioner caspase directly cleaving the substrate proteins and promotes the downstream cascade of events in apoptosis. Caspase activation degrades autophagic proteins like Beclin-1, Atg5 and Atg7, impairing the autophagic machinery and converts pro-autophagic proteins to pro-apoptotic proteins, thereby triggering apoptosis (145). The myocardial cells exhibit a stage of interrupted apoptosis, where there is contractile dysfunction with increased caspase-3 activity but normal nuclei. This prolonged pre-death stage suggests that cells have the possibility to be rescued with restoration of myocardial function. (126,146–148).

Increased caspase-3 expression is found in the hearts with end-stage heart failure and ventricular arrhythmias and considerable reduction of this protease is seen in patients with left ventricular assisted device (LVAD) support. Over-expressing cardiac specific caspase-3 in mice induced myofibrillar ultrastructural damages and lethality was also reported in caspase-3 transgenic mice with increased infarct size when subjected to myocardial ischemia-reperfusion injury (148). DOX treatment induces apoptosis in cardiomyocytes and rat cardiac ventricles by activating caspase-3 (149). In consistence with data published by peers, the present study also reports a dose-dependent increase in caspase-3 activity of H9c2 cells in an *in vitro* model of DOX cardiotoxicity. Although the exact mechanism of caspase-3 activation by DOX remains unclear, H<sub>2</sub>O<sub>2</sub> induced ROS is predominantly considered as the mediator of caspase-3 activation in cardiomyocytes in contrast to caspase-3 activation mediated by p53 in tumour cells (150).

#### 4.1.2 Doxorubicin inhibits acidification and induces lysosomal dysfunction in cardiomyocytes

With high rates of oxygen consumption and aerobic respiration, the post-mitotic myocardial cells are highly susceptible to damage associated with pathological conditions such as aging and disease. Due to the lack of proliferative and renewal capacities, myocardial cells depend extensively on the intracellular recycling mechanisms for their survival. Lysosomes, being the key organelles demonstrating degradative and salvaging capabilities, are vital in preserving the viability of these cells. Autophagic clearance of damaged and

defective proteins and organelles in the cell carried out by lysosomes maintains cardiomyocyte homeostasis and longevity. Cells when subjected to stress, activate autophagy to get rid of the malfunctional cellular structures formed in response to various stimuli. Insufficient autophagy in stressed cells could result in the accumulation of ROS and induction of apoptosis. In cardiomyocytes, proper lysosomal function and autophagy is of utmost importance as the respiratory organelle mitochondria is actively functioning and often suffers from oxidative damage and should be recycled (50). Autophagic flux impairment has been implicated in doxorubicin cardiotoxicity and our lab has reported this previously. Increased steady-state LC3-II levels indicates activation of autophagic flux or downstream blockage of autophagic vacuole processing. Bafilomycin A, the inhibitor of late stage autophagy, increased the LC3-II protein levels in saline-treated cardiomyocytes. Compared to the saline-treated cells, Bafilomycin A treatment did not further increase the LC3-II protein levels in doxorubicin-treated cardiomyocytes suggesting a block in the autophagic flux (117).

The hydrolytic enzymes within the lysosomes are tightly regulated by the pH within the organelle. An acidic pH of 4.5-5 is essential for the enzymatic activity in the interior of lysosomes. The interior perimeter of the lysosome is protected from the attack from its own enzymes with the help of a glycocalyx lining. The pH gradient is generated and maintained with the help of protons pumped into the lysosomal lumen by the V-ATPase pump. ATP hydrolysis at the cytoplasmic  $V_1$  domain of V-ATPase imports protons via the membrane-embedded  $V_0$  domain. The pumping mechanism is tightly regulated by the reversible assembly of the domains and has been described in detail in the first chapter. Disorders in lysosomal acidification have been implicated in several neurodegenerative diseases, Crohn's disease and lipotoxicity (151–153). Doxorubicin treatment inhibited the lysosomal acidification in neonatal rat ventricular myocytes resulting in the disruption of autophagic flux and accumulation of ROS (52), leading to cell death.

Using the V-ATPase inhibitor Bafilomycin A as a positive control, the lysosomal acidification defects in DOX-treated H9c2 cells have been established in this study. Compared to the control group, H9c2 cells incubated with Bafilomycin A and Doxorubicin showed similar alterations in lysosomal pH. The results obtained indicate that Doxorubicin inhibits V-ATPase, prevents the acidification of lysosomes, and impairs the autophagic machinery in cardiomyocytes. Since Bafilomycin A impaired V-ATPase activity partly by inhibiting the subunit c of  $V_0$  domain, DOX mediated inhibition of V-ATPase subunits was worth investigating. Preliminary results from an ongoing research in our laboratory have

indeed identified DOX mediated modification on the subunit d of the V-ATPase V<sub>0</sub> domain. Interestingly, none of the other subunits from the V<sub>1</sub> or V<sub>0</sub> domains showed any alterations.

### 4.1.3 NMN confers protection against Doxorubicin-induced toxicity and death in cardiomyocytes

NAD<sup>+</sup> homeostasis in the cell is vital for regulating cellular bioenergetics as it is an important co-factor for many intracellular enzymatic reactions. Altered NAD<sup>+</sup> homeostasis and depleted levels of NAD<sup>+</sup> have been linked to aging and development of several diseases of the brain, heart, liver, skeletal muscle, kidney, and gut. Decreased levels of NAD<sup>+</sup> have been linked to multiple cardiac pathologies. Overactivation of the NAD<sup>+</sup> consuming enzymes in the heart leads to the depletion of the cofactor and affects the normal functioning of the cells in the organ. In cardiomyocytes too, as in other cells, NAD<sup>+</sup> is critical for the maintaining the fuel oxidation. NAD<sup>+</sup> gets reduced to NADH, which get re-oxidised in the mitochondria to produce ATP in a process termed as oxidative phosphorylation. This process generates about 95 % of the cardiac ATP content. The phosphorylated NAD<sup>+</sup>, NADP<sup>+</sup>, is an essential component in the pentose phosphate pathway generating NADPH and ribose 5-phosphate. NADPH is involved in lipid biosynthesis and protects against ROS. In models of cardiac dysfunction, NAD<sup>+</sup> supplementation using precursors re-establishes the depleted NAD<sup>+</sup> pools and normalized the redox reactions in the cell (94,154).

The NAD<sup>+</sup> precursor, NMN, have shown promising therapeutic effects on various cardiovascular complications. NMN prevented ischemic injury and increased sirtuin activity and vasodilatory function in rodent models of heart ischemia/reperfusion. This NAD<sup>+</sup> precursor also showed potential to reverse left ventricular contractile dysfunction in animal models (94). Our lab has recently reported the protective effect of another NAD<sup>+</sup> precursor, NR in ameliorating Doxorubicin-induced cardiotoxicity in mice via modulating the NAD<sup>+</sup>/SIRT1 pathway (117). This study for the first time demonstrates the potential of NMN in preventing toxic effects of Doxorubicin in an *in vitro* cell culture model. Both NAD<sup>+</sup> and NMN improved the viability of H9c2 cells and prevented the increases in LDH release and caspase-3 activity. Based on the results from this study, NMN attenuated the cell damage in Doxorubicin treated cells and prevented cell death.

Orally administered NMN is rapidly absorbed and converted to NAD<sup>+</sup> in peripheral organs and is retained longer in the body than other NAD<sup>+</sup> intermediates (101). A clinical

trial to investigate the safety profile of NMN revealed no side effects up to single oral doses of 0.5 gram/day in healthy men. NMN was effectively metabolised and did not cause any adverse clinical symptoms in the subjects. The biochemical analysis revealed normal ranges of serum creatinine, chloride, and blood glucose levels (155). Another clinical trial to investigate the effects of NMN on cardiometabolic functions are currently underway and is expected to be completed soon (156). Bioavailability and therapeutic value of NMN can hence be exploited and has the potential to be translated in mitigating Doxorubicin cardiotoxicity.

#### **4.1.4 NMN protects cardiomyocytes from Doxorubicin-induced alterations in lysosomal pH**

As mentioned earlier, efficient lysosome functioning is critical in post-mitotic cells like cardiomyocytes. Insufficient autophagy in cardiomyocytes lead to the accumulation of defective organelles like mitochondria and damaged proteins in cell and contributes to the ROS generation leading to oxidative stress. Lysosomal acidification by V-ATPase is vital in maintaining autophagic flux. NR supplementation prevented lysosomal alkalinization in Doxorubicin- treated adult cardiomyocytes (117). The current study also validated the effects of NAD<sup>+</sup> supplementation in preventing pH increases in cardiomyocytes in response to DOX treatment. Treatment with NMN blocked the effects of Doxorubicin on the lysosomal pH of H9c2 cells. NAD<sup>+</sup> treatment also showed similar results suggesting the NMN mediated lysosomal pH preservation could be facilitated by the conservation of the NAD<sup>+</sup> pool in H9c2 cells. Since lysosomal pH is maintained by V-ATPase activity, it is possible that NAD<sup>+</sup> may veil the proton pump from the deleterious effects of Doxorubicin. Hence, we postulated that the hyperacetylation of the V-ATPase V<sub>0</sub>d subunit induced by Doxorubicin identified in our laboratory, could be prevented by NMN.

#### **4.1.5 Bafilomycin A abrogates the protective effects of NMN in Doxorubicin-induced cardiotoxicity**

Doxorubicin inhibits lysosomal acidification in cardiomyocytes by inhibiting V-ATPase and blocking proton transport (52). To clarify the role of V-ATPases in Doxorubicin mediated cardiotoxicity, Bafilomycin A, a specific V-ATPase inhibitor, was used to inhibit

the proton transport mechanism in H9c2 cells. NAD<sup>+</sup> upregulation was unable to rescue the cells from lysosomal pH increases, when Bafilomycin A was incubated with Doxorubicin. The protection imparted by NMN in preventing lysosomal pH alterations in H9c2 cells were hence abrogated suggesting a modulatory role of NAD<sup>+</sup> on the V-ATPase pump activity.

Bafilomycin A inhibits lysosomal acidification by binding to the c subunit of the V-ATPase V<sub>0</sub> domain and as mentioned earlier, we have preliminary results from our lab validating a similar *modus operandi* of Doxorubicin on the proton pump. Since NAD<sup>+</sup> and NMN failed to protect the lysosomal pH of DOX-treated H9c2 cells in the presence of the V-ATPase inhibitor, it was anticipated that NAD<sup>+</sup> upregulation might be exerting its effects via modulating V-ATPase.

#### 4.1.6 NMN prevents hyperacetylation of the d subunit of V-ATPase pump V<sub>0</sub> domain

NMN supplementation restores the NAD<sup>+</sup> levels and stimulates the activity of the NAD<sup>+</sup> dependent lysine deacetylase SIRT1 in the heart. SIRT1 inhibitor splitomycin prevented the protective effects of NMN in heart ischemia-reperfusion injury justifying the role of SIRT1 pathway in NAD<sup>+</sup> mediated cardio protection (130). Hyperacetylation of various autophagy related proteins and transcription factors including TFEB have been implicated in several cardiovascular complications. Activation of DNA repair enzymes like PARPs deplete the NAD<sup>+</sup> reserves in the cells and constrain the deacetylation activity of sirtuins. Under normal physiological conditions, PARPs are also deacetylated and inhibited by sirtuins to preserve the NAD<sup>+</sup> levels in cardiomyocytes. But damages to the DNA leads to NAD<sup>+</sup> consumption due to PARP activation and inhibition of sirtuin activity (157). Doxorubicin induced epigenetic modifications such as DNA methylation and histone modifications exacerbate the toxic effects of the drug on cardiomyocytes by altering the gene expression (158). Our lab has previously reported robust increase in p53 acetylation in cardiomyocytes treated with Doxorubicin. NAD<sup>+</sup> supplementation prevented the acetylation, but this protective effect was abolished when the cells were co-incubated with the SIRT1 inhibitor, EX-527, highlighting the role of NAD<sup>+</sup> mediated deacetylation as a defensive phenomenon in Doxorubicin cardiotoxicity (117).



In line with the ongoing research in our laboratory on DOX-induced cardiotoxicity, this study explored the potential of NMN assisted deacetylation mechanism on the DOX-induced hyperacetylation on the V-ATPase V<sub>0</sub>d1 subunit. Pre-incubating neonatal cardiomyocytes with NMN prevented hyperacetylation as evidenced by co-immunoprecipitation and western blotting experiments. Thus, a unique role of the NAD<sup>+</sup> precursor, NMN, was established in this study which could open doors for further meritorious investigations. Preventing the hyperacetylation of the V-ATPase d1 subunit is assumed to be a possible mechanism of NMN mediated inhibition of lysosomal pH increases in Doxorubicin treated cells.

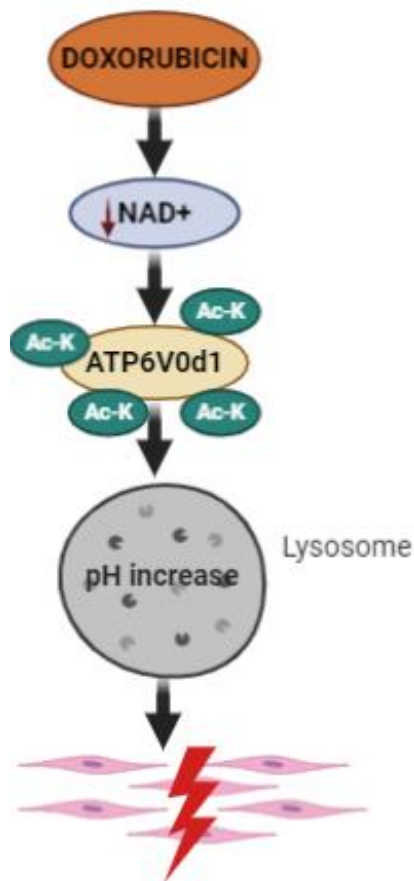
The V-ATPase d subunit is ubiquitously expressed and links the proteolipid c ring of V<sub>0</sub> and the central stalk of V<sub>1</sub> (55). Subunit d is also hydrophilic and is located on the cytoplasmic side of the c ring. Binding sites for the D and F subunits of the V<sub>1</sub> domain are present on subunit d and it is a vital protein of the V-ATPase rotary complex comprising of D, F and proteolipid ring (159). Unless complexed with the V<sub>0</sub> domain, d doesn't bind to the D subunit of central stalk (60). During disassembly of the V-ATPase domains, subunit a separates from the V<sub>1</sub> subunit and binds to d, preventing its rotation (58). Crystal structure and electron microscopic analysis suggests that the d subunit serves as a socket to attach central stalk subunits of V<sub>1</sub> onto the V<sub>0</sub> phospholipid ring, coupling the two domains (160). Subunit d dissociates from the membrane on treating with alkaline reagents such as Na<sub>2</sub>CO<sub>3</sub> or 5M urea and at a pH of 11.5 in *in vitro* experiments. Moreover, subunit d is the only component of V<sub>0</sub> that is not an integral membrane protein (63). Based on all these literatures, it is logical to assume that subunit d is prone to acetylation modifications when cells are subjected to Doxorubicin treatment either directly by DOX/ROS or indirectly by NAD<sup>+</sup>/SIRT inhibition.

## 4.2 Concluding Remarks

This study uncovers a novel role of NMN in establishing the basal autophagic machinery in DOX treated cardiomyocytes by improving impaired lysosome acidification. The d subunit of V-ATPase V<sub>0</sub> sector is the only protein in the membranous domain of the proton pump to be localised to the periphery of the lysosomal membrane and could be prone to modifications by DOX directly or indirectly. It is an important regulator of proton

transport and hence hyperacetylation could account for DOX-induced lysosomal dysfunction in cardiomyocytes. Pre-incubation with the NAD<sup>+</sup> precursor, NMN, averted hyperacetylation of the V-ATPase d subunit in DOX-treated cardiomyocytes. Also, NMN and NAD<sup>+</sup> imparted protection to H9c2 cardiomyocyte cells from Doxorubicin toxicity by preventing cell injury and lysosomal pH alterations (Figure 4.1). Based on these findings and the safety profile of NMN, this molecule could be credibly considered as a beneficial drug in ameliorating Doxorubicin cardiotoxicity.

**A**



**B**

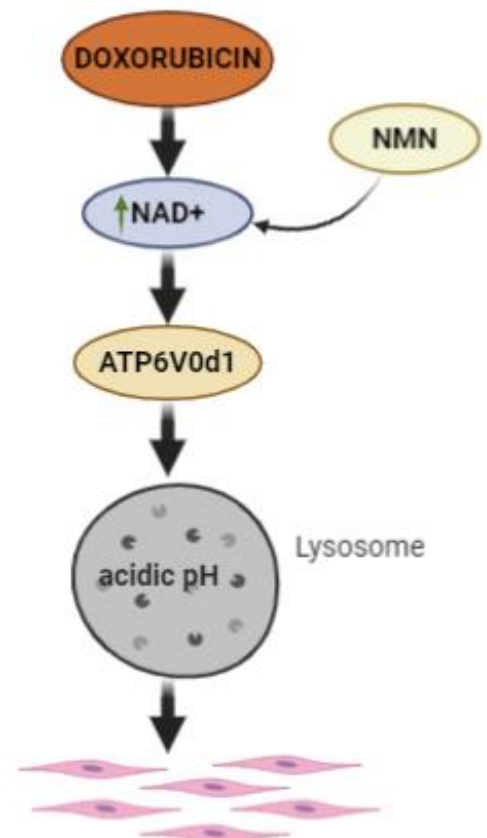


**Figure 4.1: Schematic illustration of the study.** (A) Doxorubicin depletes the NAD<sup>+</sup> content and stimulates hyperacetylation of ATP6V0d1 thereby preventing lysosomal acidification and inducing cardiomyocyte cell toxicity. (B) NAD<sup>+</sup> precursor, NMN, supplements the NAD<sup>+</sup> pools depleted by Doxorubicin and prevents the hyperacetylation of ATP6V0d1 and hence maintains acidic lysosomal pH and prevents cardiomyocyte cell toxicity.

## 4.3 Limitations

1) Direct evidence of NAD<sup>+</sup> upregulation by NMN in H9c2 cells has not been included in this study. However, this has been reported by multiple researchers and our lab also has unpublished data of NAD<sup>+</sup> upregulation by NMN in H9c2 cells.

2) This study has focussed on therapeutic scope of NMN in *in vitro* models of Doxorubicin cardiotoxicity. Though NMN has shown cardioprotective effects in *in vivo* models of cardiac complications and NR has shown potential in rodent models of Doxorubicin cardiotoxicity, additional studies are required for validating the protective effects of NMN in Doxorubicin cardiotoxicity.

3) Though pharmacological inhibitors such as Bafilomycin A, serves the purpose in providing mechanistic evidence of V-ATPase inhibition, genetic manipulations would have supported the claim further.

4) NMN indeed did prevent hyperacetylation of ATP6V0d1 and inhibited lysosomal pH increases in Doxorubicin treated cardiomyocytes, but other mechanisms of protection on lysosomal functioning and autophagic flux in Doxorubicin cardiotoxicity may exist which warrants further investigations.

5) Inclusion of *in vitro* lysosomal imaging techniques would have aided the intention of this study and would have spiked the visual interest of readers as well.

## 4.4 Future Directions

NAD<sup>+</sup> mediated protection in Doxorubicin cardiotoxicity is speculated to include the sirtuin pathway. Though our lab has reported the involvement of SIRT1 in the protective mechanism of NR in Doxorubicin cardiotoxicity using pharmacological inhibitors (117), we intent to further verify this, in the mechanism of protection imparted by NMN as well. Pharmacological interventions and genetic manipulations will be used to elucidate the role of sirtuins, particularly SIRT1, using *in vitro* and *in vivo* models of disease.

Negative regulation of TFEB, the master regulator of lysosome biogenesis has been implicated in the progression of Doxorubicin cardiotoxicity (161). Acetylation of TFEB prevents its activation and stalls the synthesis of several proteins in the autophagic machinery (99). The role of NAD<sup>+</sup> upregulation in augmenting TFEB function and lysosome biogenesis will be evaluated in future experiments.

The acetylation patterns on ATP6V0d1 in response to Doxorubicin treatment will be investigated using mass spectrophotometry. Individual site mutations will be generated at the identified acetylation sites through gene mutagenesis and the vital acetylation sites impacting the efficient functioning of V-ATPase will be explored. Using genetic manipulations, the role of ATP6V0d1 will be studied in *in vivo* models of Doxorubicin cardiotoxicity as well.

## 5 References

1. Cancer statistics at a glance - Canadian Cancer Society [Internet]. www.cancer.ca. [cited 2020 May 14]. Available from: <https://www.cancer.ca:443/en/cancer-information/cancer-101/cancer-statistics-at-a-glance/?region=on>
2. DeVita VT, Chu E. A History of Cancer Chemotherapy. *Cancer Res.* 2008 Nov 1;68(21):8643–53.
3. Angelis AD, Cappetta D, Urbanek LB and K. Doxorubicin Cardiotoxicity: Multiple Targets and Translational Perspectives. *Cardiotoxicity* [Internet]. 2018 Nov 14 [cited 2020 Jun 22]; Available from: <https://www.intechopen.com/books/cardiototoxicity/doxorubicin-cardiotoxicity-multiple-targets-and-translational-perspectives>
4. Ewer MS, Von Hoff DD, Benjamin RS. A Historical Perspective of Anthracycline Cardiotoxicity. *Heart Fail Clin.* 2011 Jul;7(3):363–72.
5. McGowan JV, Chung R, Maulik A, Piotrowska I, Walker JM, Yellon DM. Anthracycline Chemotherapy and Cardiotoxicity. *Cardiovasc Drugs Ther.* 2017;31(1):63–75.
6. Cutts SM, Swift LP, Pillay V, Forrest RA, Nudelman A, Rephaeli A, et al. Activation of clinically used anthracyclines by the formaldehyde-releasing prodrug pivaloyloxymethyl butyrate. *Mol Cancer Ther.* 2007 Apr 1;6(4):1450–9.
7. Martins-Teixeira MB, Carvalho I. Antitumour Anthracyclines: Progress and Perspectives. *ChemMedChem.* 2020 May 7;cmdc.202000131.
8. Doxorubicin Market Size Is Expected To Reach \$1.38 Billion By 2024 [Internet]. [cited 2020 Jun 7]. Available from: <https://www.grandviewresearch.com/press-release/global-doxorubicin-market>
9. Baxter-Holland M, Dass CR. Doxorubicin, mesenchymal stem cell toxicity and antitumour activity: implications for clinical use. *J Pharm Pharmacol.* 2018;70(3):320–7.
10. Lee JB, Zhou S, Chiang M, Zang X, Kim TH, Kagan L. Interspecies prediction of pharmacokinetics and tissue distribution of doxorubicin by physiologically-based pharmacokinetic modeling. *Biopharm Drug Dispos.* 2020 Apr 28;bdd.2229.
11. Tacar O, Sriamornsak P, Dass CR. Doxorubicin: an update on anticancer molecular action, toxicity and novel drug delivery systems. *J Pharm Pharmacol.* 2013 Feb 1;65(2):157–70.
12. Rivankar S. An overview of doxorubicin formulations in cancer therapy. *J Cancer Res Ther.* 2014 Dec;10(4):853–8.
13. Taymaz-Nikerel H, Karabekmez ME, Eraslan S, Kirdar B. Doxorubicin induces an extensive transcriptional and metabolic rewiring in yeast cells. *Sci Rep* [Internet]. 2018 Sep 12 [cited 2019 Dec 9];8. Available from: <https://www.ncbi.nlm.nih.gov/pmc/articles/PMC6135803/>
14. Agudelo D, Bourassa P, Bérubé G, Tajmir-Riahi H-A. Intercalation of antitumor drug doxorubicin and its analogue by DNA duplex: Structural features and biological implications. *Int J Biol Macromol.* 2014 May 1;66:144–50.

15. Doxorubicin Redox Biology: Redox Cycling, Topoisomerase Inhibition, and Oxidative Stress. - Abstract - Europe PMC [Internet]. [cited 2020 May 17]. Available from: <https://europepmc.org/article/PMC/5921833>
16. Themes UFO. Topoisomerase II Inhibitors: Anthracyclines [Internet]. Oncohematol Key. 2016 [cited 2020 May 17]. Available from: <https://oncohemakey.com/topoisomerase-ii-inhibitors-anthracyclines/>
17. Finn NA, Findley HW, Kemp ML. A Switching Mechanism in Doxorubicin Bioactivation Can Be Exploited to Control Doxorubicin Toxicity. *PLoS Comput Biol* [Internet]. 2011 Sep 15 [cited 2020 May 17];7(9). Available from: <https://www.ncbi.nlm.nih.gov/pmc/articles/PMC3174179/>
18. Volkova M, Russell R. Anthracycline Cardiotoxicity: Prevalence, Pathogenesis and Treatment. *Curr Cardiol Rev*. 2011 Nov;7(4):214–20.
19. Santos DS dos, Goldenberg RC dos S. Doxorubicin-Induced Cardiotoxicity: From Mechanisms to Development of Efficient Therapy. *Cardiotoxicity* [Internet]. 2018 Nov 5 [cited 2020 May 19]; Available from: <https://www.intechopen.com/books/cardiotoxicity/doxorubicin-induced-cardiotoxicity-from-mechanisms-to-development-of-efficient-therapy>
20. Chatterjee K, Zhang J, Honbo N, Karliner JS. Doxorubicin Cardiomyopathy. *Cardiology*. 2010 Jan;115(2):155–62.
21. Wenningmann N, Knapp M, Ande A, Vaidya TR, Ait-Oudhia S. Insights into Doxorubicin-induced Cardiotoxicity: Molecular Mechanisms, Preventive Strategies, and Early Monitoring. *Mol Pharmacol*. 2019 Aug;96(2):219–32.
22. Zhu H. Doxorubicin-Induced Cardiotoxicity. *Cardiotoxicity* [Internet]. 2018 Nov 5 [cited 2020 May 19]; Available from: <https://www.intechopen.com/books/cardiotoxicity/doxorubicin-induced-cardiotoxicity>
23. Octavia Y, Tocchetti CG, Gabrielson KL, Janssens S, Crijns HJ, Moens AL. Doxorubicin-induced cardiomyopathy: From molecular mechanisms to therapeutic strategies. *J Mol Cell Cardiol*. 2012 Jun 1;52(6):1213–25.
24. Puma N, Ruggiero A, Ridola V, Maurizi P, Lazzareschi I, Attinà G, et al. Anthracycline-related cardiotoxicity: risk factors and therapeutic options in childhood cancers. *Signa Vitae - J Intensive Care Emerg Med*. 2008 Apr 1;3(1):30–4.
25. Meiners B, Shenoy C, Zordoky BN. Clinical and preclinical evidence of sex-related differences in anthracycline-induced cardiotoxicity. *Biol Sex Differ* [Internet]. 2018 Aug 29 [cited 2020 Jun 3];9. Available from: <https://www.ncbi.nlm.nih.gov/pmc/articles/PMC6114275/>
26. Aminkeng F, Ross CJD, Rassekh SR, Hwang S, Rieder MJ, Bhavsar AP, et al. Recommendations for genetic testing to reduce the incidence of anthracycline-induced cardiotoxicity. *Br J Clin Pharmacol*. 2016;82(3):683–95.
27. Xiao B, Hong L, Cai X, Mei S, Zhang P, Shao L. The true colors of autophagy in doxorubicin-induced cardiotoxicity (Review). *Oncol Lett*. 2019 Sep 1;18(3):2165–72.
28. Koleini N, Kardami E. Autophagy and mitophagy in the context of doxorubicin-induced cardiotoxicity. *Oncotarget*. 2017 Apr 7;8(28):46663–80.

29. Hanna AD, Lam A, Tham S, Dulhunty AF, Beard NA. Adverse Effects of Doxorubicin and Its Metabolic Product on Cardiac RyR2 and SERCA2A. *Mol Pharmacol*. 2014 Oct;86(4):438–49.
30. Liu J, Mao W, Ding B, Liang C. ERKs/p53 signal transduction pathway is involved in doxorubicin-induced apoptosis in H9c2 cells and cardiomyocytes. *Am J Physiol - Heart Circ Physiol*. 2008 Nov;295(5):H1956–65.
31. Cappetta D, De Angelis A, Sapio L, Prezioso L, Illiano M, Quaini F, et al. Oxidative Stress and Cellular Response to Doxorubicin: A Common Factor in the Complex Milieu of Anthracycline Cardiotoxicity [Internet]. *Oxidative Medicine and Cellular Longevity*. 2017 [cited 2018 Sep 27]. Available from: <https://www.hindawi.com/journals/omcl/2017/1521020/>
32. Lemasters JJ, Nieminen A-L. *Mitochondria in Pathogenesis*. Springer Science & Business Media; 2007. 533 p.
33. Zhang X, Chen S, Huang K, Le W. Why should autophagic flux be assessed? *Acta Pharmacol Sin*. 2013 May;34(5):595–9.
34. Jung CH, Ro S-H, Cao J, Otto NM, Kim D-H. mTOR regulation of autophagy. *FEBS Lett*. 2010 Apr 2;584(7):1287–95.
35. Kim J, Russell R, Yuan H, Guan K-L. AMPK and mTOR in nutrient signaling and autophagy regulation. *FASEB J*. 2013 Apr 1;27(1\_supplement):99.1-99.1.
36. Hardie DG. AMPK and autophagy get connected. *EMBO J*. 2011 Feb 16;30(4):634–5.
37. Kim J, Kundu M, Viollet B, Guan K-L. AMPK and mTOR regulate autophagy through direct phosphorylation of Ulk1. *Nat Cell Biol*. 2011 Feb;13(2):132–41.
38. Roach PJ. AMPK → ULK1 → Autophagy. *Mol Cell Biol*. 2011 Aug 1;31(15):3082–4.
39. Zhao M, Klionsky DJ. AMPK-Dependent Phosphorylation of ULK1 Induces Autophagy. *Cell Metab*. 2011 Feb 2;13(2):119–20.
40. Zachari M, Ganley IG. The mammalian ULK1 complex and autophagy initiation. *Essays Biochem*. 2017 Dec 12;61(6):585–96.
41. Abounit K, Scarabelli TM, McCauley RB. Autophagy in mammalian cells. *World J Biol Chem*. 2012 Jan 26;3(1):1–6.
42. Glick D, Barth S, Macleod KF. Autophagy: cellular and molecular mechanisms. *J Pathol*. 2010 May;221(1):3–12.
43. Rubinsztein DC, Shpilka T, Elazar Z. Mechanisms of Autophagosome Biogenesis. *Curr Biol*. 2012 Jan 10;22(1):R29–34.
44. Katsuragi Y, Ichimura Y, Komatsu M. p62/SQSTM1 functions as a signaling hub and an autophagy adaptor. *FEBS J*. 2015 Oct 2;282(24):4672–8.
45. Reggiori F, Ungermann C. Autophagosome Maturation and Fusion. *J Mol Biol*. 2017 Feb 17;429(4):486–96.

46. Nakamura S, Yoshimori T. New insights into autophagosome–lysosome fusion. *J Cell Sci.* 2017 Apr 1;130(7):1209–16.
47. Song Q, Meng B, Xu H, Mao Z. The emerging roles of vacuolar-type ATPase-dependent Lysosomal acidification in neurodegenerative diseases. *Transl Neurodegener.* 2020 May 11;9(1):17.
48. Wang X, Wu WKK, Cho CH, Sung JJY, Yu J. Reduced Lysosomal Acidification Induce p53 and Unfolded Protein Response in Mice With Nutritional Steatohepatitis. *Clin Gastroenterol Hepatol.* 2015 Jul 1;13(7):e83.
49. Liu Y, Steinbusch LKM, Nabben M, Kapsokalyvas D, van Zandvoort M, Schönleitner P, et al. Palmitate-Induced Vacuolar-Type H<sup>+</sup>-ATPase Inhibition Feeds Forward Into Insulin Resistance and Contractile Dysfunction. *Diabetes.* 2017 Jun;66(6):1521–34.
50. Terman A, Kurz T, Gustafsson B, Brunk UT. The Involvement of Lysosomes in Myocardial Aging and Disease. *Curr Cardiol Rev.* 2008 May;4(2):107–15.
51. Chi C, Riching AS, Song K. Lysosomal Abnormalities in Cardiovascular Disease. *Int J Mol Sci* [Internet]. 2020 Jan 27 [cited 2020 May 25];21(3). Available from: <https://www.ncbi.nlm.nih.gov/pmc/articles/PMC7036830/>
52. Li DL, Wang ZV, Ding G, Tan W, Luo X, Criollo A, et al. Doxorubicin Blocks Cardiomyocyte Autophagic Flux by Inhibiting Lysosome Acidification. *Circulation.* 2016 Apr 26;133(17):1668–87.
53. Ruffin VA, Salameh AI, Boron WF, Parker MD. Intracellular pH regulation by acid-base transporters in mammalian neurons. *Front Physiol* [Internet]. 2014 [cited 2020 Aug 17];5. Available from: <https://www.frontiersin.org/articles/10.3389/fphys.2014.00043/full>
54. FUTAI M, SUN-WADA G-H, WADA Y, MATSUMOTO N, NAKANISHI-MATSUI M. Vacuolar-type ATPase: A proton pump to lysosomal trafficking. *Proc Jpn Acad Ser B Phys Biol Sci.* 2019 Jun 11;95(6):261–77.
55. Cotter K, Stransky L, McGuire C, Forgac M. Recent Insights into the Structure, Regulation and Function of the V-ATPases. *Trends Biochem Sci.* 2015 Oct;40(10):611–22.
56. Maxson ME, Grinstein S. The vacuolar-type H<sup>+</sup>-ATPase at a glance – more than a proton pump. *J Cell Sci.* 2014 Dec 1;127(23):4987–93.
57. Parra KJ, Chan C-Y, Chen J. *Saccharomyces cerevisiae* Vacuolar H<sup>+</sup>-ATPase Regulation by Disassembly and Reassembly: One Structure and Multiple Signals. *Eukaryot Cell.* 2014 Jun;13(6):706–14.
58. Vasanthakumar T, Rubinstein JL. Structure and Roles of V-type ATPases. *Trends Biochem Sci.* 2020 Apr;45(4):295–307.
59. Sun-Wada G-H, Wada Y, Futai M. Diverse and essential roles of mammalian vacuolar-type proton pump ATPase: toward the physiological understanding of inside acidic compartments. *Biochim Biophys Acta BBA - Bioenerg.* 2004 Jul 23;1658(1):106–14.
60. Abbas YM, Wu D, Bueler SA, Robinson CV, Rubinstein JL. Structure of V-ATPase from the mammalian brain. *Science.* 2020 Mar 13;367(6483):1240–6.



61. Toei M, Saum R, Forgac M. Regulation and Isoform Function of the V-ATPases. *Biochemistry*. 2010 Jun 15;49(23):4715–23.
62. Pamarthy S, Kulshrestha A, Katara GK, Beaman KD. The curious case of vacuolar ATPase: regulation of signaling pathways. *Mol Cancer* [Internet]. 2018 Feb 15 [cited 2018 Sep 25];17. Available from: <https://www.ncbi.nlm.nih.gov/pmc/articles/PMC5815226/>
63. Owegi MA, Pappas DL, Finch MW, Bilbo SA, Resendiz CA, Jacquemin LJ, et al. Identification of a Domain in the Vo Subunit d That Is Critical for Coupling of the Yeast Vacuolar Proton-translocating ATPase. *J Biol Chem*. 2006 Oct 6;281(40):30001–14.
64. Bhargava A, Voronov I, Wang Y, Glogauer M, Kartner N, Manolson MF. Osteopetrosis mutation R444L causes endoplasmic reticulum retention and misprocessing of vacuolar H<sup>+</sup>-ATPase a3 subunit. *J Biol Chem*. 2012 Aug 3;287(32):26829–39.
65. Holliday LS. Vacuolar H<sup>+</sup>-ATPase: An Essential Multitasking Enzyme in Physiology and Pathophysiology [Internet]. Vol. 2014, *New Journal of Science*. Hindawi; 2014 [cited 2020 May 12]. p. e675430. Available from: <https://www.hindawi.com/journals/njos/2014/675430/>
66. McGuire C, Cotter K, Stransky L, Forgac M. Regulation of V-ATPase Assembly and Function of V-ATPases in Tumor Cell Invasiveness. *Biochim Biophys Acta*. 2016 Aug;1857(8):1213–8.
67. Oot RA, Couoh-Cardel S, Sharma S, Stam NJ, Wilkens S. Breaking up and making up: The secret life of the vacuolar H<sup>+</sup>-ATPase. *Protein Sci Publ Protein Soc*. 2017 May;26(5):896–909.
68. Sharma S, Oot RA, Wilkens S. Role of the H subunit C-terminal domain in the assembly of the vacuolar H<sup>+</sup>-ATPase. *bioRxiv*. 2018 Aug 14;391656.
69. du Toit A, Hofmeyr J-HS, Gniadek TJ, Loos B. Measuring autophagosome flux. *Autophagy*. 2018 Jul 20;14(6):1060–71.
70. Mauvezin C, Nagy P, Juhász G, Neufeld TP. Autophagosome–lysosome fusion is independent of V-ATPase-mediated acidification. *Nat Commun*. 2015 May 11;6:7007.
71. McGuire CM, Forgac M. Glucose starvation increases V-ATPase assembly and activity in mammalian cells through AMP kinase and phosphatidylinositide 3-kinase/Akt signaling. *J Biol Chem*. 2018 Jun 8;293(23):9113–23.
72. Dröse S, Altendorf K. Bafilomycins and concanamycins as inhibitors of V-ATPases and P-ATPases. *J Exp Biol*. 1997 Jan 1;200(1):1–8.
73. Huss M, Wiczorek H. Inhibitors of V-ATPases: old and new players. *J Exp Biol*. 2009 Feb 1;212(3):341–6.
74. Bockelmann S, Menche D, Rudolph S, Bender T, Grond S, von Zezschwitz P, et al. Archazolid A binds to the equatorial region of the c-ring of the vacuolar H<sup>+</sup>-ATPase. *J Biol Chem*. 2010 Dec 3;285(49):38304–14.
75. Osteresch C, Bender T, Grond S, Zezschwitz P von, Kunze B, Jansen R, et al. The Binding Site of the V-ATPase Inhibitor Apicularen Is in the Vicinity of Those for Bafilomycin and Archazolid. *J Biol Chem*. 2012 Sep 14;287(38):31866–76.

76. Sørensen MG, Henriksen K, Neutzsky-Wulff AV, Dziegiel MH, Karsdal MA. Diphyllin, a Novel and Naturally Potent V-ATPase Inhibitor, Abrogates Acidification of the Osteoclastic Resorption Lacunae and Bone Resorption. *J Bone Miner Res.* 2007;22(10):1640–8.
77. Ding L, Guo Z, Xu H, Li T, Wang Y, Tao H. The Inhibitory Effect of Celangulin V on the ATP Hydrolytic Activity of the Complex of V-ATPase Subunits A and B in the Midgut of *Mythimna separata*. *Toxins.* 2019 22;11(2).
78. Mauvezin C, Neufeld TP. Bafilomycin A1 disrupts autophagic flux by inhibiting both V-ATPase-dependent acidification and Ca-P60A/SERCA-dependent autophagosome-lysosome fusion. *Autophagy.* 2015 Sep 14;11(8):1437–8.
79. Fedele AO, Proud CG. Chloroquine and bafilomycin A mimic lysosomal storage disorders and impair mTORC1 signalling. *Biosci Rep [Internet].* 2020 Apr 28 [cited 2020 May 13];40(4). Available from: <https://www.ncbi.nlm.nih.gov/pmc/articles/PMC7189491/>
80. Mangieri LR, Mader BJ, Thomas CE, Taylor CA, Luker AM, Tse TE, et al. ATP6V0C Knockdown in Neuroblastoma Cells Alters Autophagy-Lysosome Pathway Function and Metabolism of Proteins that Accumulate in Neurodegenerative Disease. *PLOS ONE.* 2014 Apr 2;9(4):e93257.
81. Wang S, Wong L-Y, Neumann D, Liu Y, Sun A, Antoons G, et al. Augmenting Vacuolar H<sup>+</sup>-ATPase Function Prevents Cardiomyocytes from Lipid-Overload Induced Dysfunction. *Int J Mol Sci [Internet].* 2020 Feb 23 [cited 2020 Jun 5];21(4). Available from: <https://www.ncbi.nlm.nih.gov/pmc/articles/PMC7073192/>
82. Lorkowski Shuhui Wang, Brubaker Gregory, Gulshan Kailash, Smith Jonathan D. V-ATPase (Vacuolar ATPase) Activity Required for ABCA1 (ATP-Binding Cassette Protein A1)-Mediated Cholesterol Efflux. *Arterioscler Thromb Vasc Biol.* 2018 Nov 1;38(11):2615–25.
83. Pizarro M, Troncoso R, Martínez GJ, Chiong M, Castro PF, Lavandero S. Basal autophagy protects cardiomyocytes from doxorubicin-induced toxicity. *Toxicology.* 2016 Aug;370:41–8.
84. Elhassan YS, Philp AA, Lavery GG. Targeting NAD<sup>+</sup> in Metabolic Disease: New Insights Into an Old Molecule. *J Endocr Soc.* 2017 Jul 1;1(7):816–35.
85. Zhang D-X, Zhang J-P, Hu J-Y, Huang Y-S. The potential regulatory roles of NAD<sup>+</sup> and its metabolism in autophagy. *Metabolism.* 2016 Apr;65(4):454–62.
86. Nakagawa T, Guarente L. Sirtuins at a glance. *J Cell Sci.* 2011 Mar 15;124(6):833–8.
87. Morales JC, Li L, Fattah FJ, Dong Y, Bey EA, Patel M, et al. Review of Poly (ADP-ribose) Polymerase (PARP) Mechanisms of Action and Rationale for Targeting in Cancer and Other Diseases. *Crit Rev Eukaryot Gene Expr.* 2014;24(1):15–28.
88. Deaglio S, Malavasi F. The CD38/CD157 mammalian gene family: An evolutionary paradigm for other leukocyte surface enzymes. *Purinergic Signal.* 2006 Jun;2(2):431–41.
89. Johnson S, Imai S. NAD<sup>+</sup> biosynthesis, aging, and disease. *F1000Research [Internet].* 2018 Feb 1 [cited 2019 Sep 30];7. Available from: <https://www.ncbi.nlm.nih.gov/pmc/articles/PMC5795269/>
90. Sultani G, Samsudeen AF, Osborne B, Turner N. NAD<sup>+</sup> : A key metabolic regulator with great therapeutic potential. *J Neuroendocrinol.* 2017 Oct;29(10):e12508.

91. Brazill JM, Li C, Zhu Y, Zhai RG. NMNAT: It's an NAD<sup>+</sup> Synthase... It's a Chaperone... It's a Neuroprotector. *Curr Opin Genet Dev*. 2017 Jun;44:156–62.
92. Yoshino J, Baur JA, Imai S. NAD<sup>+</sup> Intermediates: The Biology and Therapeutic Potential of NMN and NR. *Cell Metab*. 2018 Mar 6;27(3):513–28.
93. Verdin E. NAD<sup>+</sup> in aging, metabolism, and neurodegeneration. *Science*. 2015 Dec 4;350(6265):1208–13.
94. Katsyuba E, Romani M, Hofer D, Auwerx J. NAD<sup>+</sup> homeostasis in health and disease. *Nat Metab*. 2020 Jan;2(1):9–31.
95. Walker Matthew A., Tian Rong. Raising NAD in Heart Failure. *Circulation*. 2018 May 22;137(21):2274–7.
96. Grant R, Berg J, Mestayer R, Braidy N, Bennett J, Broom S, et al. A Pilot Study Investigating Changes in the Human Plasma and Urine NAD<sup>+</sup> Metabolome During a 6 Hour Intravenous Infusion of NAD<sup>+</sup>. *Front Aging Neurosci* [Internet]. 2019 [cited 2019 Nov 11];11. Available from: <https://www.frontiersin.org/articles/10.3389/fnagi.2019.00257/full>
97. Han X, Tai H, Wang X, Wang Z, Zhou J, Wei X, et al. AMPK activation protects cells from oxidative stress-induced senescence via autophagic flux restoration and intracellular NAD<sup>+</sup> elevation. *Aging Cell*. 2016 Jun 1;15(3):416–27.
98. Hsieh C-L, Hsieh S-Y, Huang H-M, Lu S-L, Omori H, Zheng P-X, et al. Nicotinamide Increases Intracellular NAD<sup>+</sup> Content to Enhance Autophagy-Mediated Group A Streptococcal Clearance in Endothelial Cells. *Front Microbiol* [Internet]. 2020 [cited 2020 May 13];11. Available from: <https://www.frontiersin.org/articles/10.3389/fmicb.2020.00117/full#B27>
99. Sedlackova L, Korolchuk VI. The crosstalk of NAD, ROS and autophagy in cellular health and ageing. *Biogerontology*. 2020 Jun 1;21(3):381–97.
100. Poddar SK, Sifat AE, Haque S, Nahid NA, Chowdhury S, Mehedi I. Nicotinamide Mononucleotide: Exploration of Diverse Therapeutic Applications of a Potential Molecule. *Biomolecules* [Internet]. 2019 Jan 21 [cited 2020 Jun 8];9(1). Available from: <https://www.ncbi.nlm.nih.gov/pmc/articles/PMC6359187/>
101. Mills KF, Yoshida S, Stein LR, Grozio A, Kubota S, Sasaki Y, et al. Long-Term Administration of Nicotinamide Mononucleotide Mitigates Age-Associated Physiological Decline in Mice. *Cell Metab*. 2016 Dec 13;24(6):795–806.
102. Grozio A, Mills KF, Yoshino J, Bruzzone S, Sociali G, Tokizane K, et al. Slc12a8 is a nicotinamide mononucleotide transporter. *Nat Metab*. 2019 Jan;1(1):47–57.
103. Yoshino J, Mills KF, Yoon MJ, Imai S. Nicotinamide mononucleotide, a key NAD<sup>(+)</sup> intermediate, treats the pathophysiology of diet- and age-induced diabetes in mice. *Cell Metab*. 2011 Oct 5;14(4):528–36.
104. Choi S-E, Fu T, Seok S, Kim D-H, Yu E, Lee K-W, et al. Elevated microRNA-34a in obesity reduces NAD<sup>+</sup> levels and SIRT1 activity by directly targeting NAMPT. *Aging Cell* [Internet]. 2013 Dec [cited 2020 Jun 8];12(6). Available from: <https://www.ncbi.nlm.nih.gov/pmc/articles/PMC3838500/>

105. Yamamoto T, Byun J, Zhai P, Ikeda Y, Oka S, Sadoshima J. Nicotinamide Mononucleotide, an Intermediate of NAD<sup>+</sup> Synthesis, Protects the Heart from Ischemia and Reperfusion. *PLoS ONE* [Internet]. 2014 Jun 6 [cited 2020 Jun 8];9(6). Available from: <https://www.ncbi.nlm.nih.gov/pmc/articles/PMC4048236/>
106. Klimova N, Fearnow A, Long A, Kristian T. NAD<sup>+</sup> precursor modulates post-ischemic mitochondrial fragmentation and reactive oxygen species generation via SIRT3 dependent mechanisms. *Exp Neurol*. 2020 Mar;325:113144.
107. Hong W, Mo F, Zhang Z, Huang M, Wei X. Nicotinamide Mononucleotide: A Promising Molecule for Therapy of Diverse Diseases by Targeting NAD<sup>+</sup> Metabolism. *Front Cell Dev Biol* [Internet]. 2020 Apr 28 [cited 2020 Jun 8];8. Available from: <https://www.ncbi.nlm.nih.gov/pmc/articles/PMC7198709/>
108. Lee CF, Chavez JD, Garcia-Menendez L, Choi Y, Roe ND, Chiao YA, et al. Normalization of NAD<sup>+</sup> Redox Balance as a Therapy for Heart Failure. *Circulation*. 2016 Sep 20;134(12):883–94.
109. Martin AS, Abraham DM, Hershberger KA, Bhatt DP, Mao L, Cui H, et al. Nicotinamide mononucleotide requires SIRT3 to improve cardiac function and bioenergetics in a Friedreich's ataxia cardiomyopathy model. *JCI Insight*. 2017 Jul 20;2(14).
110. Shirakabe Akihiro, Ikeda Yoshiyuki, Sciarretta Sebastiano, Zablocki Daniela K., Sadoshima Junichi. Aging and Autophagy in the Heart. *Circ Res*. 2016 May 13;118(10):1563–76.
111. Terman A, Kurz T, Navratil M, Arriaga EA, Brunk UT. Mitochondrial Turnover and Aging of Long-Lived Postmitotic Cells: The Mitochondrial–Lysosomal Axis Theory of Aging. *Antioxid Redox Signal*. 2010 Feb 15;12(4):503–35.
112. Schiattarella GG, Hill JA. Therapeutic Targeting of Autophagy in Cardiovascular Disease. *J Mol Cell Cardiol*. 2016 Jun;95:86–93.
113. Kane Alice E., Sinclair David A. Sirtuins and NAD<sup>+</sup> in the Development and Treatment of Metabolic and Cardiovascular Diseases. *Circ Res*. 2018 Sep 14;123(7):868–85.
114. Hanf A, Oelze M, Manea A, Li H, Münzel T, Daiber A. The anti-cancer drug doxorubicin induces substantial epigenetic changes in cultured cardiomyocytes. *Chem Biol Interact*. 2019 Nov 1;313:108834.
115. Hsu C-P, Hariharan N, Alcendor RR, Oka S, Sadoshima J. Nicotinamide phosphoribosyltransferase regulates cell survival through autophagy in cardiomyocytes. *Autophagy*. 2009 Nov 16;5(8):1229–31.
116. Ruan Y, Dong C, Patel J, Duan C, Wang X, Wu X, et al. SIRT1 Suppresses Doxorubicin-Induced Cardiotoxicity by Regulating the Oxidative Stress and p38MAPK Pathways. *Cell Physiol Biochem*. 2015;35(3):1116–24.
117. Zheng D, Zhang Y, Zheng M, Cao T, Wang G, Zhang L, et al. Nicotinamide riboside promotes autolysosome clearance in preventing doxorubicin-induced cardiotoxicity. *Clin Sci Lond Engl 1979*. 2019 Jul 15;133(13):1505–21.
118. Vassilopoulos A, Pennington JD, Andresson T, Rees DM, Bosley AD, Fearnley IM, et al. SIRT3 Deacetylates ATP Synthase F1 Complex Proteins in Response to Nutrient- and Exercise-Induced Stress. *Antioxid Redox Signal*. 2014 Aug 1;21(4):551–64.

119. Rahman M, Nirala NK, Singh A, Zhu LJ, Taguchi K, Bamba T, et al. *Drosophila* Sirt2/mammalian SIRT3 deacetylates ATP synthase  $\beta$  and regulates complex V activity. *J Cell Biol.* 2014 Jul 21;206(2):289–305.
120. Finbow ME, Harrison MA. The vacuolar H<sup>+</sup>-ATPase: a universal proton pump of eukaryotes. *Biochem J.* 1997 Jun 15;324(Pt 3):697–712.
121. Rajman L, Chwalek K, Sinclair DA. Therapeutic potential of NAD-boosting molecules: the in vivo evidence. *Cell Metab.* 2018 Mar 6;27(3):529–47.
122. Branco AF, Pereira SP, Gonzalez S, Gusev O, Rizvanov AA, Oliveira PJ. Gene Expression Profiling of H9c2 Myoblast Differentiation towards a Cardiac-Like Phenotype. *PLOS ONE.* 2015 Jun 29;10(6):e0129303.
123. New Insights About Doxorubicin-Induced Toxicity to Cardiomyoblast-Derived H9C2 Cells and Dexrazoxane Cytoprotective Effect: Contribution of In Vitro 1H-NMR Metabonomics. - Abstract - Europe PMC [Internet]. [cited 2020 May 23]. Available from: <https://europepmc.org/article/med/32153402>
124. Turakhia S, Venkatakrisnan CD, Dunsmore K, Wong H, Kuppusamy P, Zweier JL, et al. Doxorubicin-induced cardiotoxicity: direct correlation of cardiac fibroblast and H9c2 cell survival and aconitase activity with heat shock protein 27. *Am J Physiol-Heart Circ Physiol.* 2007 Nov 1;293(5):H3111–21.
125. Vallyathan V, Castranova V, Shi X. *Oxygen/Nitrogen Radicals: Cell Injury and Disease.* Springer Science & Business Media; 2012. 393 p.
126. Communal C, Sumandea M, de Tombe P, Narula J, Solaro RJ, Hajjar RJ. Functional consequences of caspase activation in cardiac myocytes. *Proc Natl Acad Sci U S A.* 2002 Apr 30;99(9):6252–6.
127. Li S, Wang W, Niu T, Wang H, Li B, Shao L, et al. Nrf2 Deficiency Exaggerates Doxorubicin-Induced Cardiotoxicity and Cardiac Dysfunction [Internet]. Vol. 2014, *Oxidative Medicine and Cellular Longevity.* Hindawi; 2014 [cited 2020 May 23]. p. e748524. Available from: <https://www.hindawi.com/journals/omcl/2014/748524/>
128. Isa HI, Ferreira GCH, Crafford JE, Botha CJ. Epoxyscillirosidine Induced Cytotoxicity and Ultrastructural Changes in a Rat Embryonic Cardiomyocyte (H9c2) Cell Line. *Toxins* [Internet]. 2019 May 21 [cited 2020 Aug 17];11(5). Available from: <https://www.ncbi.nlm.nih.gov/pmc/articles/PMC6563272/>
129. Diguët Nicolas, Trammell Samuel A.J., Tannous Cynthia, Deloux Robin, Piquereau Jérôme, Mougénot Nathalie, et al. Nicotinamide Riboside Preserves Cardiac Function in a Mouse Model of Dilated Cardiomyopathy. *Circulation.* 2018 May 22;137(21):2256–73.
130. Nadtochiy SM, wang YT, Nehrke K, Munger J, Brookes PS. Cardioprotection by nicotinamide mononucleotide (NMN): Involvement of glycolysis and acidic pH. *J Mol Cell Cardiol.* 2018 Aug;121:155–62.
131. Canada PHA of. Cancer - About Us [Internet]. aem. 2009 [cited 2020 Jun 9]. Available from: <https://www.canada.ca/en/public-health/services/chronic-diseases/cancer/cancer-about-us.html>

132. Impact of antioxidant supplementation on chemotherapeutic efficacy: A systematic review of the evidence from randomized controlled trials - ScienceDirect [Internet]. [cited 2018 Oct 1]. Available from:  
<https://www.sciencedirect.com/science/article/pii/S0305737207000278?via%3Dihub>
133. Bansal N, Adams MJ, Ganatra S, Colan SD, Aggarwal S, Steiner R, et al. Strategies to prevent anthracycline-induced cardiotoxicity in cancer survivors. *Cardio-Oncol*. 2019 Dec 2;5(1):18.
134. Langer SW. Dexrazoxane for the treatment of chemotherapy-related side effects. *Cancer Manag Res*. 2014 Sep 15;6:357–63.
135. Koleini N, Kardami E. Autophagy and mitophagy in the context of doxorubicin-induced cardiotoxicity. *Oncotarget*. 2017 Apr 7;8(28):46663–80.
136. Unverferth BJ, Magorien RD, Balcerzak SP, Leier CV, Unverferth DV. Early changes in human myocardial nuclei after doxorubicin. *Cancer*. 1983 Jul 15;52(2):215–21.
137. Zhao L, Zhang B. Doxorubicin induces cardiotoxicity through upregulation of death receptors mediated apoptosis in cardiomyocytes. *Sci Rep* [Internet]. 2017 Mar 16 [cited 2018 Oct 1];7. Available from: <https://www.ncbi.nlm.nih.gov/pmc/articles/PMC5353581/>
138. Maejima Y, Adachi S, Ito H, Hirao K, Isobe M. Induction of premature senescence in cardiomyocytes by doxorubicin as a novel mechanism of myocardial damage. *Aging Cell*. 2008;7(2):125–36.
139. Thenappan T, Stulak JM, Agarwal R, Maltais S, Shah P, Eckman P, et al. Early intervention for lactate dehydrogenase elevation improves clinical outcomes in patients with the HeartMate II left ventricular assist device: Insights from the PREVENT study. *J Heart Lung Transplant*. 2018 Jan 1;37(1):25–32.
140. Piper C, Horstkotte D, Bock A-K, Wudel E, Schultheiß H-P, Dörner A. Myocardial lactate dehydrogenase patterns in volume or pressure overloaded left ventricles. *Eur J Heart Fail*. 2002;4(5):587–91.
141. Kemp M, Donovan J, Higham H, Hooper J. Biochemical markers of myocardial injury. *BJA Br J Anaesth*. 2004 Jul 1;93(1):63–73.
142. Suguro M, Kanda Y, Yamamoto R, Chizuka A, Hamaki T, Matsuyama T, et al. High serum lactate dehydrogenase level predicts short survival after vincristine-doxorubicin-dexamethasone (VAD) salvage for refractory multiple myeloma. *Am J Hematol*. 2000 Oct;65(2):132–5.
143. Sawa Y, Taketani S, Kawaguchi N, Kagisaki K, Onishi S, Matsuda H. DNA Fragmentation is a Possible Mechanism for Heart Failure in Cardiomyopathy. In: Takeda N, Nagano M, Dhalla NS, editors. *The Hypertrophied Heart* [Internet]. Boston, MA: Springer US; 2000 [cited 2020 Jun 9]. p. 363–74. (Progress in Experimental Cardiology). Available from: [https://doi.org/10.1007/978-1-4615-4423-4\\_29](https://doi.org/10.1007/978-1-4615-4423-4_29)
144. Qasim M, Bukhari S, Ghani M, Masoud M, Huma T, Arshad M, et al. Relationship of oxidative stress with elevated level of DNA damage and homocysteine in cardiovascular disease patients. *Pak J Pharm Sci*. 2016 Dec 1;29:2297–302.
145. Wu H, Che X, Zheng Q, Wu A, Pan K, Shao A, et al. Caspases: A Molecular Switch Node in the Crosstalk between Autophagy and Apoptosis. *Int J Biol Sci*. 2014 Sep 13;10(9):1072–83.

146. Pop C, Salvesen GS. Human Caspases: Activation, Specificity, and Regulation. *J Biol Chem*. 2009 Aug 14;284(33):21777–81.
147. Roy\* S. Caspases at the Heart of the Apoptotic Cell Death Pathway [Internet]. American Chemical Society; 2000 [cited 2020 Jun 9]. Available from: <https://pubs.acs.org/doi/pdf/10.1021/tx000109k>
148. Yang B, Ye D, Wang Y. Caspase-3 as a therapeutic target for heart failure. *Expert Opin Ther Targets*. 2013 Mar;17(3):255–63.
149. Michihiko U, Yoshihiko K, Koh-ichi Y, Nobuyuki M, Motoyuki I, Takashi M, et al. Doxorubicin Induces Apoptosis by Activation of Caspase-3 in Cultured Cardiomyocytes In Vitro and Rat Cardiac Ventricles In Vivo. *J Pharmacol Sci*. 2006 Jan 1;101(2):151–8.
150. Wang S, Konorev EA, Kotamraju S, Joseph J, Kalivendi S, Kalyanaraman B. Doxorubicin Induces Apoptosis in Normal and Tumor Cells via Distinctly Different Mechanisms INTERMEDIACY OF H2O2- AND p53-DEPENDENT PATHWAYS. *J Biol Chem*. 2004 Jun 11;279(24):25535–43.
151. Colacurcio DJ, Nixon RA. Disorders of lysosomal acidification—The emerging role of v-ATPase in aging and neurodegenerative disease. *Ageing Res Rev*. 2016 Dec 1;32:75–88.
152. Trudeau KM, Colby AH, Zeng J, Las G, Feng JH, Grinstaff MW, et al. Lysosome acidification by photoactivated nanoparticles restores autophagy under lipotoxicity. *J Cell Biol*. 2016 Jul 4;214(1):25–34.
153. Bonam SR, Wang F, Muller S. Lysosomes as a therapeutic target. *Nat Rev Drug Discov*. 2019;18(12):923–48.
154. Matasic DS, Brenner C, London B. Emerging potential benefits of modulating NAD<sup>+</sup> metabolism in cardiovascular disease. *Am J Physiol-Heart Circ Physiol*. 2017 Dec 22;314(4):H839–52.
155. Irie J, Inagaki E, Fujita M, Nakaya H, Mitsuishi M, Yamaguchi S, et al. Effect of oral administration of nicotinamide mononucleotide on clinical parameters and nicotinamide metabolite levels in healthy Japanese men. *Endocr J*. 2020 Feb 28;67(2):153–60.
156. Clinical Trial on Glucose Metabolism Disorders: NMN supplement, Placebo [Internet]. [cited 2020 Jun 10]. Available from: <https://ichgcp.net/clinical-trials-registry/NCT03151239>
157. Bindu S, Pillai VB, Gupta MP. Role of Sirtuins in Regulating Pathophysiology of the Heart. *Trends Endocrinol Metab*. 2016 Aug;27(8):563–73.
158. Kumari H, Huang W-H, Chan MWY. Review on the Role of Epigenetic Modifications in Doxorubicin-Induced Cardiotoxicity. *Front Cardiovasc Med* [Internet]. 2020 May 7 [cited 2020 Aug 18];7. Available from: <https://www.ncbi.nlm.nih.gov/pmc/articles/PMC7221144/>
159. Cipriano DJ, Wang Y, Bond S, Hinton A, Jefferies KC, Qi J, et al. Structure and regulation of the vacuolar ATPases. *Biochim Biophys Acta BBA - Bioenerg*. 2008 Jul 1;1777(7):599–604.
160. Smith AN, Jouret F, Bord S, Borthwick KJ, Al-Lamki RS, Wagner CA, et al. Vacuolar H<sup>+</sup>-ATPase d2 Subunit: Molecular Characterization, Developmental Regulation, and Localization to Specialized Proton Pumps in Kidney and Bone. *J Am Soc Nephrol*. 2005 May;16(5):1245–56.

161. Bartlett JJ, Trivedi PC, Pulinilkunnil T. Autophagic dysregulation in doxorubicin cardiomyopathy. *J Mol Cell Cardiol.* 2017 Mar;104:1–8.



## Curriculum Vitae

**Name:** Nima Nalin

**Post-secondary Education and Degrees:** Western University  
London, Ontario, Canada  
2018-2020 M.Sc.

Amrita University  
Kerala, India  
2007-2009 M.Sc.

Mahatma Gandhi University  
Kerala, India  
2004-2007 B.Sc.

**Honours and Awards:** Western Graduate Research Scholarship  
2018-2020

**Related Work Experience:** Research Assistant  
United Arab Emirates University  
2014-2018